Coastal and epipelagic habitats of the estuary and Gulf of St. Lawrence

J.-D. Dutil, S. Proulx, P. S. Galbraith, J. Chassé, N. Lambert and C. Laurian

Institut Maurice-Lamontagne
850 route de la Mer
C.P. 1000
Mont-Joli, Québec
G5H 3Z4

2012

Canadian Technical Report of Fisheries and Aquatic Sciences 3009

Fisheries and Oceans Canada | Pêches et Océans Canada

Canada

Canadian Technical Report of Fisheries and Aquatic Sciences

Technical reports contain scientific and technical information that contributes to existing knowledge but which is not normally appropriate for primary literature. Technical reports are directed primarily toward a worldwide audience and have an international distribution. No restriction is placed on subject matter and the series reflects the broad interests and policies of Fisheries and Oceans Canada, namely, fisheries and aquatic sciences.

Technical reports may be cited as full publications. The correct citation appears above the abstract of each report. Each report is abstracted in the data base *Aquatic Sciences and Fisheries Abstracts*.

Technical reports are produced regionally but are numbered nationally. Requests for individual reports will be filled by the issuing establishment listed on the front cover and title page.

Numbers 1-456 in this series were issued as Technical Reports of the Fisheries Research Board of Canada. Numbers 457-714 were issued as Department of the Environment, Fisheries and Marine Service, Research and Development Directorate Technical Reports. Numbers 715-924 were issued as Department of Fisheries and Environment, Fisheries and Marine Service Technical Reports. The current series name was changed with report number 925.

Rapport technique canadien des sciences halieutiques et aquatiques

Les rapports techniques contiennent des renseignements scientifiques et techniques qui constituent une contribution aux connaissances actuelles, mais qui ne sont pas normalement appropriés pour la publication dans un journal scientifique. Les rapports techniques sont destinés essentiellement à un public international et ils sont distribués à cet échelon. Il n'y a aucune restriction quant au sujet; de fait, la série reflète la vaste gamme des intérêts et des politiques de Pêches et Océans Canada, c'est-à-dire les sciences halieutiques et aquatiques.

Les rapports techniques peuvent être cités comme des publications à part entière. Le titre exact figure au-dessus du résumé de chaque rapport. Les rapports techniques sont résumés dans la base de données *Résumés des sciences aquatiques et halieutiques*.

Les rapports techniques sont produits à l'échelon régional, mais numérotés à l'échelon national. Les demandes de rapports seront satisfaites par l'établissement auteur dont le nom figure sur la couverture et la page du titre.

Les numéros 1 à 456 de cette série ont été publiés à titre de Rapports techniques de l'Office des recherches sur les pêcheries du Canada. Les numéros 457 à 714 sont parus à titre de Rapports techniques de la Direction générale de la recherche et du développement, Service des pêches et de la mer, ministère de l'Environnement. Les numéros 715 à 924 ont été publiés à titre de Rapports techniques du Service des pêches et de la mer, ministère des Pêches et de l'Environnement. Le nom actuel de la série a été établi lors de la parution du numéro 925.

Canadian Technical Report of
Fisheries and Aquatic Sciences 3009

2012

COASTAL AND EPIPELAGIC HABITATS OF THE ESTUARY AND GULF OF ST. LAWRENCE

by

J.-D. Dutil, S. Proulx, P. S. Galbraith, J. Chassé, N. Lambert and C. Laurian

Institut Maurice-Lamontagne
850 route de la Mer
C.P. 1000
Mont-Joli, Québec
G5H 3Z4

© Her Majesty the Queen in Right of Canada, 2012.

Cat. No. Fs 97-6/3009E
Cat. No. Fs 97-6/3009E-PDF

ISSN 0706-6457 (Print version)
ISSN 1488-5379 (Online version)

Correct citation for this publication:

Dutil, J.-D., S. Proulx, P. S. Galbraith, J. Chassé, N. Lambert and C. Laurian. 2012. Coastal and epipelagic habitats of the estuary and Gulf of St. Lawrence. Can. Tech. Rep. Fish. Aquat. Sci. 3009: ix + 87 pp.

TABLE OF CONTENTS

List of Tables iii
List of Figures iv
List of Appendices vii
Abstract viii
Résumé ix
Introduction 1
Materials and Methods 2
Spatial reference system 2
Landscape features 4
Satellite imagery 5
3D circulation model 6
Shoreline classification and pre-spill databases 8
Other parameters 8
Statistical analyses 9
Results 10
Mapping individual variables 11
Mapping using a set of criteria 13
Habitat classification 13
Discussion 15
Acknowledgements 18
References 19

LIST OF TABLES

Table 1. Characteristics of benthic and pelagic cells (39,337 marine cells with a non-tidal zone area > 0) in the estuary and Gulf of St. Lawrence. "No of cells" is the total count of cells by category. Planimetric areas (km^2) and "lenght of coastline" represent sum values by category. Other variables are mean values by category. 22

LIST OF FIGURES

Figure 1. The study area included the middle and lower St. Lawrence estuary, and the Gulf of St. Lawrence east to Cabot Strait and the Strait of Belle Isle. Solid red lines indicate the limits of the study area and subareas. The 200 m isobath south of the Laurentian Channel arbitrarily divides the northern and southern Gulf. The Saguenay Fjord was not included in the study. (1) Prince Edward Island, (2) Cape Breton, (3) Miscou Island, (4) Anticosti, (5) Gaspé Peninsula, (6) West Coast of Newfoundland, (7) Quebec Lower North Shore, (8) Shediac Valley, (9) Manicouagan Peninsula, (10) Pointe-des-Monts, (11) Mingan Islands, (12) Cape St. Georges, (13) Baie des Chaleurs, (14) Northumberland Strait.....23

Figure 2. Coastal area showing the mapping grid and cell address designation. The 100 km² cells are designated by column number (increasing from left to right) and row number (increasing from top to bottom), as described in Dutil et al. (2011). The 6.25 km² cells are designated by adding a suffix letter ranging from a to p and increasing through the alphabet column-wise and then row-wise. Hatched areas indicate the tidal zone and the blue line indicates the cut-off limit of river estuaries. 24

Figure 3. The area of the non-tidal zone within each cell was categorized as being benthic (B) or pelagic (P) based on two binary variables (BENTHIC_B and PELAGIC_B). Cells with the whole seafloor at depths shallower than 30 m have a BENTHIC_B value of 1 and a PELAGIC_B value of 0; cells with the whole seafloor at depths greater than 30 m have a PELAGIC_B value of 1 and a BENTHIC_B value of 0. Cells with a mixed situation have BENTHIC_B and PELAGIC_B values of 1. I, cells with TIDAL_A value > 0 and NONTIDAL_A value = 0. The plan view is on the left and the sectional view on the right. 25

Figure 4. Study area showing the coastal zone down to the 30 m isobath (dark blue). 26

Figure 5. Length of the coastline (km) in the northeastern Gulf as determined by the low tide mark (mainland and islands).....27

Figure 6. Sinuosity of the coastline (mainland only) in the northeastern Gulf, determined as the ratio of the length of the coastline at low tide, and the corresponding straight-line distance. 28

Figure 7. Total number of discrete landscape features emerged at low tide in the northeastern Gulf: islands with associated tidal zone and patches of tidal zones forming islands at low tide.....29

Figure 8. Maximum depth (m) of the portion of the seafloor less than 30 m deep. Only benthic cells are shown. 30

Figure 9. Standard deviation of depth (m) for the portion of the seafloor less than 30 m deep. Only benthic cells are shown. 31

Figure 10. Maximum slope (degrees) of the portion of the seafloor less than 30 m deep. Only benthic cells are shown. 32

Figure 11. Sum area of the tidal zone (km^2) accessible based on the eight nearest neighbours. Only benthic cells are shown. 33

Figure 12. Maximum sum value of all tide components (cm) during a 50 d period (17 October to 5 December, 2007). Tidal amplitude has been multiplied by two to yield tidal range. 34
Figure 13. Minimum mean monthly temperature at the surface (°C) as predicted by the 3D model (0–6.2 m layer). 35
Figure 14. Maximum mean monthly temperature at the surface (°C) as predicted by the 3D model (0–6.2 m layer). 36
Figure 15. Number of weeks with sea surface temperature below 2°C. 37
Figure 16. Number of weeks with sea surface temperature between 6 and 10°C. 38
Figure 17. Number of weeks with sea surface temperature between 14 and 18°C. 39
Figure 18. Number of degree-days above 2°C from week 31 to week 40. 40
Figure 19. Sea surface temperature (°C) at the end of May (week 21). 41
Figure 20. Mean salinity predicted by the 3D model at the surface (0–6.2 m layer). 42
Figure 21. Mean salinity at DEPTHMEAN (on the bottom or at 30 m for BENTHIC_B=0 cells), as predicted from the corresponding layer by the 3D model. 43
Figure 22. Freshwater runoff influence in winter (period from January to March), as predicted by the 3D model, and calculated as 1-(MSAL/35), where MSAL is the average salinity of the water column from the surface down to 36.7 m, and "35" is the maximum salinity of seawater. 44
Figure 23. Freshwater runoff influence in spring (period from April to June), as predicted by the 3D model, and calculated as 1-(MSAL/35), where MSAL is the average salinity of the water column from the surface down to 36.7 m, and "35" is the maximum salinity of seawater. 45
Figure 24. Freshwater runoff influence in summer (period from July to September), as predicted by the 3D model, and calculated as 1-(MSAL/35), where MSAL is the average salinity of the water column from the surface down to 36.7 m, and "35" is the maximum salinity of seawater. 46
Figure 25. Freshwater runoff influence in fall (period from October to December), as predicted by the 3D model, and calculated as 1-(MSAL/35), where MSAL is the average salinity of the water column from the surface down to 36.7 m, and "35" is the maximum salinity of seawater. 47
Figure 26. Mean turbidity in spring (period from April to June). Source: NASA, satellite AQUA, MODIS spectroradiometer-based estimate of the diffuse attenuation coefficient of seawater at 490 nm (m^{-1}). 48
Figure 27. Mean turbidity in fall (period from October to December). Source: NASA, satellite AQUA, MODIS spectroradiometer-based estimate of the diffuse attenuation coefficient of seawater at 490 nm (m^{-1}). 49
Figure 28. First day of the year when mean ice thickness is greater than 5 cm. 50
Figure 29. Number of years when ice thickness reached the 5 cm mark (14 years of record). 51
Figure 30. Direction of the horizontal current at the surface (0–6.2 m layer), coded into eight categories of 45 degrees each, code 1 (north) including angles from 337.5 to 360 degrees and from 0 to 22.5 degrees, code 2 angles from 22.5 to 67.5 degrees, etc. 52

Figure 31. Direction of the horizontal current at DEPTHMEAN (on the bottom or at 30 m for BENTHIC_B=0 cells), coded into eight categories of 45 degrees each, code 1 (north) including angles from 337.5 to 360 degrees and from 0 to 22.5 degrees, code 2 angles from 22.5 to 67.5 degrees, etc. 53
Figure 32. Mean horizontal current velocity (m/s) predicted by the 3D model at the surface (0–6.2 m layer). 54
Figure 33. Mean horizontal current velocity (m/s) at the depth value set by DEPTHMEAN (on the bottom or at 30 m for BENTHIC_B=0 cells), as predicted from the corresponding layer by the 3D model. 55
Figure 34. Minimum horizontal current velocity (m/s) predicted by the 3D model at the surface (0–6.2 m layer). 56
Figure 35. Maximum horizontal current velocity (m/s) at the depth value set by DEPTHMEAN (on the bottom or at 30 m for BENTHIC_B=0 cells), as predicted from the corresponding layer by the 3D model. 57
Figure 36. Mean tidal current (cm/sec) associated with the M2 component of the tide. 58
Figure 37. Mean annual wind speed (m/sec). 59
Figure 38. Simpson-Hunter water column stability parameter, mean value for a 50 d period (17 October to 5 December, 2007). This parameter is unitless; values near 0 indicate strong mixing, high values indicate a stratified water column. 60
Figure 39. Coastal habitat less than 10 m deep by depth and exposure category in the Baie des Chaleurs, Miscou Island and Miramichi areas. The figure was drawn from Cairns et al. (2012, figure 23). 61
Figure 40. Cells located within 50 km of all of the following features in the Shoreline Classification and Pre-spill database: sand beach, marsh, and mud flat (light blue areas). Within light blue areas, dark areas indicate cells located within 10 km of known eelgrass beds. 62
Figure 41. Pelagic cells exhibiting low mean values of the Simpson-Hunter water column stability parameter (< 4.5) and mean tidal current velocities > 7 cm/sec, broken down by mean annual turbidity. 63
Figure 42. Cells classified as being brackish (brown and beige shades) or more saline (dark blue). Blue: mean bottom salinity > 30, maximum surface salinity > 32, and freshwater influence <0.09; beige: mean bottom salinity < 30, maximum surface salinity < 32, and freshwater influence > 0.08; brown: mean bottom salinity < 24. 64
Figure 43. Cells classified as belonging to an arctic environment (blue shades) or a more temperate environment (brown shades). Blue: years with ice > 5 cm = 14, number of weeks with temperature below 2°C > 21, number of degree-days above 2°C from week 31 to week 40 < 850, and minimum surface temperature <-0.5 °C; brown: mirror values for the same parameters. Both categories are broken down by maximum surface temperature. 65
Figure 44. Tree diagram showing 16 clusters formed at an average distance of 0.35. Clusters were determined using a disjoint (i.e., non-hierarchical) cluster analysis based on Euclidean

distances (FASTCLUS procedure; SAS software). Outliers (clusters of less than 30 cells) were detected and re-assigned to the remaining clusters. The output from this analysis was analyzed with the CLUSTER procedure (unweighted pair-group averages to determine the hierarchy among clusters and, indirectly, among the 39,337 cells in the study area (see method 2 in Materials and Methods). 66

Figure 45. Spatial distribution of seven clusters of cells based on 103 habitat descriptors and representing 80% of all cells in the study area. The analysis suggested 16 different clusters; two small clusters appeared to be made of scattered cells and were grouped with their nearest neighbour, resulting in 14 different clusters considered to represent a classification of the pelagic and coastal habitats in the estuary and Gulf of St. Lawrence (see method 2 in Materials and Methods). 67

Figure 46. Spatial distribution of seven clusters of cells based on 103 habitat descriptors, mainly located near the coastline and representing 20% of all cells in the study area. The analysis suggested 16 different clusters; two small clusters appeared to be made of scattered cells and were grouped with their nearest neighbour, resulting in 14 different clusters considered to represent a classification of the pelagic and coastal habitats in the estuary and Gulf of St. Lawrence (see method 2 in Materials and Methods). 68

Figure 47. Spatial distribution of seven clusters of cells based on 21 habitat descriptors and representing 84% of all cells in the study area. The 103 original variables were clustered (VARCLUS procedure; SAS software) and a subset of 21 variables selected (see method 4 in Materials and Methods). Different shades indicate different habitat categories....69

Figure 48. Habitat diversity determined as the number of different habitat categories within a distance of 11.5 km from each cell centroid (shades of blue in the background; deeper colours indicate a higher count, i.e., greater diversity). Kernel density estimation contours are overlaid. 70

LIST OF APPENDICES

Appendix 1. List of variables used to describe marine cells in the Microsoft Access® database with short descriptions. 71

Appendix 2. Description of variables in the Microsoft Access® database with regard to their characteristics and scale of measurement. 79

Appendix 3. Variables issued from remote sensing observations (italics) and 3D modelling (plain text). 85

Appendix 4. Variables and number of cells with null or missing data. Cells with null data were coded "-8888", those with missing data were coded "-9999". Variables not listed had no null or missing data. 87

ABSTRACT

Dutil, J.-D., S. Proulx, P. S. Galbraith, J. Chassé, N. Lambert and C. Laurian. 2012. Coastal and epipelagic habitats of the estuary and Gulf of St. Lawrence. Can. Tech. Rep. Fish. Aquat. Sci. 3009: ix + 87 pp.

A database is presented that describes the pelagic and benthic habitats of the 0–30 m surface layer in the estuary and Gulf of St. Lawrence. A grid made of 6.25 km^2 cells (2.5 x 2.5 km) was used to aggregate the data. Each of the 39,337 cells overlapping the marine environment was characterized using landscape, hydrographic, and oceanographic parameters determined from observations (including satellite imagery), a 3D circulation model, and published and unpublished material available at local and regional scales. The low tide limit was taken as the upper (0 m) boundary, but neighbouring landscape features, such as the proximity to freshwater inflows, surface area of the tidal zone, and characteristics of the shoreline, were also taken into consideration. The dataset includes 130 descriptors: cell location parameters such as cell address, latitude and longitude, and distance to the coast; landscape features such as depth, slope, insulosity, coastline development, shore material and characteristics, degree of protection from the open sea, sensitivity of the shoreline to sea-level rise, and relative importance of the benthic and pelagic environments; hydrographic and oceanographic parameters such as distance to the nearest stream or river and its drainage area and mean annual flow, tidal range, vertical and horizontal currents, sea-surface climatology, ice conditions, salinity and temperature at various depths, stability of the water column. A total of 103 variables were used to classify cells into 14 different habitats. Coastal areas, particularly in the southern Gulf, appear to be more diversified locally than midshore and offshore habitats, which formed large patches of more uniform characteristics. The dataset provides useful information on the spatial extent of major coastal epipelagic habitats in the study area. The information can be used for mapping purposes and for analyses of species-habitat relationships, a key requirement for conservation, integrated management, or species-at-risk recovery planning purposes.

RÉSUMÉ

Dutil, J.-D., S. Proulx, P. S. Galbraith, J. Chassé, N. Lambert and C. Laurian. 2012. Coastal and epipelagic habitats of the estuary and Gulf of St. Lawrence. Can. Tech. Rep. Fish. Aquat. Sci. 3009: ix + 87 pp.

Une base de données géospatiales a été créée décrivant les habitats de la couche de surface entre 0 et 30 m de profondeur dans l'estuaire et le Golfe du Saint-Laurent. Les caractéristiques topographiques, hydrographiques et océanographiques de 39,337 cellules de 6.25 km² (2.5 x 2.5 km) qui chevauchent le milieu marin ont été obtenues de diverses sources: données publiées ou non publiées, imagerie satellitaire, modèle de circulation 3D. Bien que la limite des basses eaux ait été retenue comme limite supérieure de la couche de surface, certains paramètres propres à la côte ont été inclus, notamment la proximité des rivières, les caractéristiques du rivage, et la superficie accessible de la zone intertidale. La base de données comporte 130 descripteurs, à une échelle locale ou régionale, qui portent sur la topographie (localisation des cellules, la pente, la profondeur, l'insulosité, la complexité de la côte, le type de rivage, l'exposition aux vagues, la sensibilité à l'érosion, l'importance relative des milieux pélagiques et benthiques), l'hydrographie et l'océanographie (distance de la rivière la plus proche, son débit et son aire drainée, amplitude des marées, force des courants horizontaux et verticaux, climatologie en surface, salinité et température à diverses profondeurs, stabilité de la colonne d'eau, glaces). Cent-trois de ces descripteurs ont servi à la classification de 14 habitats. Les habitats sont en général plus diversifiés ou fragmentés dans la zone côtière, notamment dans le sud du Golfe. Ce jeu de données peut servir à la cartographie thématique du territoire et de ses principaux habitats côtiers et épipélagiques. Il se prête également à l'analyse des relations entre espèces et habitats, mettant ainsi davantage à notre portée la prestation d'avis écosystémiques en matière de conservation, d'écocertification, de gestion intégrée, et de protection de l'habitat des espèces en péril.

INTRODUCTION

There is a growing concern and a growing need to be concerned about the health of coastal ecosystems. The human population is growing and population densities are increasing exponentially, particularly in the coastal areas (De Sherbinin et al. 2007). Since sustainable development practices are not the norm, the nearshore landscape becomes progressively modified and coastal ecosystems are affected most intensively (Adam 2002). Coastal areas are also increasingly exposed to changes in freshwater runoff quality and regime, resulting from mining, forestry, and agriculture and urbanization activities and practices. High nutrient loads in large rivers have caused the largely hypoxic conditions now observed in many estuaries and extending to large areas in the coastal zone and beyond (Rabalais et al. 2002). Climate change, associated with sea level rise and increased storm frequency and intensity, will also take its toll on coastal wetland habitats known to be of great importance to critical life stages of many marine species (Scavia et al. 2002).

Environmental organizations strive to foster the sound practices required to preserve the so-called ecosystem services (Costanza et al. 1997), i.e., the capacity of marine ecosystems to contribute to our well-being. Environmental managers have to reconcile this view with the day-to-day need to make decisions about projects of all kinds. For Canada's oceans, different tools are considered: marine protected areas (MPAs), conservation objectives for ecologically and biologically significant areas (EBSAs), and integrated management within large ocean management areas (LOMAs) (Ricketts and Harrison 2007). Other considerations include environmental risk assessment and critical habitat of species at risk. The estuary and Gulf of St. Lawrence is one of the five priority LOMAs selected for the implementation of the integrated management framework. Ten EBSAs (Savenkoff et al. 2007) and five areas of interest for MPAs have been identified within the estuary and Gulf of St. Lawrence.

Whether considering potential MPA or EBSA networks, or making decisions as to the relative importance of an area based on its uniqueness or value towards sustaining a significant production, managers are greatly assisted by the availability of a habitat inventory and classification. An atlas of North American coastal and oceanic ecoregions has been published describing 24 different ecoregions (Wilkinson et al. 2009). Within that framework, the estuary and Gulf of St. Lawrence is part of the Acadian-Atlantic ecoregion (no. 7) and is divided into two geomorphological regions, the Acadian Shelf sub-region (7.2) and the Laurentian/Esquiman Channel sub-region (7.4). Within sub-region 7.2, three coastal areas were defined (neritic areas excluding the channels): the St. Lawrence estuary including the part of the Gulf west of Anticosti Island (7.2.1, St. Lawrence Estuarine Area), the northern Gulf (7.2.2, North Gulf Neritic), and the southern Gulf (7.2.3, Magdalen Shallows). More recently and using a grid made of 100 km^2 cells, a hierarchical classification of the seabed was proposed for the estuary and Gulf of St. Lawrence (Dutil et al. 2011). Thirteen different megahabitats were identified based on physiographic and oceanographic features, four of them located in deep water. The more shallow-water habitats appeared to differ between the northern (5 megahabitats) and southern (4 megahabitats) Gulf. A dataset was created that allows mapping habitat diversity and characteristics and, most importantly, allows spatial analyses based on habitat characteristics as well as species, assemblages, fishing, or other human activities.

In the estuary and Gulf of St. Lawrence, previous efforts considered a large number of potential EBSAs and, based on expert opinion, identified ten areas of greatest importance (Savenkoff et al. 2007). Relative importance was assessed by the degree of overlap between different layers of information, with each layer being assigned a score reflecting its classification under a set of pre-defined criteria. For instance, Chabot et al. (2007) examined the distribution and abundance of 44 different invertebrate species observed in annual bottom trawl surveys and identified 17 potential EBSAs for the area considered. While the workshops were successful at identifying EBSAs, no database was created that integrated all the physical, chemical, and biological characteristics of the habitats. The spatial boundaries of the EBSAs could not be precisely determined, and experts focused on midshore and offshore resources (roughly areas deeper than 30 m), given data availability and criteria selected. Thus coastal areas received little attention. Furthermore, in contrast to other studies designed so as to specifically address the coastal habitats (Gromack et al. 2010), the megahabitat database provided by Dutil et al. (2011) used a scale inappropriate for classifying habitats in the coastal zone.

The present report uses a finer scale (6.25 km^2 cells) and more descriptors of landscape, hydrographic and oceanographic processes to describe the coastal and pelagic habitats of the St. Lawrence down to a depth of 30 m. This information can be used for mapping purposes (individual variables or combinations of variables) and for analyses of species-habitat relationships. The dataset may also provide a classification of coastal, midshore and offshore megahabitats of the surface layer in the St. Lawrence whether for conservation, integrated management, or species-at-risk recovery planning purposes.

MATERIALS AND METHODS

For a description and exhaustive list of variables used in this report, refer to Appendices 1 and 2 .

SPATIAL REFERENCE SYSTEM

Dutil et al. (2011) described and classified the benthic habitats of the estuary and Gulf of St. Lawrence. The description and classification unit was a 100 km^2 square cell (10 km x 10 km) whose designation referred to a rectangular grid. The grid was made of equal-sized 100 km^2 cells with each cell being designated by column number from left to right (n=115) and row number from top to bottom (n=85). In the present study, which included the middle and lower estuary, excluding the Saguenay Fjord, and the northern and southern Gulf east up to Cabot Strait and the Strait of Belle Isle (Figure 1), the 100 km^2 cells were sub-divided into 16 smaller square cells of 6.25 km^2 (2.5 km x 2.5 km). Smaller cells were designated by column and row number of the original grid supplemented with a letter suffix ranging from a to p, increasing through the alphabet column-wise and then row-wise (Figure 2). To minimize distortion, the grid was projected using a Lambert conformal conic projection (NAD 1983 Quebec Lambert, false easting: 0.00000000, false northing: 0.00000000, central meridian: -68.50000000, standard parallel 1: 46.00000000, standard parallel 2: 60.00000000, latitude of origin: 44.00000000). Distance and planimetric areas (*areas* herein) of cell features are thus marginally underestimated northward by roughly 1% north of Anticosti Island and 2% at the northern tip of the study area (Strait of Belle Isle). Mapping and spatial analyses were done using ESRI ArcGIS version 10.0, ArcMap

version 10.0 Service Pack 3 (ArcView and ArcEditor, Build 3600) with the Spatial Analyst extension, and Geo Wizards Version 10.1 (Built 18 Jan 2012) software.

Each cell was classified as being marine, intertidal, or terrestrial using the high and low tide marks (Figure 2). Those marks were determined using NRCan CANVEC topographic map products[1] (1:50,000; downloaded in January 2009), considering their universal coverage at a large scale. The high tide mark was determined as the limit between the land and water layers. The low tide mark (0 m depth) was determined as the lower limit of the tidal zone in areas with a tidal zone, and as the limit between the land and water layers elsewhere. In the case of estuaries, the inner boundary was set as the approximate limit of salt penetration (Cairns et al. 2012). When this limit was unknown, it was estimated based on two criteria, the location of the upstream limit of the tidal zone and a marked narrow passage of the river above the tidal zone (Figure 2). These criteria may not correspond to the exact limit of salt penetration into the estuaries, but this was not considered to bias other cell features to any significant degree, particularly in small rivers. Terrestrial cells (cells located outside the high tide mark) were removed from further analyses. The area of the tidal zone (TIDAL_A) within each remaining cell was calculated as the area of the cell between the low tide mark and the high tide mark. This is based on the non-permanency feature of the NRCan CANVEC map products and thus it excludes the area of tidal pools. The area of the non-tidal zone within each cell (NONTIDAL_A) was calculated as the total area of the cell minus the area of the tidal zone and minus the area of land (mainland and islands). In the present report, some of the major islands were considered as part of the mainland: Miscou, Anticosti, Cape Breton, Iles-de-la-Madeleine, Newfoundland, and Prince Edward Island. Areas are in square kilometers unless otherwise specified.

A total of 39,337 cells, referred to as *marine cells* herein, were located partly or entirely below the low tide mark and thus include both cells with and cells without an intertidal zone. Their physiographic and oceanographic features were compiled as a table in the spatial database (Microsoft Access® database Table *Habitat_descriptors_of_marine_cells*) for the purpose of mapping coastal and pelagic habitats of surface waters (0–30 m). In that table, the fields OBJECTID[2] and SHAPE were generated by ArcGIS. OBJECTID is a unique ID field for each entry (each cell in the grid) in the database. SHAPE designates the data type (Geometry-Polygon). Variable COL_ROW designates the large cells address (e.g., 36-59), and variable CELL_ID designates the small cells address (e.g., 36-59-a); smaller cells are referred to as *cells* herein. LATITUDE and LONGITUDE refer to the position of the cell centroid. Habitat descriptors for these 39,337 marine cells are described below and are listed in Appendices 1 and 2 with a short description. Cells located entirely above the low tide mark (370 cells), i.e., cells with TIDAL_A>0 and NONTIDAL_A=0, are listed in a separate table of the dataset (Microsoft Access® database Table *Tidal_area_of_non_marine_cells*), but their physiographic and oceanographic characteristics were not described.

---

[1] (http://www.geogratis.ca/geogratis/en/download/topographic.html)

[2] Variable names appear in capital letters throughout.

LANDSCAPE FEATURES

Since the non-tidal zone varies in depth up to a maximum at 527 m, the 0–30 m surface layer may or may not reach the seafloor. The area of the non-tidal zone within each marine cell (NONTIDAL_A) was split into a benthic (BENTHIC_A; size of the area less than 30 m deep) and a pelagic (PELAGIC_A; size of the area more than 30 m deep) zone. This zonation allowed a classification of marine cells into three categories based on two binary variables (BENTHIC_B and PELAGIC_B). *Benthic cells* are those having a BENTHIC_B value of 1 and a PELAGIC_B value of 0. *Pelagic cells* are those having a BENTHIC_B value of 0 and a PELAGIC_B value of 1.The third category is made of marine cells having both BENTHIC_B and PELAGIC_B values of 1. This classification scheme is shown diagrammatically in Figure 3.

Ecotone effects may be expected to occur at the interface between land and water because there is a marked transition in the ecology characteristics of those two environments. Shore complexity was described using two variables. The length of the coastline (LCOAST) was determined by the low tide mark (mainland and islands). The distance to the coastline (DCOAST) was determined as the distance between the cell centroid and the coastline (km) as determined by the low tide mark (mainland only). Sinuosity (SCOAST_P) was determined as the ratio of the length of the coastline (mainland only), as determined by the low tide mark, and the corresponding straight-line distance. Topographic complexity was further described by insulosity (INSULOSI_P and INSULOSI_F). INSULOSI_P was determined as a ratio of two areas: (1) the sum area of islands, tidal zones associated with islands, and patches of tidal zones forming islands at low tide (i.e., mainland and contiguous tidal zones were excluded), and (2) the sum area of non-tidal zones, islands, tidal zones associated with islands, and patches of tidal zones forming islands at low tide. INSULOSI_F was taken as the total number of discrete landscape features emerged at low tide, i.e., islands with associated tidal zone and patches of tidal zones forming islands at low tide.

The degree of protection from the open sea was determined as described in Cairns et al. (2012) and ICES (2009) and was expressed as a percentage of the non-tidal zone area falling into the sheltered (SHELTERE_P), semi-exposed (SEMIEXPO_P), or exposed (EXPOSED_P) category. RISK1_C and RISK2 are based on a sensitivity index proposed by Shaw et al. (1998). The index measures the risk of erosion of the coast as a result of sea-level rise. We were unable to obtain the source data (seven variables) or the index values, so the index categories shown on the map in Shaw et al. (1998) were used (low, moderate, and high vulnerability). RISK1_C reports the dominant index category within the cell whereas RISK2 measures the distance between the cell centroid and the nearest high-sensitivity coastal segment (most sensitive to sea-level rise; index values > 15.0). RISK1_C was not available for islands (see above).

The depths correspond to the height of the water column at low tide. Bathymetric data were obtained from the Canadian Hydrographic Service. The number of depth observations available per cell varied considerably depending on depth and sounding technology, from a few observations in the worst cases (deep channels) to thousands of observations with multibeam acoustic surveys. Near shore, the digital data available were supplemented by digitizing depth observations from nautical charts at the finest

scale available for the area considered. Those data were submitted to spatial interpolation (natural neighbour method, 20 m distance interval). Maximum cell depth (CELLDEPTH), and depth and slope characteristics of the portion of the seafloor less than 30 m deep were obtained from interpolated values: mean depth (DEPTHMEAN), minimum (DEPTHMIN) and maximum depth (DEPTHMAX), standard deviation of depth (DEPTHSTD), mean slope (SLOPEMEAN), minimum (SLOPEMIN) and maximum slope (SLOPEMAX), and standard deviation of slope (SLOPESTD). The slope was calculated as the maximum difference in elevation between adjacent raster cells divided by the horizontal distance between the raster nodes. Mean, minimum, maximum, and standard deviation of slope were set to 0.0 for strictly pelagic cells (BENTHIC_B=0 and PELAGIC_B=1). For cells classified as BENTHIC_B=1 and with a very small value for BENTHIC_A (ca. 520 cells), CELLDEPTH as well as depth and slope characteristics of the portion of the seafloor less than 30 m deep are reported as being 0 or close to 0. This should be interpreted as resulting from two situations: (1) cell and non-tidal areas barely overlapped; (2) cell and non-tidal areas overlapped in bays and river estuaries with no data for depth. In both situations, CELLDEPTH and depth and slope characteristics were obtained only from the low tide mark (0 m observations).

SATELLITE IMAGERY

The sea surface temperature (SST) data were obtained from the National Oceanic and Atmospheric Administration (NOAA). The raw data were derived from satellite imagery, using the advanced very high resolution radiometer (AVHRR) technology, and processed using the Terascan® software to detect clouds and project the results on a georeferenced grid of 1 km resolution. While SST data are available from 1985, weekly average temperatures at each grid node were calculated for the period 1994–2010 because the period 1985–1993 was characterized by a cool anomaly (Galbraith et al. 2012). From January to March, ice conditions are such that few or no observations were available over large areas. Missing data were estimated through spatial interpolation of average temperatures for the period 1994–2010 (natural neighbour method). The following parameters were determined: maximum weekly temperature reached (SSTMAX); number of weeks with temperature below 2°C (SSTWKS1_F), between 2 and 6°C (SSTWKS2_F), between 6 and 10°C (SSTWKS3_F), between 10 and 14°C (SSTWKS4_F), between 14 and 18°C (SSTWKS5_F), and above 18°C (SSTWKS6_F); consecutive weeks with temperature below 6°C from January 1 (SSTMARK1_F), below 10°C from January 1 (SSTMARK2_F), and below 14°C from January 1 (SSTMARK3_F); surface temperature at week 21 (week beginning May 20, SSTWK21), surface temperature at week 30 (week beginning July 22, SSTWK30); number of degree-days above 2°C from week 21 to week 30 (SSTDD1) and from week 31 to week 40 (week beginning September 30) (SSTDD2). Since surface temperatures at each grid node are calculated based on years when no ice interfered, average temperatures for the 1994–2010 period may be representative of milder winter conditions, but the above-mentioned parameters would not be affected.

Ice cover data were obtained from the Canadian Ice Service (Environment Canada). Five parameters were used to describe the timing and extent of ice conditions based on 14 years of record (5 km grid): the first and last day of the year when ice thickness was greater than 5 cm (ICEBEG and ICEEND), and duration of the ice period as number of days when ice thickness was greater than 5 cm (ICEDUR_F).

ICERECUR_F indicates the number of years when ice thickness reached the 5 cm mark (maximum 14 years) and ICETHICK the maximal ice thickness averaged over years.

Turbidity data were downloaded from the National Aeronautics and Space Administration (NASA) as obtained using a moderate resolution imaging spectroradiometer (MODIS) on the AQUA satellite. Values are based on point estimates (4 km grid) of the diffuse attenuation coefficient of seawater at 490 nm (m^{-1}) for the 2002–2011 period. Higher values indicate greater turbidity, i.e., a stronger attenuation of light. The following parameters were determined, based on monthly mean values: mean annual turbidity (TURBIDMEAN), minimum and maximum monthly turbidity (TURBIDMIN and TURBIDMAX), and mean turbidity for each season: TURBIDWR (January to March), TURBIDSG (April to June), TURBIDSR (July to September), and TURBIDFL (October to December). A summary of variables obtained from remote sensing observations is given in Appendix 3.

3D CIRCULATION MODEL

A 3D circulation model was used to characterize salinity, temperature, and currents in the upper 30 m layer. The NEMO-OPA model was applied to the Gulf of St. Lawrence, Scotian Shelf, and Gulf of Maine for hindcast studies (Brickman and Drozdowski 2012). The actual code was based on the OPA 9.0 version (Madec 2008). The model used a 1/12° (~6–8 km) grid and calculated values for different parameters in the whole water column. It is a prognostic model, meaning that the salinity and temperature fields are free to evolve with time and are only constrained through boundary conditions, freshwater runoff (78 main rivers), and surface forcing. The tides are included in the model through surface elevation at the open boundaries. The model has internal and external mode splitting and the time step is 480 s for the internal mode (baroclinic) and 8 s for the external mode (barotropic). For the purpose of our database, daily averages were generated in five depth layers and over an annual cycle. For salinity, temperature, and vertical and horizontal currents, daily values were obtained for the 2006–2010 period. Five depth layers were used: 3.1 m (0.0–6.2), 9.5 m (6.2–12.8), 16.4 m (12.8–20.0), 23.9 m (20.0–27.9), and 32.2 m (27.9–36.7).

The mean annual salinity as well as the minimum and maximum mean monthly salinity values are reported for the surface layer (SSALMEAN, SSALMIN, SSALMAX) and for the bottom layer (BSALMEAN, BSALMIN, BSALMAX) as follows: for benthic cells (BENTHIC_B=1), salinity values were obtained from the layer with the median depth value closest to the value for DEPTHMEAN, whereas for non-benthic cells (BENTHIC_B=0) salinity values were obtained from layer 5. Freshwater runoff influence was assessed relative to the maximum salinity of seawater and calculated as 1-(MSAL/35), where MSAL is the average salinity of the water column from the surface down to the bottom (maximum 36.7 m, as described above). Thus it varies from 0 to 1, with values close to 0 indicating no influence. The value is reported for each season: FWRINFSG (April to June), FWRINFSR (July to September), FWRINFFL (October to December), and FWRINFWR (January to March). The distance between each cell and the nearest model prediction value on the grid and for the same layer are reported for SSALMEAN, SSALMIN, and SSALMAX (variable SDIST3D), and BSALMEAN, BSALMIN, and BSALMAX (BDIST3D1). That distance may be greater than 6 km in

nearshore and estuarine areas, and hence SDIST3D and BDIST3D1 can be used to screen out cells that were out of the range of the model.

The same approach was used to obtain the mean annual and minimum and maximum mean monthly temperature (STEMMEAN, STEMMIN, STEMMAX, BTEMMEAN, BTEMMIN, and BTEMMAX), vertical current velocity (SVCURMEAN, SVCURMIN, SVCURMAX, BVCURMEAN, BVCURMIN, and BVCURMAX), and horizontal current velocity (SHCURMEAN, SHCURMIN, SHCURMAX, BHCURMEAN, BHCURMIN, and BHCURMAX). Horizontal current velocity does not include the tidal currents, which are reported separately. The mean seasonal temperature for the bottom of the 0–30 m layer is also given for each of the four seasons: BTEMWIN (January to March), BTEMSPR (April to June), BTEMSUM (July to September), and BTEMFAL (October to December). For vertical currents, negative values indicate descending currents and positive values ascending currents. Vertical currents were assessed between depth layers, and the top of the layer (as opposed to the median depth) was used as the reference depth. Thus the distance between each cell and the nearest model prediction value on the grid for the bottom of the 0–30 m layer may differ for vertical currents (BDIST3D2) compared to other parameters (BDIST3D1). The direction of the surface horizontal current (SHCURDIR_C) and bottom layer horizontal current (BHCURDIR_C) at DEPTHMEAN were calculated in degrees (0–360 clockwise, true north being 0°), and coded into eight categories of 45 degrees each, code 1 (north) including angles from 337.5 to 360 degrees and from 0 to 22.5 degrees, code 2 angles from 22.5 to 67.5 degrees, and so on.

Tidal range, tidal currents, and water column stability were determined from model predictions for a 50 d period (17 October to 5 December, 2007). The Simpson-Hunter water column stability parameter was determined using the predicted horizontal currents determined hourly. Values <1 indicate strong mixing, values around 1.5 indicate transitional zones, and higher values (> 2) indicate a stratified water column. The mean (SIHUMEAN), minimum (SIHUMIN), and maximum (SIHUMAX) value of the running average for 50 h periods (four tidal cycles) is reported. The tidal current (TIDECUR) was calculated based on the amplitude of the M2 tidal component. Tidal amplitude has been multiplied by 2 to yield three parameters: maximum tidal range (TIDEMAX), the maximum sum value of the main five tidal components; mean tidal range of the semi-diurnal high tide (TIDESDH), estimated as the sum of the M2 (or S2 where the S2 component had the greatest amplitude) and O1 components; mean tidal range of the semi-diurnal low tide (TIDESDL), estimated as the difference between the M2 (or S2 where the S2 component has the greatest amplitude) and O1 components. The winds are used to force the 3D ocean model, and they are provided by Environment Canada (Canadian Meteorological Centre) from the nowcasts of their forecasting system. Wind statistics could therefore be derived. Mean annual wind speed (WINDMEAN), minimum and maximum monthly wind speed (WINDMIN and WINDMAX), and mean annual wind direction WINDDIR_C are provided. WINDIR_C was coded into eight categories of 45 degrees each, as previously described. A summary of variables obtained from the 3D circulation model is given in Appendix 3.

SHORELINE CLASSIFICATION AND PRE-SPILL DATABASES

Environment Canada (Quebec and Atlantic regions) provided us access to the two regions' Shoreline Classification and Pre-spill (SCP) databases. These databases are used by several agencies to obtain information on pre-spill conditions and to provide SCAT (Shoreline Cleanup Assessment Technique) teams with timely information on access and response issues should marine oil spill emergency situations occur. A web-based GIS Management System is used to access data on shoreline segmentation, backshore and intertidal zone form and substrate, and shoreline habitat classification. That information was summarized and added to the present database using nine variables. SEGMENTID and SEGMENTLBL refer to variables Segment_ID and Segment_label, respectively, in the SCP database. This is meant to enhance interoperability between the two databases. Each cell in the study area was assigned the Segment_ID and Segment_label values of the nearest segment on the shoreline as determined based on the distance from the cell boundary to the shoreline segment. That distance is reported as variable SEGMENTDIS; a value of "0" indicates that the shoreline segment is partially or entirely enclosed within the cell boundary. Shoreline morphology (SHORMOR_C) and shoreline material (SHORMAT_C) refer to the lower intertidal form and the main substrate type in the lower intertidal zone, respectively, in the SCP web-based application. Four other descriptors report the distance between the cell and the nearest sand beach (SANDBEACH), mud flat (MUDFLAT), and anthropogenic structure and material (MANMADE) on the shoreline, as well as the nearest salt marsh (MARSH) on the shoreline and in the backshore area.

OTHER PARAMETERS

Other features of the coast and watersheds, were used as criteria for the habitat classification when they were considered relevant to processes occurring in the 0–30 m layer. The accessibility to tidal areas (TACCESS_A) was calculated as the sum of TIDAL_A values for the cell and its adjacent neighbours (maximum eight neighbours). Neighbouring cells located entirely above the low tide mark (TIDAL_A>0 and NONTIDAL_A=0) were not described or classified as part of the present report (see above), but the surface area of the tidal zone in those cells was included in the calculation of TACCESS_A.

Bottom type was determined using a map describing surface sediments and outcrops at a broad scale (Loring and Nota 1973). Cells were assigned the sediment (SEDIMENT_C) and outcrop (OUTCROP_C) code values for the corresponding zone on the map, as described in Dutil et al. (2011). Loring and Nota's (1973) work did not include the nearshore shallow areas along the coast. When a centroid was located outside of the area covered by the map, cells were assigned the sediment and outcrop code values of the nearest adjacent zone. The distance between the cell centroid and the nearest zone was determined (LORNOTDIST). English and French descriptions for sediment (SEDIMENTF, SEDIMENTE) and outcrop (OUTCROPF, OUTCROPE) codes are provided.

Eelgrass beds are an important habitat for juvenile stages of many fish species, but information on their location and spatial extent varies between regions. Their occurrence was described in a single binary variable (ZOSTERA_B) that indicated whether an eelgrass bed is known to occur within 10 km of the cell centroid (ZOSTERA_B set to 1) or not (ZOSTERA_B set to 0). Data were obtained from various

sources. Data for the west coast of Newfoundland were obtained from Anuradha S. Rao (Gordon Global Fellow, unpublished data), Robert Gregory, and Conrad Mullins (Fisheries and Oceans Canada, Newfoundland and Labrador region, unpublished data). Data for the St. Lawrence estuary and northern Gulf were obtained from Martel et al. (2009) and those for the southern Gulf were obtained from the Maritimes Wetland Inventory (Karel Allard, Environment Canada, unpublished data).

Linkages between the freshwater and marine environments were established as follows. Marine cells were identified that overlapped the low tide mark at the point of entry of a stream or river having a drainage area larger than 70 km^2 (excluding the St. Lawrence main stem). For these cells, variable FWINPUT was coded with the CELL_ID value and FWDIST was set to 0. For the other cells, FWINPUT was coded with the CELL_ID value of the nearest cell identified as a point of entry of a stream or river, and FWINPUT was set as the calculated distance between the cell centroid (km) and the nearest cell identified as a point of entry of a stream or river. FWDRAIN is the drainage area (km^2) and FWFLOW is the mean annual flow (m^3/sec) of the stream or river adjacent to FWINPUT. The mean annual flow was obtained from various sources and when not available was estimated from drainage area following methods described by Caissie and Robichaud (2009). Drainage area was estimated based on NRCan CANVEC topographic map products (1:50,000) or obtained from unpublished material (Daniel Caissie, DFO Gulf region, unpublished data; G. Chaput, H. Bowlby, C. Breau, D. Cairns, P. Cameron, M. Dionne, J. Gibson, R. Jones, and D. Reddin. Atlantic Salmon Rivers Database from Eastern Canada, unpublished manuscript, 15 January 2011 version).

In the database, missing values were coded -9999 (both numerical and alphanumerical variables); null data were coded -8888 (both numerical and alphanumerical variables) and refer to cases for which no data can be provided (irrelevant cases by definition).

The category of benthic habitat for the corresponding 100 km^2 cell (Dutil et al. 2011) was included in the database for convenience.

STATISTICAL ANALYSES

A total of 103 variables out of 128 variables available in the dataset were used in the cluster analyses. The following variables were excluded: OBJECTID, SHAPE, COL_ROW, CELL_ID, LATITUDE, LONGITUDE, SDIST3D, BDIST3D1, BDIST3D2, SEGMENTID, SEGMENTLBL, SEGMENTDIS, SHORMOR_C, SHORMAT_C, MANMADE, FWINPUT, SEDIMENTF, SEDIMENTE, OUTCROPF, OUTCROPE, LORNOTDIST, and MEGAHABITA. SCOAST_P and RISK1_C were excluded as well because most cells had null values for those descriptors. ZOSTERA_B was included in the database for convenience, but it was not used in the classification because it was considered as a biological descriptor. SEDIMENT_C and OUTCROP_C were the only non-numeric variables left and had null values for cells with the BENTHIC_B value set to 0. They were transformed into numeric variables as follows: Loring and Nota's (1973) used alphanumeric codes for describing soft sediments (e.g., 1a, 2b-2c), with the dominant category listed first and smaller number and letters indicating finer sediments. Using the dominant category only, SEDIMENT_C was transformed into a two-digit numeric variable with the first digit referring to the numeric code and the second digit referring to the letter code (for instance, 11 and 22 for 1a and 2b-2c, respectively). OUTCROP_C was transformed into

a binary variable (0= no outcrop, category R0; 1= with outcrop, categories R1, R2, R3). For non-benthic cells (BENTHIC_B=0), SEDIMENT_C and OUTCROP_C were set to 0. Variables with null or missing data are listed in Appendix 4.

Cluster analyses were performed with SAS software (version 9.3). The 103 variables used in the analysis were normalized (SAS procedure DISTANCE). Interval (INSULOSI_P, SHELTERE_P, SEMIEXPO_P, EXPOSED_P, SSTMAX, SSTWK21, SSTWK30, TURBIDMEAN, TURBIDMIN, TURBIDMAX, TURBIDWR, TURBIDSG, TURBIDSR, TURBIDFL, STEMMEAN, STEMMIN, STEMMAX, BTEMMEAN, BTEMMIN, BTEMMAX, BTEMWIN, BTEMSPR, BTEMSUM, BTEMFAL, SIHUMEAN, SIHUMIN, and SIHUMAX) and ordinal (SEDIMENT_C) variables were standardized by the range method, and ratio variables (all other variables except nominal variables BENTHIC_B, PELAGIC_B, SHCURDIR_C, BHCURDIR_C, WINDDIR_C, and OUTCROP_C) by the maximum absolute value method. Before standardization, vertical current values were transformed into absolute values, i.e., vertical current direction was not factored in the analysis, and a constant value of 11 was added to ICEBEG to make all values positive. Missing values were replaced by the mean value for the parameter (data on turbidity). No variable was weighted prior to the analysis.

Five different cluster analyses were conducted. First, a direct analysis was done using the CLUSTER procedure and normalized data for the 103 variables and 39,337 cells (method 1). Clusters were determined based on the group average method. The four other analyses used the FASTCLUS procedure. FASTCLUS performs a disjoint (i.e., non-hierarchical) cluster analysis based on Euclidean distances. Outliers (clusters of less than 30 cells) were detected and reassigned to the remaining clusters. The output from this analysis was analyzed with the CLUSTER procedure (method 2: unweighted pair-group averages; method 3: unweighted pair-group centroids) to determine the hierarchy among clusters and, indirectly, among the 39,337 cells. Alternate classifications were examined based on the same dataset and a reduced number of variables. The VARCLUS procedure was used to cluster the 103 variables (standardized values). Within each cluster of variables, one or two variables were selected that had a high squared correlation with the principal component of the cluster and a low correlation with the nearest cluster. The normalized data were scored using the principal components scoring coefficients. The procedure described above (FASTCLUS followed by CLUSTER) was applied to the selected variables (method 4) and to the principal component scores (method 5).

RESULTS

Marine cells represented a total planimetric area of 232,583 km^2 of marine environment and included both cells with (3,232) and cells without (36,105) an intertidal zone (2,001 km^2 tidal and 230,582 km^2 non-tidal) (Table 1). The tidal zone area of the 370 cells with a non-tidal zone area of 0 totaled 208 km^2. Based on NRCan CANVEC topographic map products (1:50,000), the coastline at low tide has a total length of roughly 14,000 km.

Considering the incentive for this study, which was to map and describe the coastal zone and more specifically the 0–30 m layer in areas less than 30 m deep, the coastal zone was implicitly defined as being made of benthic cells (BENTHIC_B=1), i.e., marine cells with part of the bottom less than 30 m

deep. Depths less than 30 m represented a total planimetric area of 32,092 km² and occurred in 9389 marine cells (Table 1). Benthic cells occupied a wide fringe along the coast of New Brunswick, Prince Edward Island and the Îles-de-la-Madeleine. They also occupied much of the St. Lawrence middle estuary and a narrower fringe along the lower North Shore area (Figure 4). The southern Gulf was characterized by a greater share of strictly benthic cells (BENTHIC_B=1 and PELAGIC_B=0): 68% in frequency and 78% in benthic area, representing 54% of the length of the coastline for that category of marine cells in the study area. Benthic cells adjacent to deeper waters (BENTHIC_B=1 and PELAGIC_B=1) were most frequent (56%) and represented a greater proportion of the benthic area (50%) in the northern Gulf. They added up to 88% of the length of the coastline for that category of marine cells in the study area. These cells also offered more shelters in the northern than in the southern Gulf, consistent with a greater insulosity in the northern than in the southern Gulf. These proportions are affected in part by an arbitrary and uneven division of the northern and southern Gulf (23,105 and 14,236 marine cells, respectively; 137,514 and 82,194 km² of non-tidal zone area, respectively) and by the fact that the estuary (the portion included in the study) is much smaller than the Gulf (1996 marine cells, NONTIDAL_A sums up to 10,874 km²). Based on interpolated depths, a 30 m isobath forming a continuous line bordering the mainland was drawn; mainland included Miscou, Anticosti, Cape Breton, Iles-de-la-Madeleine, Newfoundland, and Prince Edward Island. The distance from the low tide mark to the 30 m isobath averaged 2.1 km and reached a maximum value 26.8 km in the Miscou area.

MAPPING INDIVIDUAL VARIABLES

Though the main purpose of this report was to provide a dataset for exploring species-habitat relationships and identifying key areas, it can also be used to map landscape and oceanographic features of the study area individually. This subsection shows several examples of how the database can be used to provide distributional data for the study area or parts thereof.

Potential ecotone effects at the low tide mark, i.e., between the marine environment below the low tide mark and the land and tidal areas above, are more likely to occur in areas where the shoreline is complex. This is exemplified for the northeastern part of the Gulf, where the length of coastline within cells is greater along the Quebec's North Shore than along the west coast of Newfoundland (Figure 5). This is consistent with high values for sinuosity (Figure 6) and insulosity (Figure 7) along the Quebec's North Shore. Cell depth varies of course, but there was also great spatial variability in the depth and slope data for the 0–30 m layer. The flat landscape around Prince Edward Island and along the New Brunswick east coast resulted in a more abrupt transition from the tidal area to the pelagic environment north of the Gaspé Peninsula and west of Cape Breton as well as on the west coast of Newfoundland (Figure 8). However, the large band of benthic cells along the New Brunswick east coast consisted of a more uniform terrain with low intracell variability in seafloor depth (Figure 9), and more gentle slopes (Figure 10), but not necessarily a greater access to large tidal areas (Figure 11). This may reflect the combined effect of landscape and tidal range (Figure 12).

To describe the thermal environment prevailing at the surface, both model prediction and satellite observation data are provided. Daily predictions from the 3D model can be used to map the

temperature conditions at the surface and on the bottom (<30 m). Minimum and maximum mean monthly temperatures are shown in Figures 13 and 14. Satellite-derived sea surface temperature observations are provided as metrics to assess the productivity of different areas considering the needs of specific organisms. For instance, the potential rate of mortality and rate of embryonic development of fish eggs released at the surface might be assessed for different areas using these metrics, provided that the thermal requirements of the target species are known. Five of the variables based on satellite observations of sea surface temperature are presented, showing the great variability in climate conditions across the study area. The number of weeks with temperature below 2°C is greatest in the Strait of Belle Isle and along the lower North Shore, with cold conditions prevailing for more than 20 weeks in the northern Gulf in general (Figure 15). Whereas temperatures in the 6–10°C range (Figure 16) occur over a period of more than 10 weeks in the estuary and large portions of the North Shore, particularly around the Mingan Island (Havre-Saint-Pierre area), those conditions are only transitory in the southern Gulf, where temperatures in the 14–18°C range (Figure 17) occur more frequently than temperatures in the 6–10°C range. This is consistent with the sum value of degree-days above 2°C for August and September, which is three times higher in the Northumberland Strait area than in the lower estuary and along the North Shore (Figure 18). In contrast, surface temperatures at the end of May (week 21) in the St. Lawrence estuary (Figure 19) are similar to those prevailing in the southern Gulf and above those observed in the northern Gulf due to a strong influence of freshwater runoff from the St. Lawrence estuary in the spring (Figures 20 and 21). The southern half of the west coast of Newfoundland is least affected by freshwater runoff, as indicated by the low values of the four seasonal variables FWINFWR (Figure 22), FWINFSG (Figure 23), FWINFSR (Figure 24), and FWINFFL (Figure 25). Turbidity is also lowest in that area (Figure 26 and 27), and ice formation is delayed until late February (Figure 28) and occurs only sporadically (Figure 29).

Circulation patterns of the 0–30 m layer are shown for the top 6.2 m layer (Figure 30) and the bottom of the 30 m layer (Figure 31). The actual depth of the latter varies depending on the DEPTHMEAN value, i.e., it is shallower in shallow benthic cells. Not surprisingly, there is actually little difference in current direction between the surface and the bottom of the 0–30 m layer. Mean current velocity patterns are also similar between the surface (Figure 32) and the bottom (Figure 33) of the 0–30 m layer. The highest values for minimum surface current velocities (>0.10 m/s) are observed in the estuary, along the Gaspé Peninsula, around Cabot Strait, and west of Belle Isle Strait up to Havre-Saint-Pierre (Figure 34). The highest values for maximum surface current velocities (>0.21 and up to 1.74 m/s) are observed in roughly the same areas, with the exception of the estuary (Figure 35). The strongest currents are shown as beige/brown shades in these figures. The strongest tidal currents (> 8 cm/s) occur in many areas, at the straits and at the head of the main channels (Figure 36) as well as in areas characterized by high mean annual wind speeds (Figure 37). There is little variability in wind direction over the study area (not shown). Finally, mean values of the Simpson-Hunter parameter (stratification) indicate areas where oceanic fronts were mostly to occur in the period examined (mid-October to early-December); they show up as areas with contrasted values (Figure 38).

MAPPING USING A SET OF CRITERIA

For very specific purposes, several features can be selected and a subset of marine cells identified that correspond to a set of criteria, either for descriptive purposes or to obtain a habitat classification (see the next section). Below we give a few examples.

A breakdown of benthic areas less than 10 m deep by depth and exposure categories is shown in Figure 39. The figure was actually drawn from Cairns et al. (2012) in which the potential American eel brackish and saltwater habitat, defined as sheltered areas and shallow depths in coastal areas, was quantified for eastern Canadian waters. This output might be combined, for instance, with sea surface temperature metrics to assess the potential growth habitat for eel.

Based on the SCP web-based application (Environment Canada), the distance from each cell to the nearest sand beach, salt marsh, or mud flat was determined. Figure 40 shows marine cells located within 50 km of all three shoreline types. The light blue patches can be interpreted as shoreline areas suitable for spawning and as a nursery for larval and juvenile stages of various species, including sticklebacks, capelin (*Mallotus villosus*), Atlantic tomcod (*Microgadus tomcod*) and rainbow smelt (*Osmerus mordax*) (see for instance Dutil and Fortin 1983). The superimposed deep blue patches indicate known occurrences of nearby eelgrass beds in the study area. Eelgrass beds are also an important habitat for juvenile stages of several fish species (Grant and Provencher 2007).

When a portion of the non-tidal zone was more than 30 m deep, marine cells were classified as being pelagic. A large proportion of those cells were defined as being exposed (variable EXPOSED_P), but they may also differ in their degree of turbulence (Figure 41). Pelagic cells exhibiting low stratification (SIHUMEAN < 4.5) and mean tidal currents > 7 cm/s were broken down by mean annual turbidity, showing that dynamic areas differ markedly based on annual turbidity.

The next two figures classify marine cells into brackish and more saline environments (Figure 42) and into arctic and temperate environments (Figure 43). In Figure 42, blue areas indicate more saline waters (13,314 km^2), while beige (50,854 km^2) and brown (2,183 km^2) areas show cells more affected by freshwater runoff. In Figure 43, blue cells were classified as being arctic (29,204 km^2) and brown cells (42,512 km^2) as being more temperate based on several criteria (ice and temperature). Both categories are broken down by maximum surface temperature.

HABITAT CLASSIFICATION

Results obtained on the full set of data (103 variables) using the FASTCLUS and CLUSTER procedures (unweighted pair-group averages, method 2) were retained. The three criteria used to assess the number of clusters (cubic clustering criterion, pseudo F, and pseudo t^2 statistics) suggested peaks at 3, 6, 9, 16, 22, and 33 clusters. The tree diagram in Figure 44 shows the 16 clusters formed at an average distance of 0.35. The first three principal components explained 59.8, 37.7, and 1.9% of the variance, respectively. Thus the percent variance explained totalled 99.4% for the first three components and dropped below 0.5% for each additional component. Grouping data into three clusters (distance=1.05) explained 71.9% of the variance; grouping data into six (distance=0.75), nine

(distance=0.50) and 16 clusters (distance=0.35) explained 88.5, 95.4, and 97.0% of the variance, respectively.

The number of marine cells per habitat category varied from 144 (cluster OB1, habitat 1) to 10,755 (cluster CL32, habitat 4) with a median value of 1,297 cells. Out of 16 valid clusters suggested by the three criteria, two clusters appeared to be made of scattered cells and were grouped with their nearest neighbour. Cluster OB30 (285 cells) was grouped with cluster CL16 (1,740 cells), and cluster CL22 (187 cells) was grouped with cluster CL18 (3,297 cells), resulting in 14 different clusters considered to represent a classification of the pelagic and coastal habitats in the estuary and Gulf of St. Lawrence:

Habitat category	Cluster ID in Figure 44	Number of cells per habitat category
1	OB1	144
2	CL27	924
3	CL23	1,635
4	CL32	10,755
5	CL17	1,112
6	CL25	683
7	CL20	911
8	CL16, OB30	2,025
9	OB31	2,670
10	CL18, CL22	3,484
11	CL21	7,962
12	CL33	5,076
13	CL39	474
14	CL24	1,482

They are mapped in two separate figures for clarity (Figures 45 and 46).

Habitat categories determined by cluster analysis appeared to exhibit spatial coherence in the study area. Whereas different analyses yielded different sets of clusters, several clusters showed a similar spatial distribution irrespective of the methods used to cluster the data. This is exemplified by comparing Figures 45 and 47 showing the outcome of analyses run with method 2 and method 4, respectively, as described in Materials & Methods. Note in particular the split in Cabot Strait, the southwest–northeast orientation of features along the west coast of Newfoundland, the large cluster formed by cells in the estuary and along the northern Gaspé peninsula, the cluster of cells over Miscou Bank and into Shediac Valley, the distribution of clusters east and west of Anticosti, and so on. Note also the spatially fragmented patches of cells around the Îles-de-la-Madeleine and Prince Edward Island, a feature that all analyses had in common.

Based on Figures 45 and 46, a map of habitat diversity was prepared (Figure 48). Seven habitats were located mostly nearshore and included fewer cells, and seven other habitats formed larger patches of

uniform characteristics mostly in the midshore–offshore area. Coastal areas tended to be more diversified than midshore and offshore areas on a more local scale, and the southern Gulf appeared to harbour more diversified and possibly more fragmented habitats than the northern Gulf. In the estuary, the area extending from the Manicouagan Peninsula to Pointe-des-Monts appeared most diversified. In the northern Gulf, the Mingan Islands, west Anticosti, and the Belle Isle Strait area exhibited a great diversity, but the highest counts were observed in the Cape Saint George area on the west coast of Newfoundland. In the southern Gulf, the tip of the Gaspé Peninsula, Baie des Chaleurs, Îles-de-la-Madeleine, and Northumberland Strait exhibited a great diversity of habitats, with the highest counts observed east of Paspébiac (Baie des Chaleurs) and east of Pictou Island (Northumberland Strait).

DISCUSSION

The dataset prepared as part of this report represents a mixture of descriptors obtained from different sources, and potential trends over time are not accounted for in the database. The data were obtained from different time periods and at different spatial resolutions. For instance, depth was interpolated at 20 m, but the underlying dataset represented a mixture of data obtained using different technologies over a long period of time (decades). Turbidity was obtained from satellite observations made over a 10–year period and was output as a 4 km grid, resulting in very few observations by cell, in contrast to depth data. As a result, our confidence in conditions actually expected to occur in the field varies depending on the variable considered, particularly when considering individual cell values, including its habitat classification. Nevertheless the dataset adequately reflects many large-scale features of landscape and oceanographic processes occurring in the estuary and Gulf of St. Lawrence (Koutitonsky and Bugden 1991), and this might explain why the resulting habitat classification appears to be spatially coherent. Whereas some cells appear to be isolated, in most cases cells form extended patches of uniform habitat categories, thus the habitat classification could be viewed as a schematic representation of habitat categories over a broad scale. Other classification schemes of marine ecosystems have been proposed (reviewed by DFO 2009). The Commission for Environmental Cooperation (U.S.A., Canada, Mexico), classified the marine waters surrounding North America into 24 different Level I marine ecoregions, based on large-scale oceanographic features (Wiken et al. 1996; Wilkinson et al. 2009). One of those, ecoregion 7 (Acadian-Atlantic), included shelf waters from the Strait of Belle Isle (Canada) down to Cape Cod (U.S.A.) and encompassed the estuary and Gulf of St. Lawrence. The classification recognized two Level II geomorphological regions, the Acadian Shelf (ecoregion 7.2) and the Laurentian/Esquiman Channel (ecoregion 7.4), which extends out of the Gulf to slope waters. Ecoregion 7.2 was split into three different coastal regions, the St. Lawrence estuary, including part of the Gulf west of Anticosti Island (7.2.1, St. Lawrence Estuarine Area), and the northern (7.2.2, North Gulf Neritic) and southern (7.2.3, Magdalen Shallows) Gulf, excluding the channels. There are similarities between the classification proposed by Wilkinson et al. (2009) and those proposed in an earlier report for the benthic zone (Dutil et al. 2011) and in the present study for the coastal and epipelagic zone. The latter two reports used a finer scale, produced a dataset to derive the classification from, and also considered the coastal–pelagic and benthic zones separately. Provided these caveats are kept in mind, there are clear advantages in having a comprehensive dataset of habitat descriptors readily available. Managers and practitioners require a more direct access to synthetic

products. Geospatial support tools now facilitate the mapping of individual variables, such as habitat categories, and the mapping of specific zones selected on the basis of multiple criteria. They also allow overlaying that information with layers of information on human activities (stressors) and resources (goods and services), thus enabling risk assessment and decision making. The dataset can be edited as required and expanded to include social aspects as well. From a science perspective, the dataset provides additional power for exploring species–human–habitat relationships.

The coastal zone can be defined in very different ways. The Gulf of St. Lawrence could be argued to be located entirely within a coastal zone defined as the extent of the continental shelf, or a fixed distance band from the coast could be used. Whereas a fixed distance from shore may appear adequate on legal and jurisdictional grounds, other considerations should prevail when attempting to identify areas of greater importance on the basis of biological productivity. The "30 m depth" criterion used to define the coastal zone in the present study was a practical one meant to include all the areas not included in a previous study on midshore–offshores areas (Savenkoff et al. 2007). Shallower depths might be considered, for instance 10 m or 20 m, resulting in a much narrower coastal zone (Figure 8) and fewer cells: 9,417 marine cells overlapped the 30 m isobath layer compared to 7,791 marine cells at 20 m and 6,016 marine cells at 10 m, with the coastal zone limited to a very narrow fringe except in the St. Lawrence estuary and part of the southern Gulf. Other criteria might also be considered to define the seaward extent of the coastal zone. Artioli et al. (2005) defined the coastal zone as "the area that is sensible to the influence of the water discharged by rivers". Sensitivity was assessed through repeated measures at several stations and reported as the area within some value of a dispersion index based on the variance of normalized salinity values. Lessin et al. (2009) suggested using biotic criteria and concluded that gradients of chlorophyll-*a* spatial distribution could be used to determine the extent of the coastal zone. Kratzer and Tett (2009) combined both biotic and abiotic factors and explored the extent of river and terrestrial inputs seaward, looking at the contribution of each optical component to the spectral attenuation coefficient. In a stratified environment with great seasonal variability, however, the seaward extent of coastal processes is likely to vary with depth and through time. Turbidity (MODIS spectroradiometer-based estimate of the diffuse attenuation coefficient of seawater at 490 nm; Figures 26 and 27) might provide an appropriate criterion to define the coastal zone in the St. Lawrence. Under that criterion, the whole estuary, a narrow band in the northern Gulf, and a wide band in the southern Gulf would be considered as part of the coastal zone. Considering the importance of the St. Lawrence River runoff (12,000 m^3/s) relative to other tributaries of the Gulf of St. Lawrence, the area that is influenced by river discharge is largely defined by the input from the St. Lawrence River (Figures 22 to 25), pushing the zone of influence further seaward into the pelagic zone when this single criterion is used.

The main purpose of the present report was to produce a comprehensive dataset of landscape and oceanographic data for the estuary and Gulf of St. Lawrence. This work is an extension of a previous report in which a similar approach was applied to the benthic area at a broader scale (Dutil et al. 2011). The earlier work used fewer descriptors and had weaknesses in the coastal area because variables more specific to the coastal zone, e.g., sinuosity of the coastline and access to the tidal zone, were not available and were not used in the benthic megahabitat classification. Including these new variables in the analysis resulted in a clear distinction between the coastal and epipelagic midshore and offshore

habitats. However, the actual classification presented should be viewed as one of several different classifications potentially achieved with the dataset. Other classifications might be obtained using benthic cells only, using a subset of the 103 variables used in the statistical analyses, or alternately using different statistical approaches on the same data.

The dataset is made public, hoping that it will be improved as new information becomes available. Two aspects appear to be of foremost importance: shoreline and watershed inputs. The marine environment forms a large boundary with the shoreline habitats, and estuaries form a transition to the freshwater habitats. These aspects were not addressed fully in the present work although an effort was made to flag important aspects of coastal processes and habitats (sensitivity to erosion; access to tidal areas; proximity to mud flats, salt marshes, and sand beaches) and to locate each marine cell relative to major streams and rivers. These are important aspects to consider in order to better address land-based anthropogenic effects (Halpern et al. 2008) on the coastal and marine environment, considering that human activities along the coast and into the watersheds challenge the natural ecosystem processes occurring in the marine environment (Rabalais et al. 2002; Gedan et al. 2009; Lebeuf 2009).

ACKNOWLEDGEMENTS

The authors thank Karel Allard, Anthony Pouw, and Jean-François Aublet (Environment Canada), for allowing access to the SCP database; and Karel Allard (Environment Canada), Anuradha Rao, Robert Gregory, and Conrad Mullins (Department of Fisheries and Oceans), for sharing information on eelgrass beds. A preliminary version of the report was reviewed by Marc Ouellette (DFO Gulf Region) and Jean-Claude Brêthes (Université du Québec à Rimouski), and was edited by Laure Devine (DFO, Quebec Region).

REFERENCES

Adam, P. 2002. Saltmarshes in a time of change. Environ. Conserv. 29: 39-61.

Artioli, Y., G. Bendoricchio & L. Palmeri. 2005. Defining and modelling the coastal zone affected by the Po River (Italy). Ecol. Model. 184: 55-68.

Brickman, D. & A. Drozdowski. 2012. Development and validation of a regional shelf model for Maritime Canada based on the NEMO-OPA circulation model. Can. Tech. Rep. Hydrogr. Ocean Sci. 278: vii + 57 pp.

Cairns, D. K., J.-D. Dutil, S. Proulx, J. D. Mailhiot, M.-C. Bédard, A. Kervalla, L. G. Godfrey, E. M. O'Brien, S. C. Daley, E. Fournier, J. P. N. Tomie & S. C. Courtenay. 2012. An atlas and classification of aquatic habitat on the east coast of Canada, with an evaluation of usage by the American eel. Can. Tech. Rep. Fish. Aquat. Sci. 2986: v + 103 pp.

Caissie, D. & S. Robichaud. 2009. Towards a better understanding of the natural flow regimes and streamflow characteristics of rivers of the Maritime Provinces. Can. Tech. Rep. Fish. Aquat. Sci. 2843: viii+53 pp.

Chabot, D., A. Rondeau, B. Sainte-Marie, L. Savard, T. Surette & P. Archambault. 2007. Distribution of benthic invertebrates in the Estuary and Gulf of St. Lawrence. DFO Can. Sci. Adv. Sec. Res. Doc. 2007/018: viii+108 pp.

Costanza, R., R. d'Arge, R. De Groot, S. Farber, M. Grasso, B. Hannon, K. Limburg, S. Naeem, R. V. O'Neill & J. Paruelo. 1997. The value of the world's ecosystem services and natural capital. Nature 387 (6630): 253-260.

De Sherbinin, A., D. Carr, S. Cassels & L. Jiang. 2007. Population and environment. Annu. Rev. Env. Resour. 32: 345-373.

DFO. 2009. Development of a framework and principles for the biogeographic classification of Canadian marine areas. DFO Can. Sci. Adv. Sec. Sci. Adv. Rep. 2009/056: 17 pp.

Dutil, J.-D. & M. Fortin. 1983. La communauté de poissons d'un marécage intertidal de l'estuaire du Saint-Laurent. Nat. can. 110: 397-410.

Dutil, J.-D., S. Proulx, P.-M. Chouinard & D. Borcard. 2011. A hierarchical classification of the seabed based on physiographic and oceanographic features in the St. Lawrence. Can. Tech. Rep. Fish. Aquat. Sci. 2916: vii + 72 pp.

Dutil, J.-D., S. Proulx, P.-M. Chouinard & D. Borcard. 2011. A hierarchical classification of the seabed based on physiographic and oceanographic features in the St. Lawrence. Can. Tech. Rep. Fish. Aquat. Sci. 2916: vii + 72 pages.

Galbraith, P. S., P. Larouche, J. Chasse & B. Petrie. 2012. Sea-surface temperature in relation to air temperature in the Gulf of St. Lawrence: interdecadal variability and long term trends. Deep-Sea Res. Part 2 Top. Stud. Oceanogr. 77-80: 10-20.

Gedan, K. B., B. Silliman & M. Bertness. 2009. Centuries of human-driven change in salt marsh ecosystems. Ann. Rev. Mar. Sci. 1: 117-141.

Grant, C. & L. Provencher. 2007. Caractérisation de l'habitat et de la faune des herbiers de *Zostera marina* de la péninsule de Manicouagan (Québec). Rapp. tech. can. sci. halieut. aquat. 2772: viii + 65 pp.

Gromack, A., K. Allard, D. Fenton, S. Johston & J. Ford. 2010. Ecological and human use information for twenty areas on the Atlantic coast of Nova Scotia in support of conservation planning. Can. Tech. Rep. Fish. Aquat. Sci. 2880: xiv + 226 pp.

Halpern, B. S., S. Walbridge, K. A. Selkoe, C. V. Kappel, F. Micheli, C. D'Agrosa, J. F. Bruno, K. S. Casey, C. Ebert & H. E. Fox. 2008. A global map of human impact on marine ecosystems. Science 319 (5865): 948-952.

ICES. 2009. Report of the study group on anguillid eels in saline waters (SGAESAW), 16-18 March 2009, Sackville, New Brunswick, Canada, and 3-5 September 2009, Gothenburg, Sweden. ICES Council Meeting documents CM 2009/DFC 06: 183 pp.

Koutitonsky, V. & G. Bugden. 1991. The physical oceanography of the Gulf of St. Lawrence: a review with emphasis on the synoptic variability of the motion. *In* The Gulf of St. Lawrence: small ocean or big estuary. *Edited by* J.-C. Therriault. Can. Spec. Publ. Fish. Aquat. Sci. 113: 57-90.

Kratzer, S. & P. Tett. 2009. Using bio-optics to investigate the extent of coastal waters: a Swedish case study. *In* Eutrophication in Coastal Ecosystems. *Edited by* J. H. Andersen and D. J. Conley. Dev. Hydrob. 207: 169-186.

Lebeuf, M. 2009. La contamination du béluga de l'estuaire du Saint-Laurent par les polluants organiques persistants en revue. Rev. Sci. Eau 22: 199-233.

Lessin, G., V. Ossipova, I. Lips & U. Raudsepp. 2009. Identification of the coastal zone of the central and eastern Gulf of Finland by numerical modeling, measurements, and remote sensing of chlorophyll-*a*. *In* Eutrophication in Coastal Ecosystems. *Edited by* J. H. Andersen and D. J. Conley. Dev. Hydrob. 207: 187-198.

Loring, D. & D. Nota. 1973. Morphology and sediments of the Gulf of St. Lawrence. Bull. Fish. Res. Board Can. 182: xiv + 147 pp.

Madec, G. 2008. NEMO ocean engine. Note du pôle de modélisation. Institut Pierre-Simon Laplace (IPSL), France, No 27 ISSN No 1288-1619.

Martel, M.-C., L. Provencher, C. Grant, H.-F. Ellefsen & S. Pereira. 2009. Distribution and description of eelgrass beds in Québec. DFO Can. Sci. Advis. Sec. Res. Doc. 2009/050: viii + 37pp.

Rabalais, N. N., R. E. Turner & D. Scavia. 2002. Beyond science into policy: Gulf of Mexico hypoxia and the Mississippi River. Bioscience 52: 129-142.

Rabalais, N. N., R. E. Turner & W. J. Wiseman Jr. 2002. Gulf of Mexico hypoxia, AKA "The Dead Zone". Annu. Rev. Ecol. Syst. 33: 235-263.

Ricketts, P. & P. Harrison. 2007. Coastal and ocean management in Canada: moving into the 21st century. Coast. Manage. 35: 5-22.

Savenkoff, C., M.-N. Bourassa, D. Baril & H. P. Benoît. 2007. Identification des zones d'importance écologique et biologique pour l'estuaire et le golfe du Saint-Laurent. DFO Can. Sci. Adv. Sec. Res. Doc. 2007/015: 49 pp.

Scavia, D., J. C. Field, D. F. Boesch, R. W. Buddemeier, V. Burkett, D. R. Cayan, M. Fogarty, M. A. Harwell, R. W. Howarth & C. Mason. 2002. Climate change impacts on US coastal and marine ecosystems. Estuaries Coasts 25: 149-164.

Shaw, J., R. B. Taylor, D. L. Forbes, M.-H. Ruz & S. Solomon. 1998. Sensitivity of the coasts of Canada to sea-level rise. Geological survey of Canada Bulletin 505: 114 pp.

Wiken, E. B., D. Gauthier, I. Marshall, K. Lawton & H. Hirvonen. 1996. A perspective on Canada's ecosystems: an overview of the terrestrial and marine ecozones. Canadian Council on Ecological Areas. Occasional Papers no 14: 99 pp.

Wilkinson, T., E. Wiken, J. Bezaury-Creel, T. Hourigan, T. Agardy, H. Herrmann, L. Janishevski, C. Madden, L. Morgan & M. Padilla. 2009. Marine ecoregions of North America. Commission for Environmental Cooperation. Montreal, Canada: 200 pp.

Table 1. Characteristics of benthic and pelagic cells (39,337 marine cells with a non-tidal zone area > 0) in the estuary and Gulf of St. Lawrence. "No of cells" is the total count of cells by category. Planimetric areas (km^2) and "lenght of coastline" represent sum values by category. Other variables are mean values by category.

	Benthic only (BENTHIC_B=1 and PELAGIC_B=0)				Benthic and pelagic (BENTHIC_B=1 and PELAGIC_B=1)				Pelagic only (BENTHIC_B=0 and PELAGIC_B=1)			
	Estuary	Northern Gulf	Southern Gulf	Study area	Estuary	Northern Gulf	Southern Gulf	Study area	Estuary	Northern Gulf	Southern Gulf	Study area
No of cells	545	1,209	3,800	5,554	420	2,155	1,260	3,835	1,031	19,741	9,176	29,948
Tidal zone area (km^2)	472.4	479.1	796.6	1748.2	101.0	146.9	4.9	252.9	0	0	0	0
Non-tidal zone area (km^2)	2,151.3	2,786.3	17,215.8	22,153.4	2,279.4	11,508.0	7,669.0	21,456.5	6,443.7	123,219.5	57,308.9	186,972.1
Benthic area (km^2)	2,151.3	2,786.3	1,7215.8	22,153.4	1,053.9	4,946.8	3,937.7	9,938.5	0	0	0	0
Pelagic area (km^2)	0	0	0	0	1,225.4	6,568.3	3,731.3	11,525.0	6,443.7	123,219.5	57,308.9	18,6972.1
Length of coastline (km)	961.9	4,932.3	6,893.1	12,787.4	427.0	5,743.2	342.5	6,512.8	0	0	0	0
Sinuosity of coastline	1.201	1.453	1.446	1.424	1.229	1.415	1.260	1.370	-	-	-	-
Insulosity-proportion	0.090	0.079	0.067	0.075	0.050	0.068	0.038	0.066	0	<0.001	0	<0.001
Insulosity-frequency	0.092	0.567	0.014	0.076	0.011	0.558	<0.001	0.193	0	<0.001	0	<0.001
Proportion sheltered	0.009	0.347	0.095	0.125	<0.001	0.044	<0.001	0.015	0	0	0	0
Proportion semi-exposed	0.682	0.116	0.048	0.101	0.300	0.075	0.006	0.059	<0.001	0.002	<0.001	<0.001
Proportion exposed	0.235	0.326	0.742	0.606	0.683	0.788	0.992	0.873	0.997	0.999	0.999	0.999

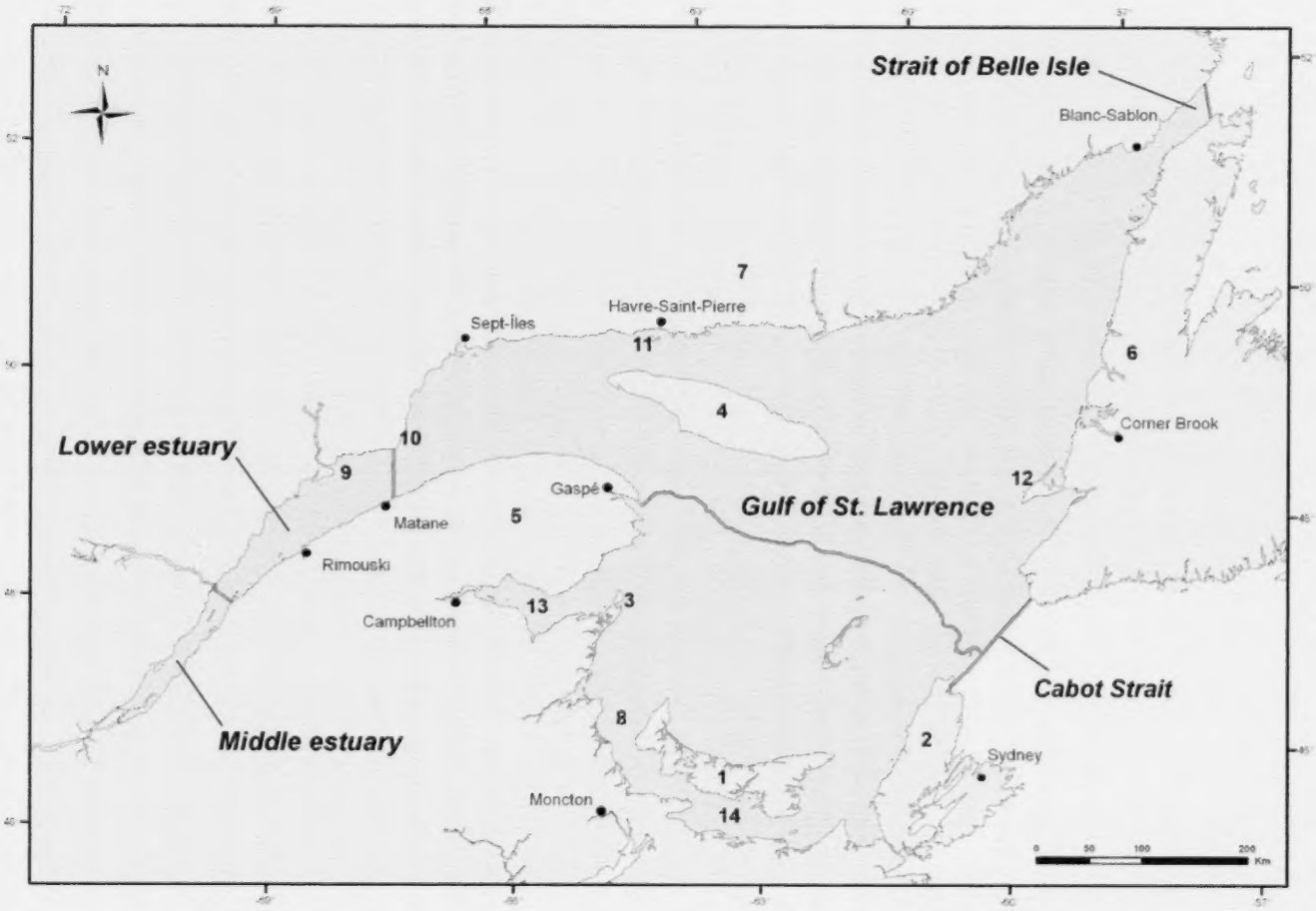

Figure 1. The study area included the middle and lower St. Lawrence estuary, and the Gulf of St. Lawrence east to Cabot Strait and the Strait of Belle Isle. Solid red lines indicate the limits of the study area and subareas. The 200 m isobath south of the Laurentian Channel arbitrarily divides the northern and southern Gulf. The Saguenay Fjord was not included in the study. (1) Prince Edward Island, (2) Cape Breton, (3) Miscou Island, (4) Anticosti, (5) Gaspé Peninsula, (6) West Coast of Newfoundland, (7) Quebec Lower North Shore, (8) Shediac Valley, (9) Manicouagan Peninsula, (10) Pointe-des-Monts, (11) Mingan Islands, (12) Cape St. Georges, (13) Baie des Chaleurs, (14) Northumberland Strait.

Figure 2. Coastal area showing the mapping grid and cell address designation. The 100 km² cells are designated by column number (increasing from left to right) and row number (increasing from top to bottom), as described in Dutil et al. (2011). The 6.25 km² cells are designated by adding a suffix letter ranging from a to p and increasing through the alphabet column-wise and then row-wise. Hatched areas indicate the tidal zone and the blue line indicates the cut-off limit of river estuaries.

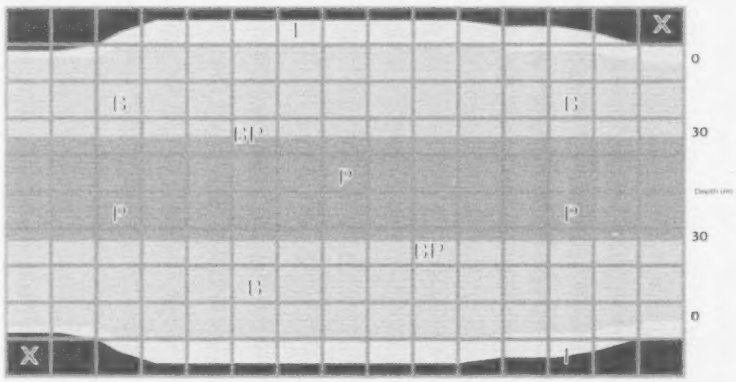

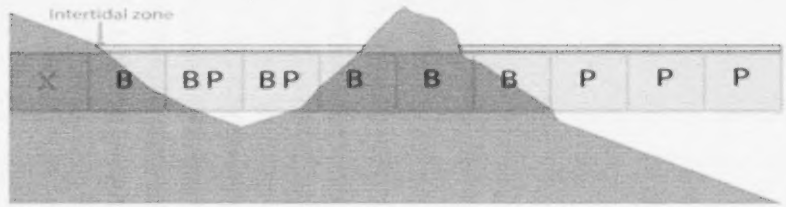

Figure 3. The area of the non-tidal zone within each cell was categorized as being benthic (B) or pelagic (P) based on two binary variables (BENTHIC_B and PELAGIC_B). Cells with the whole seafloor at depths shallower than 30 m have a BENTHIC_B value of 1 and a PELAGIC_B value of 0; cells with the whole seafloor at depths greater than 30 m have a PELAGIC_B value of 1 and a BENTHIC_B value of 0. Cells with a mixed situation have BENTHIC_B and PELAGIC_B values of 1. I, cells with TIDAL_A value > 0 and NONTIDAL_A value = 0. The plan view is on the left and the sectional view on the right.

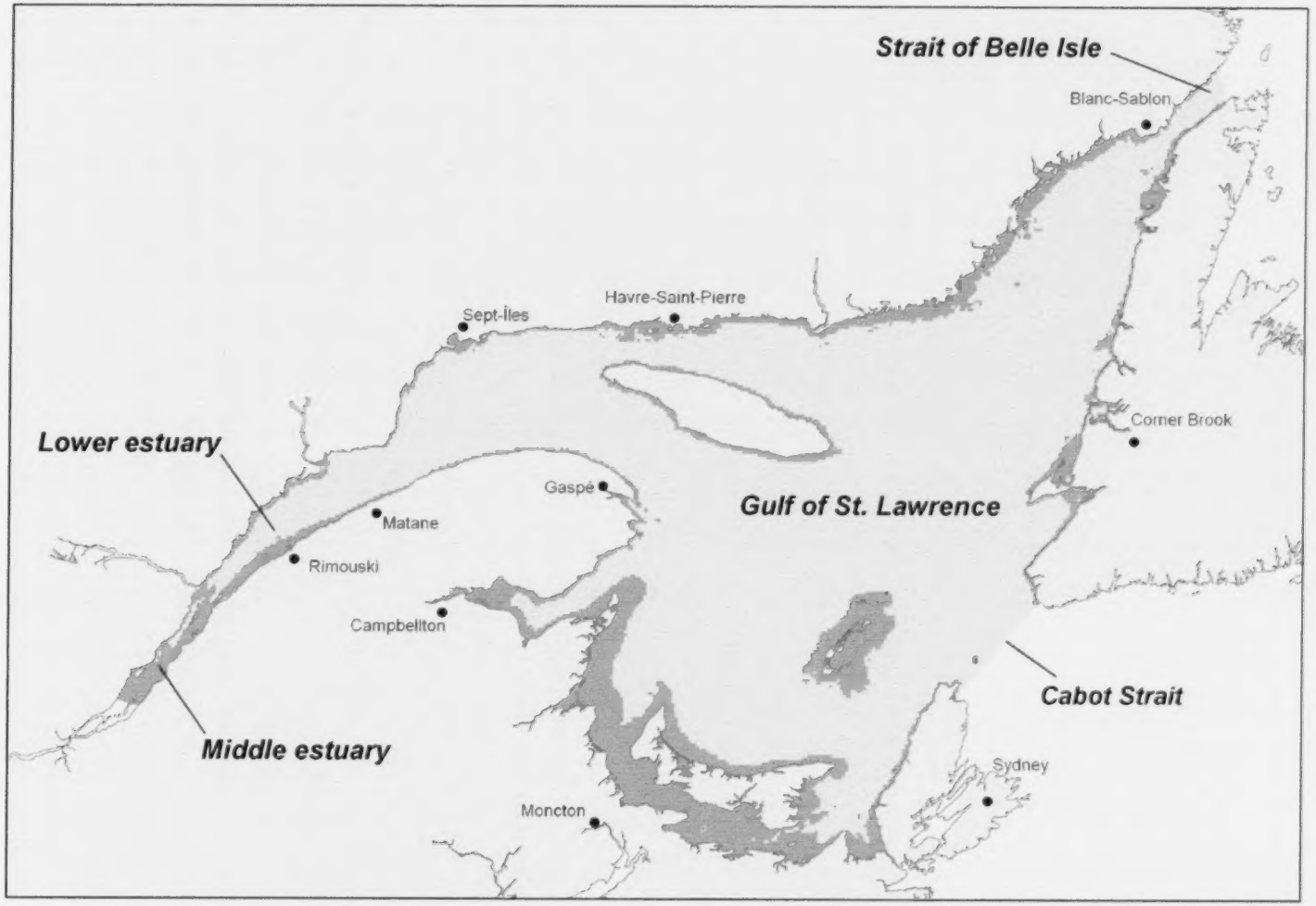

Figure 4. Study area showing the coastal zone down to the 30 m isobath (dark blue).

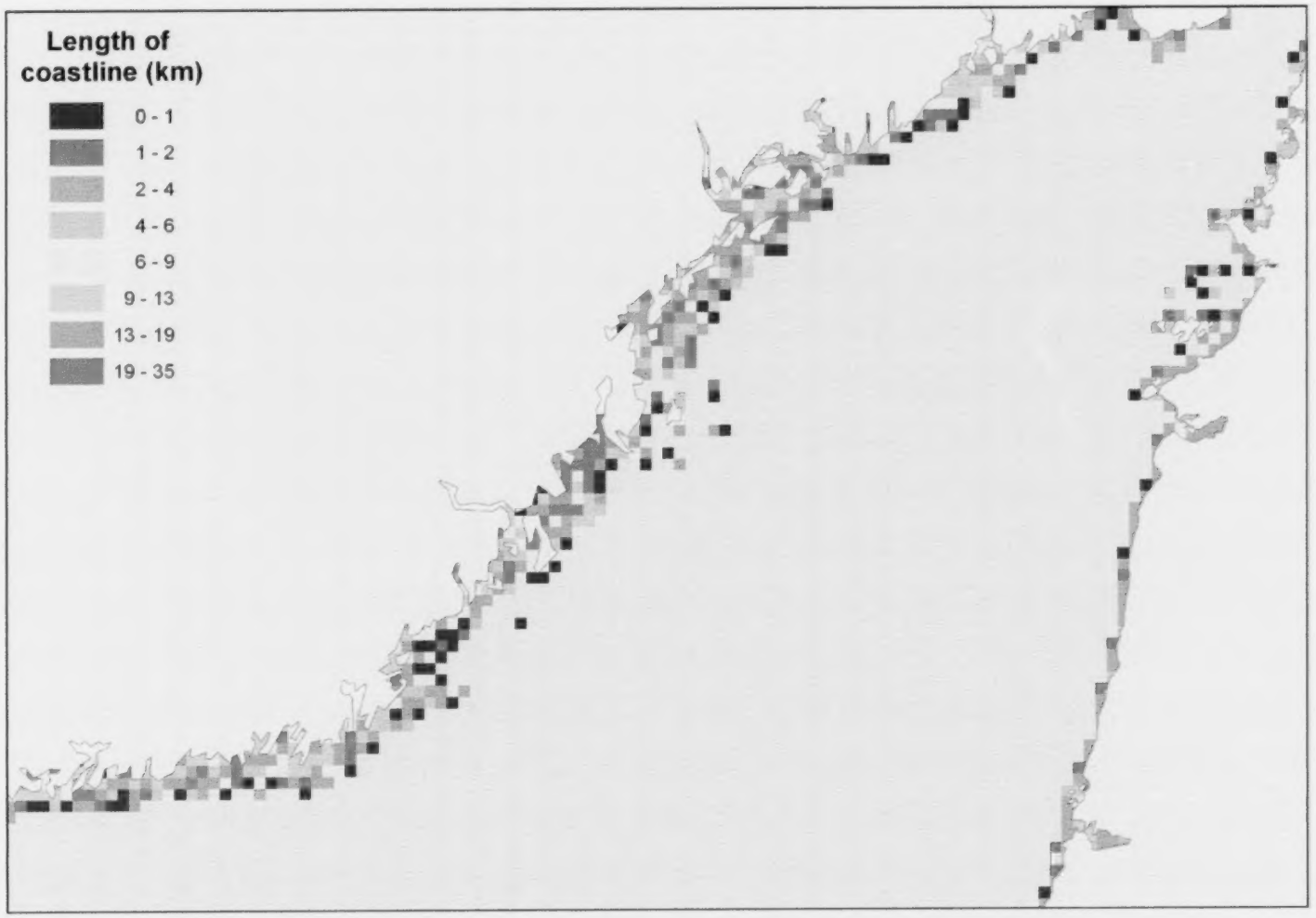

Figure 5. Length of the coastline (km) in the northeastern Gulf as determined by the low tide mark (mainland and islands).

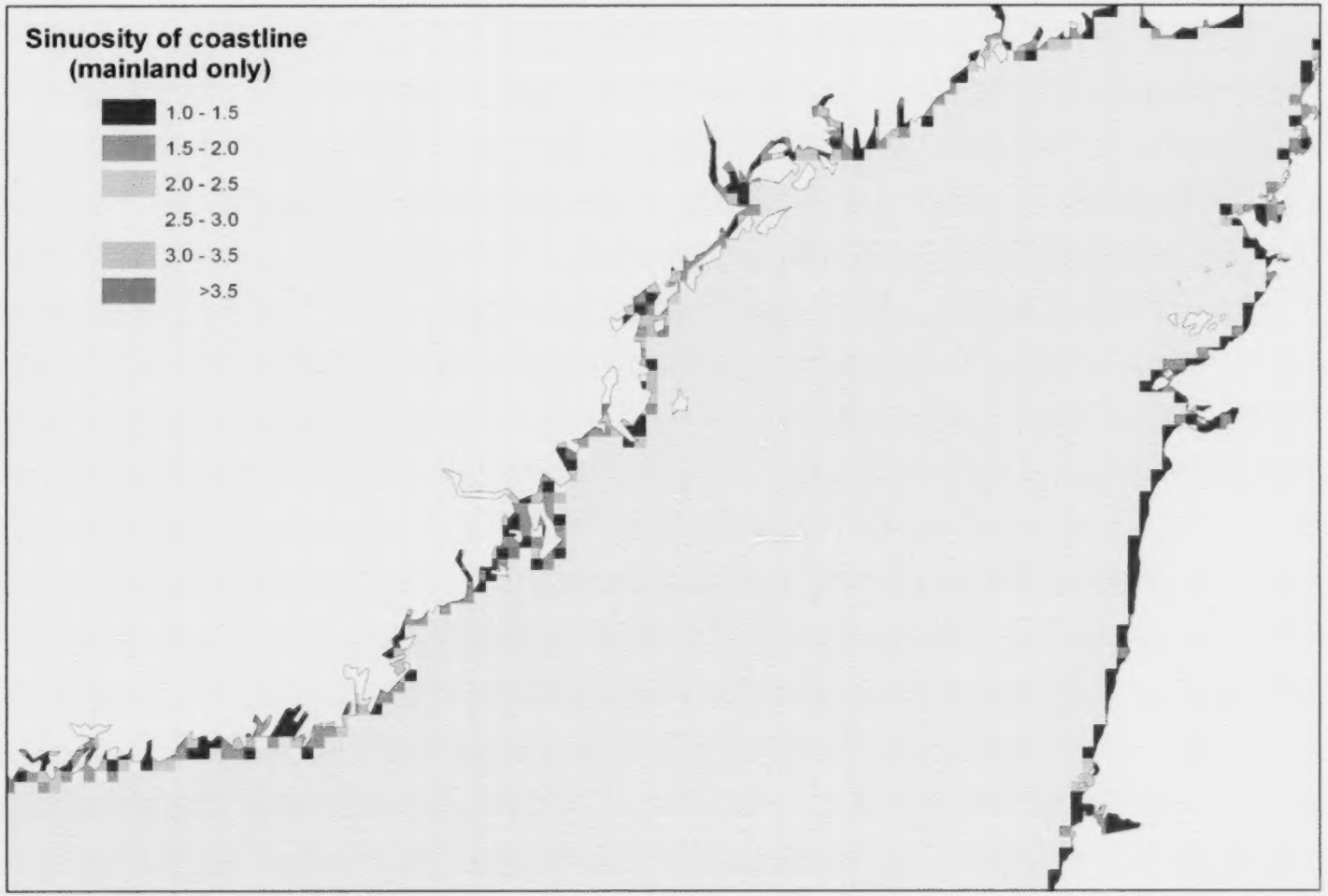

Figure 6. Sinuosity of the coastline (mainland only) in the northeastern Gulf, determined as the ratio of the length of the coastline at low tide, and the corresponding straight-line distance.

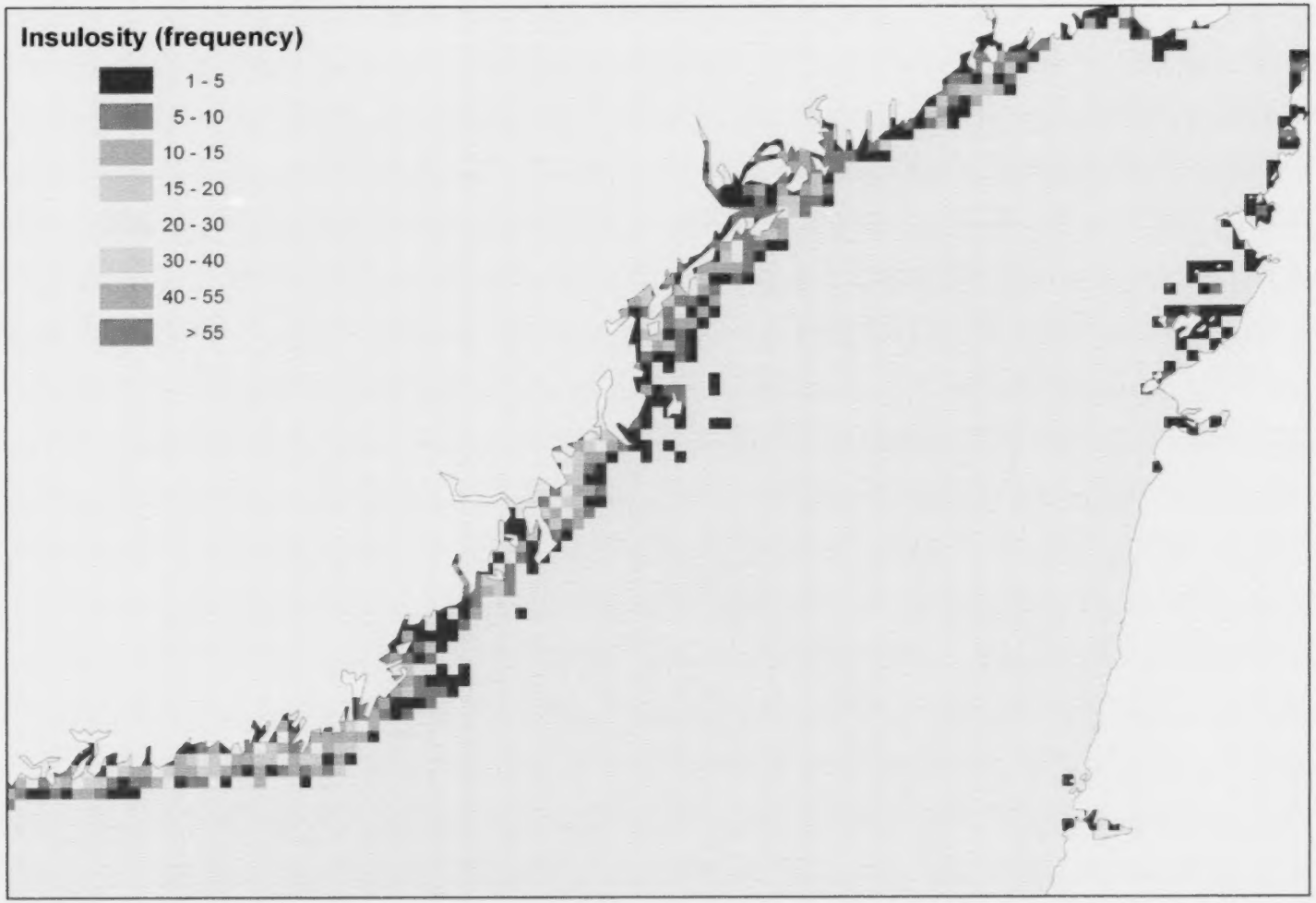

Figure 7. Total number of discrete landscape features emerged at low tide in the northeastern Gulf: islands with associated tidal zone and patches of tidal zones forming islands at low tide.

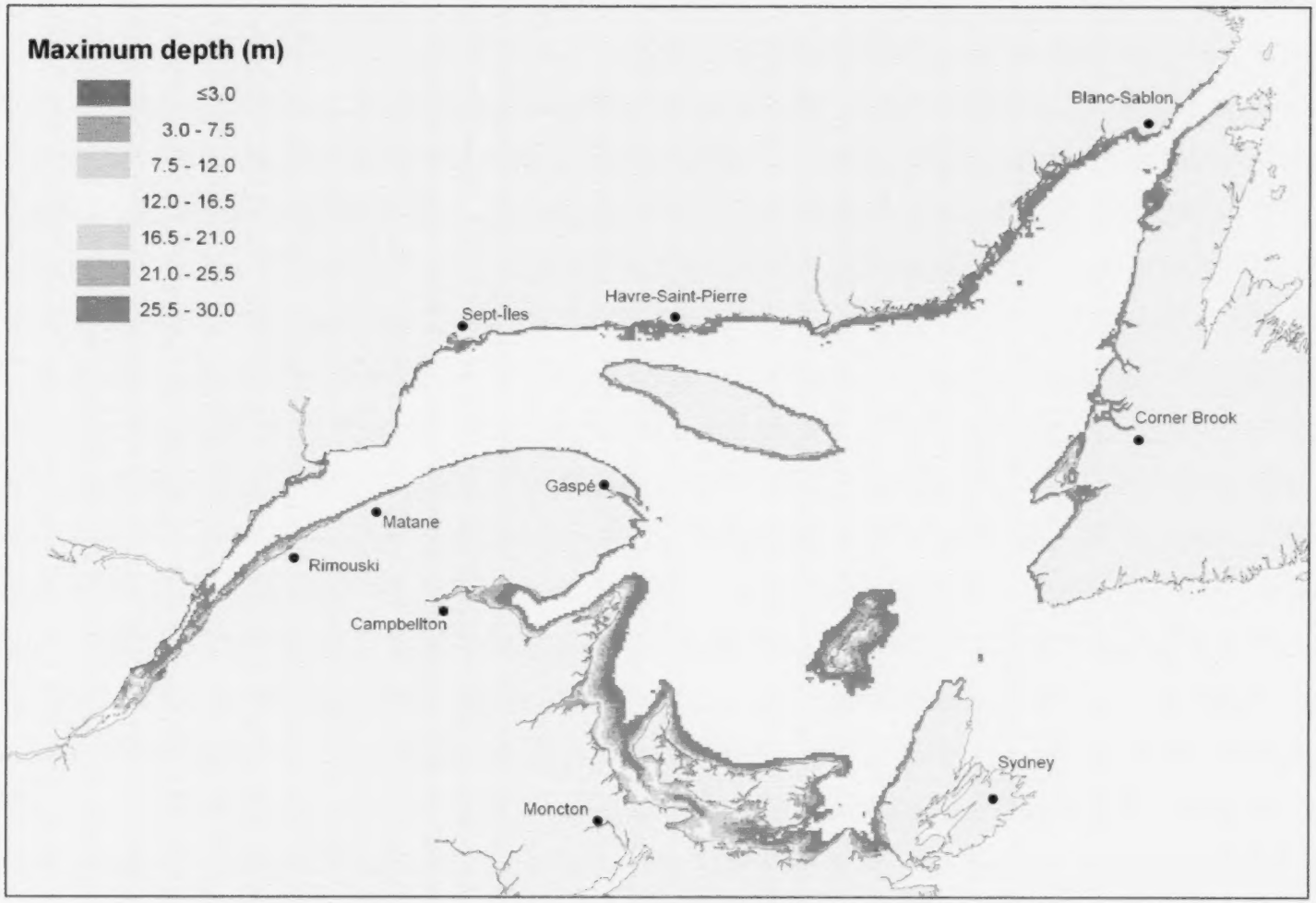

Figure 8. Maximum depth (m) of the portion of the seafloor less than 30 m deep. Only benthic cells are shown.

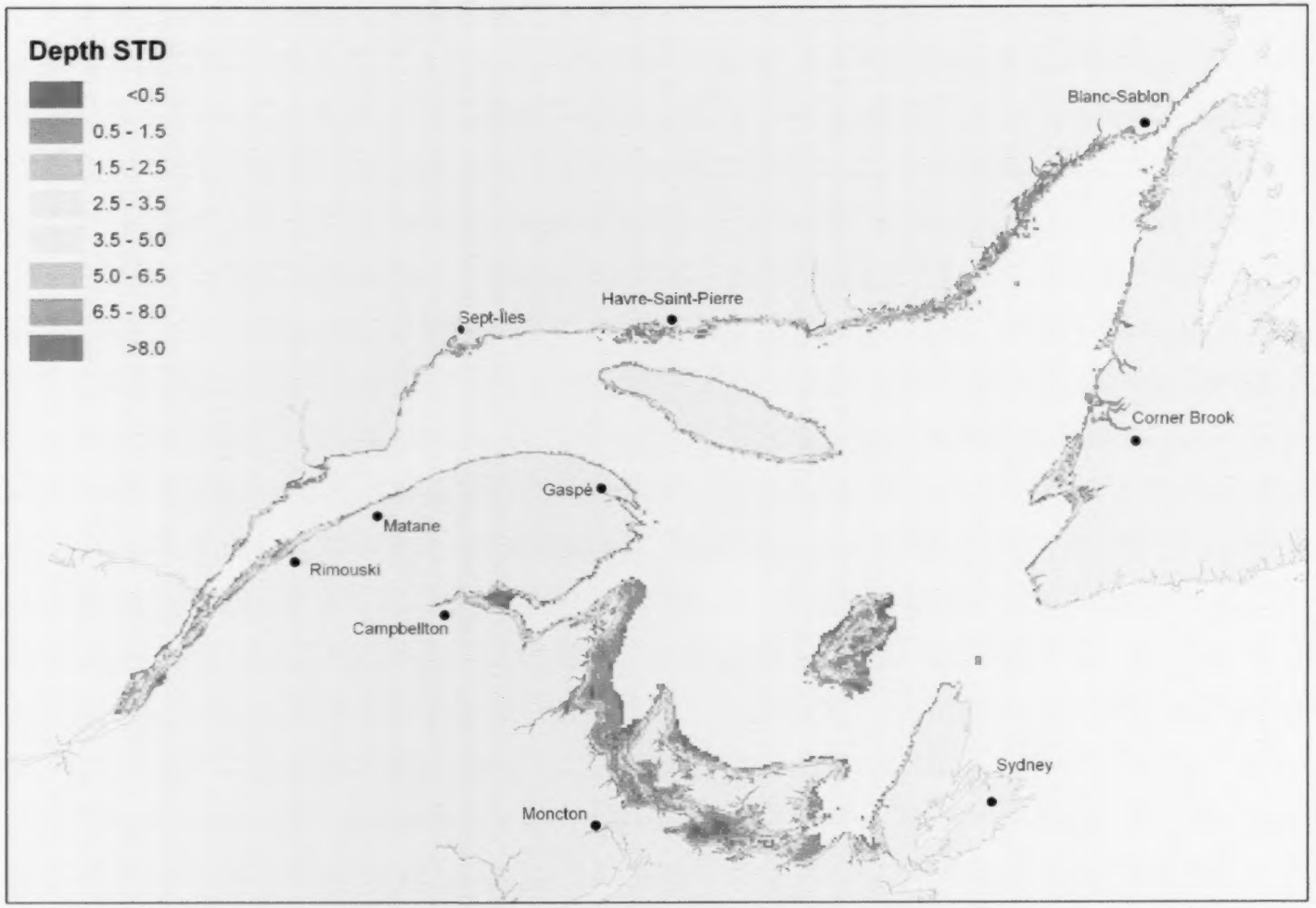

Figure 9. Standard deviation of depth (m) for the portion of the seafloor less than 30 m deep. Only benthic cells are shown.

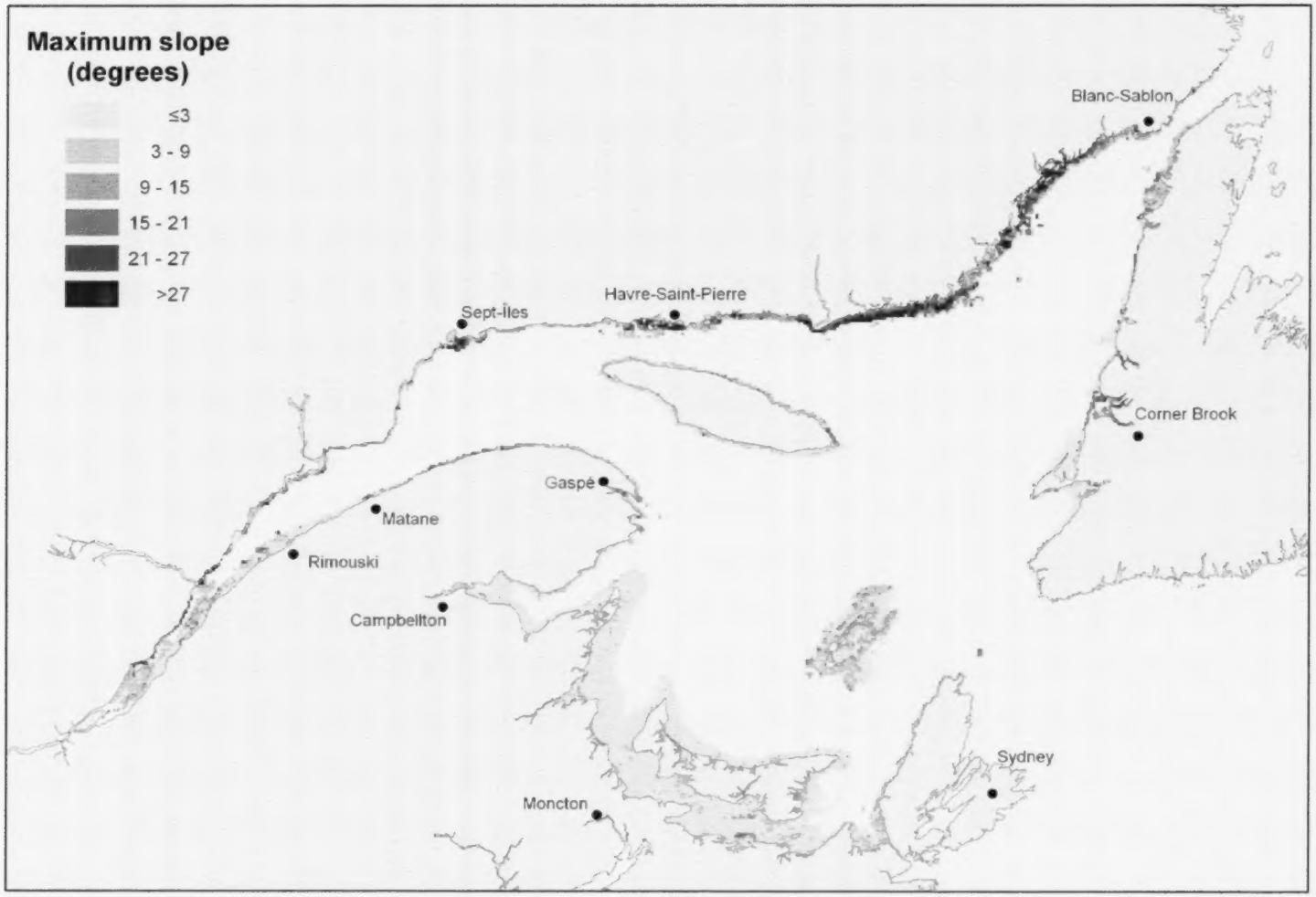

Figure 10. Maximum slope (degrees) of the portion of the seafloor less than 30 m deep. Only benthic cells are shown.

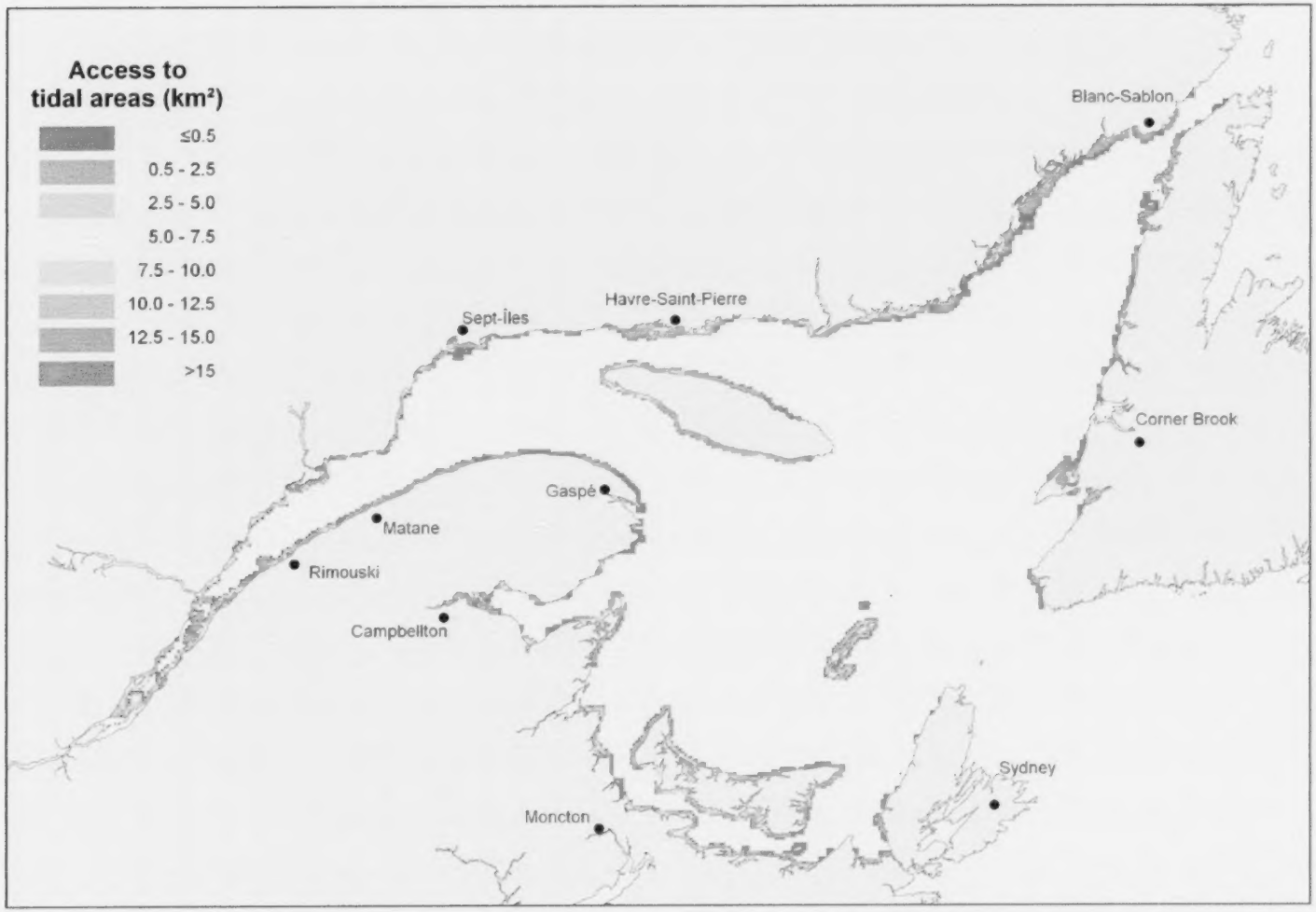

Figure 11. Sum area of the tidal zone (km^2) accessible based on the eight nearest neighbours. Only benthic cells are shown.

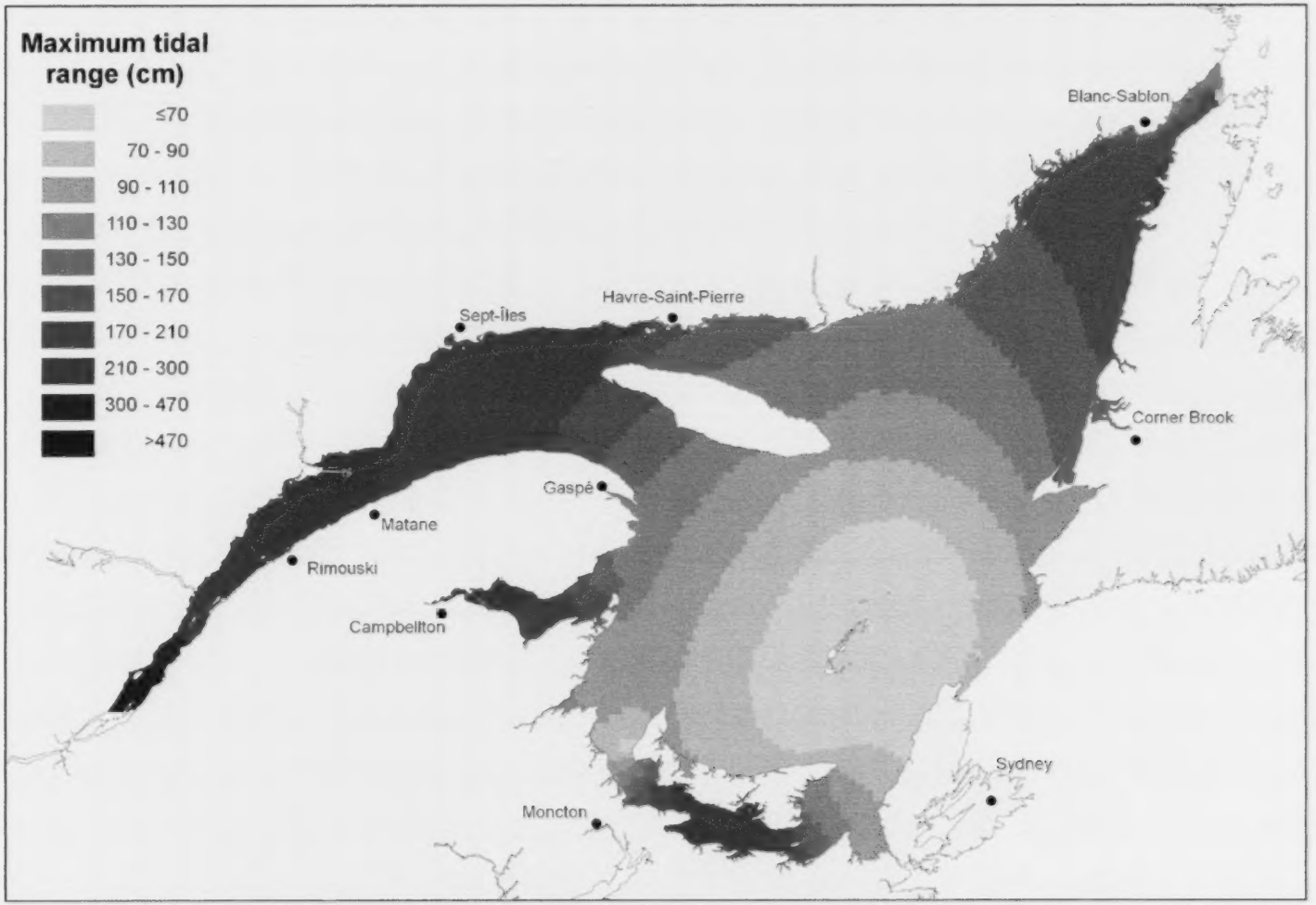

Figure 12. Maximum sum value of all tide components (cm) during a 50 d period (17 October to 5 December, 2007). Tidal amplitude has been multiplied by two to yield tidal range.

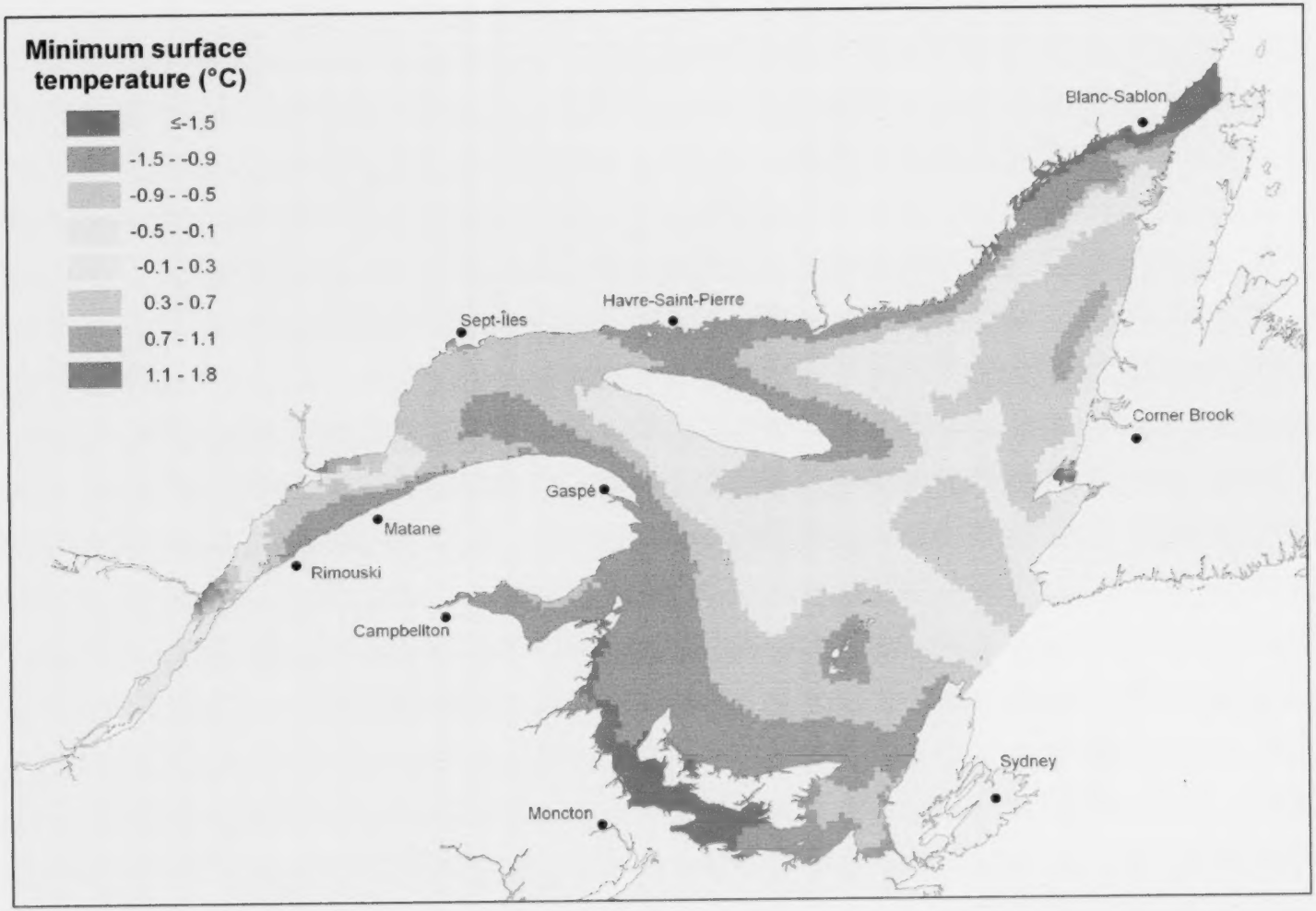

Figure 13. Minimum mean monthly temperature at the surface (°C) as predicted by the 3D model (0–6.2 m layer).

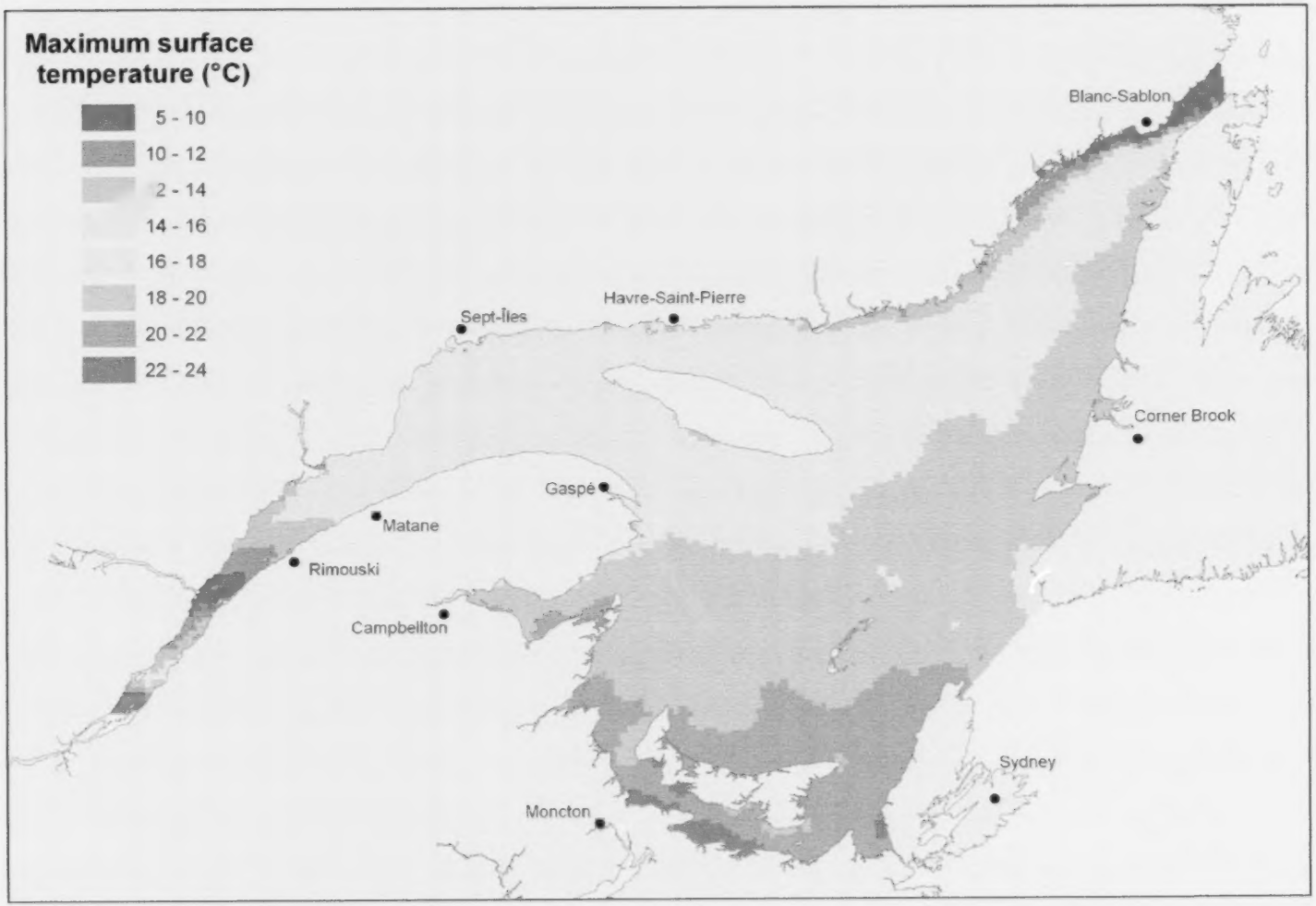

Figure 14. Maximum mean monthly temperature at the surface (°C) as predicted by the 3D model (0–6.2 m layer).

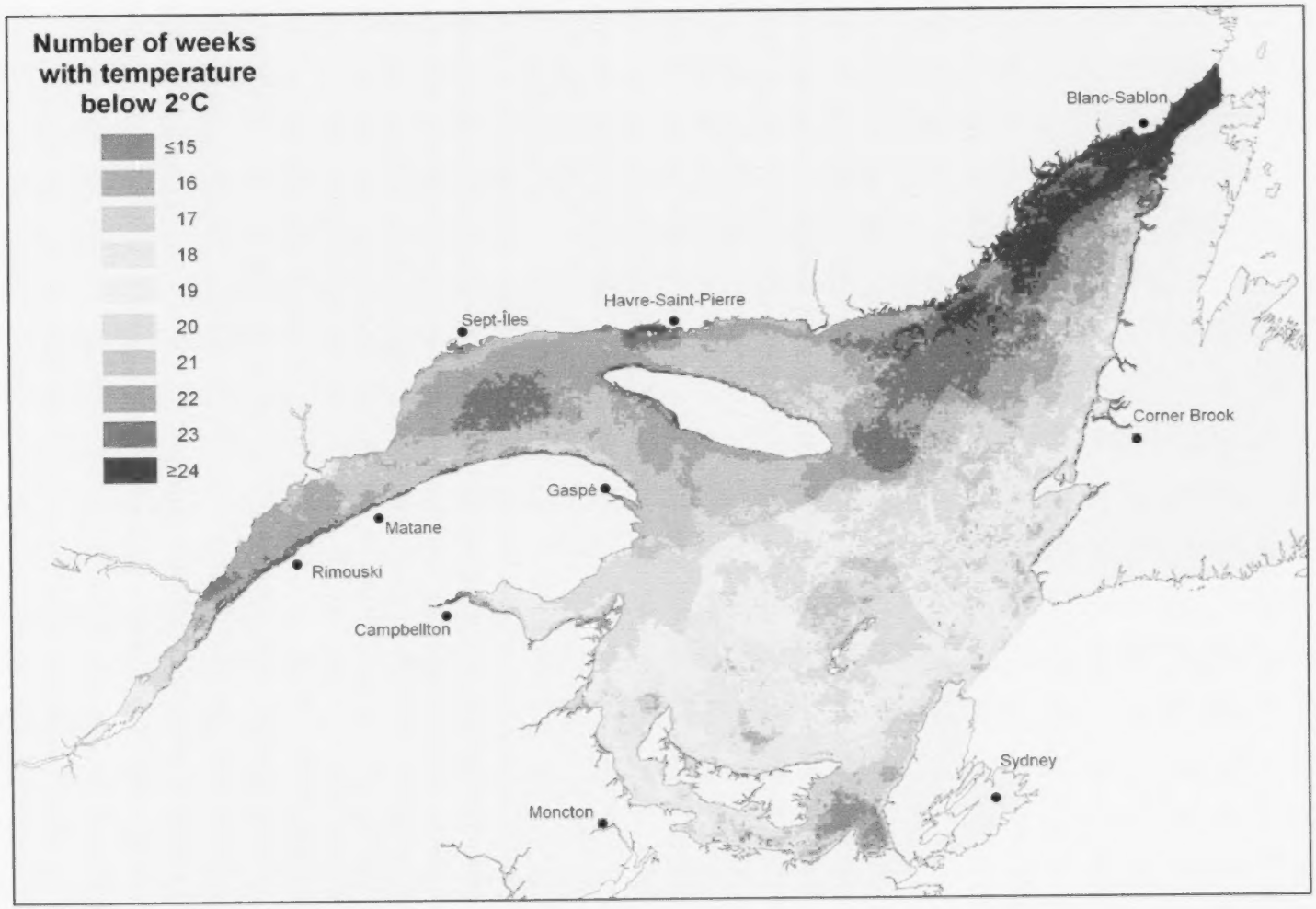

Figure 15. Number of weeks with sea surface temperature below 2°C.

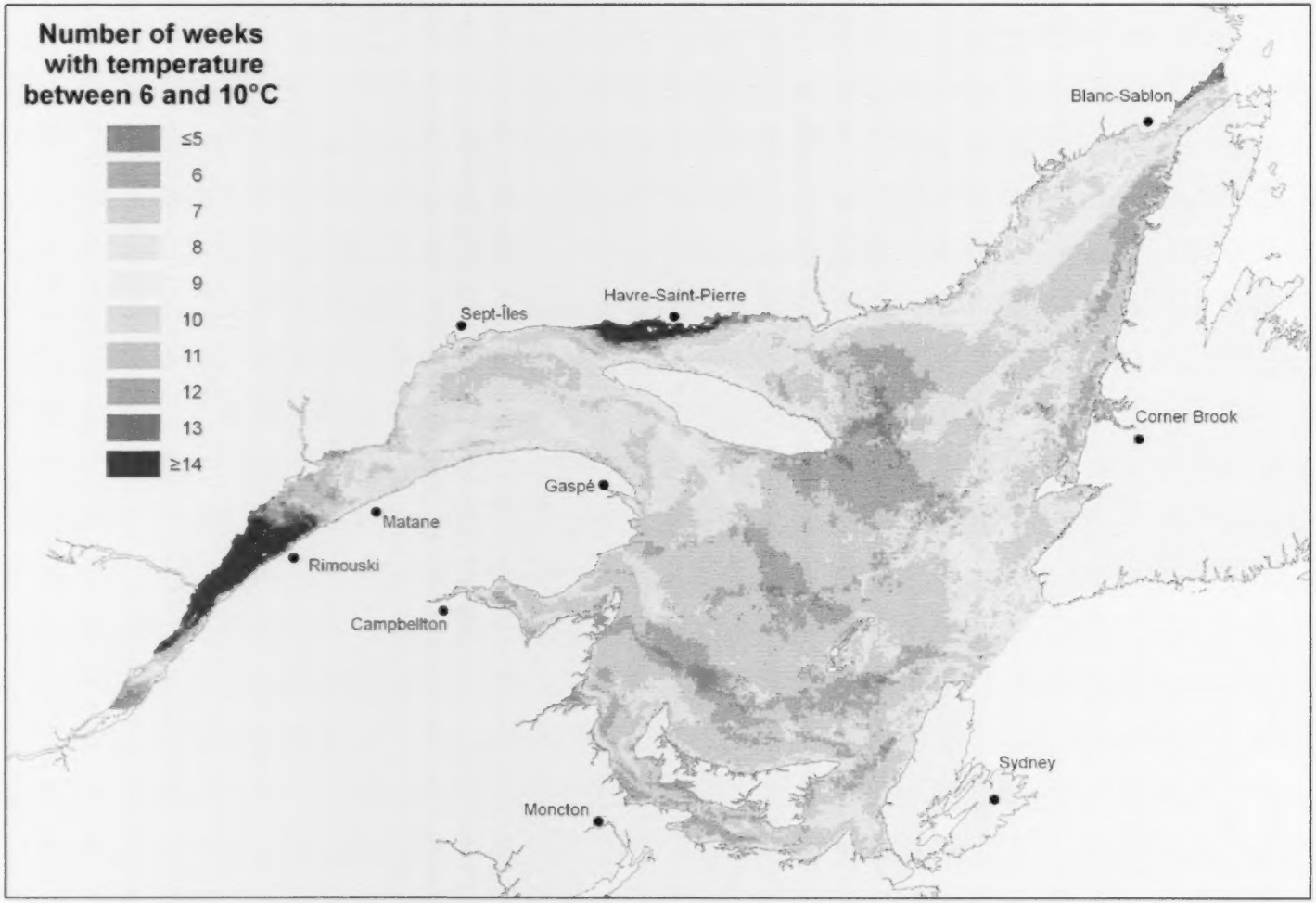

Figure 16. Number of weeks with sea surface temperature between 6 and 10°C.

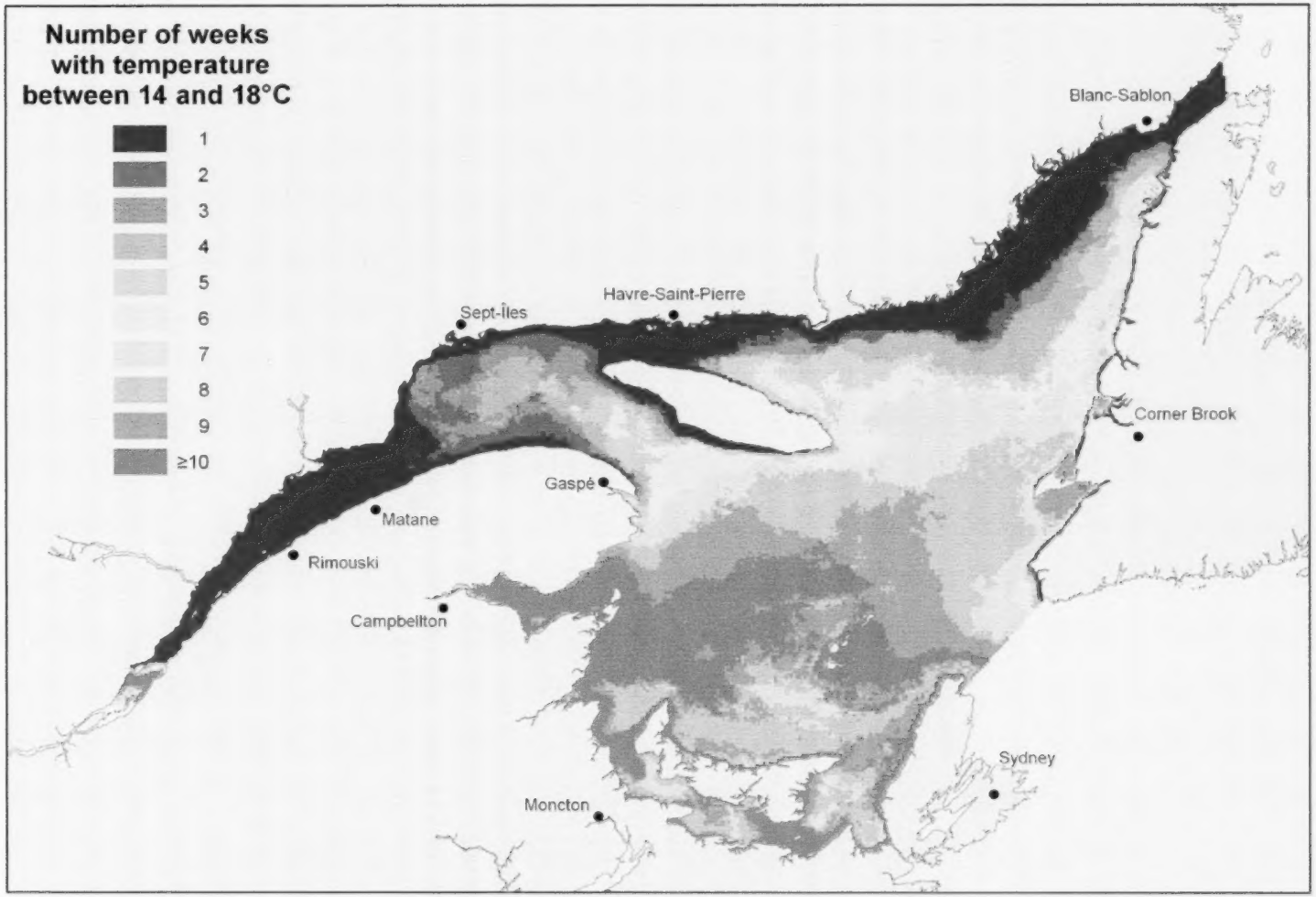

Figure 17. Number of weeks with sea surface temperature between 14 and 18°C.

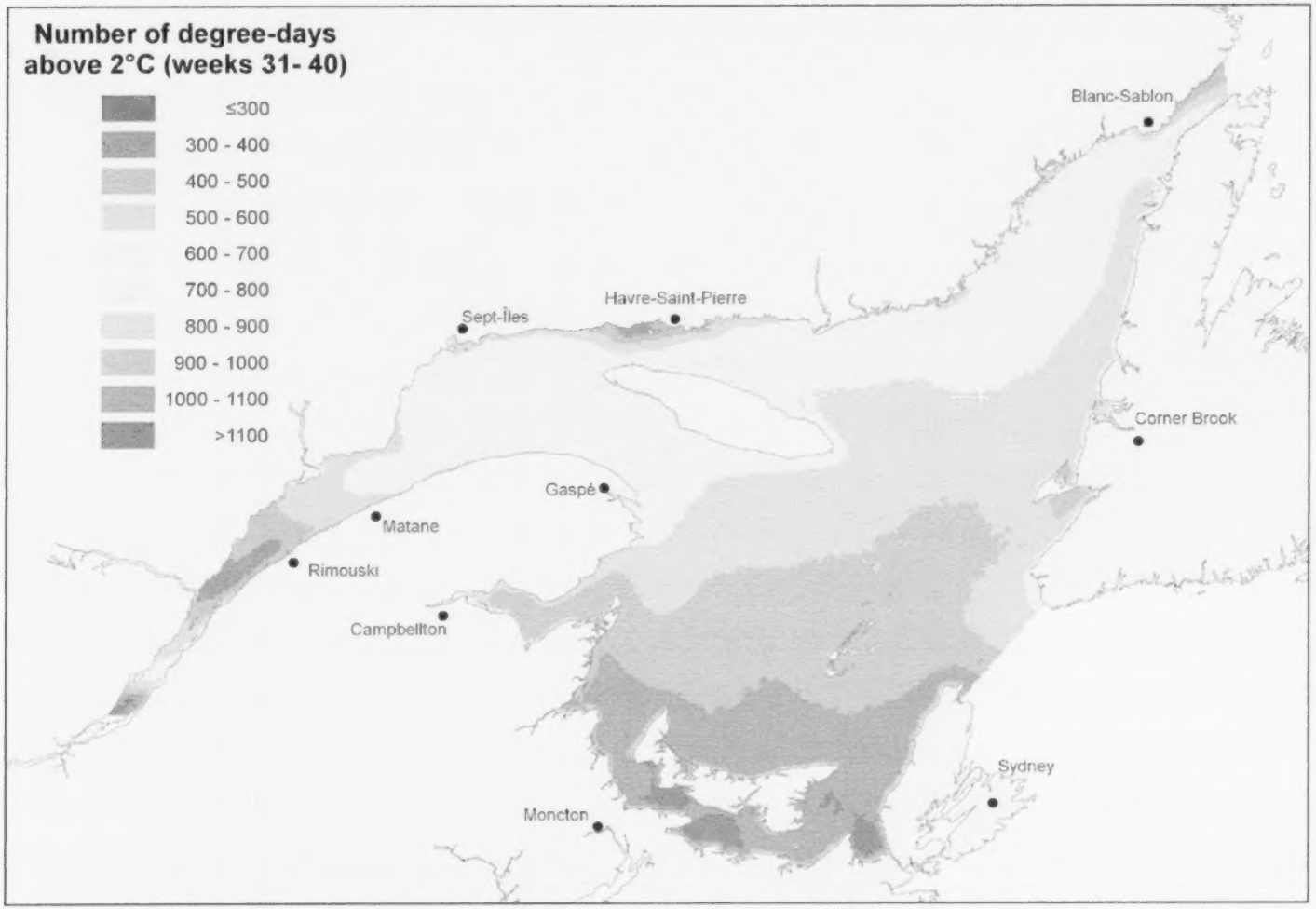

Figure 18. Number of degree-days above 2°C from week 31 to week 40.

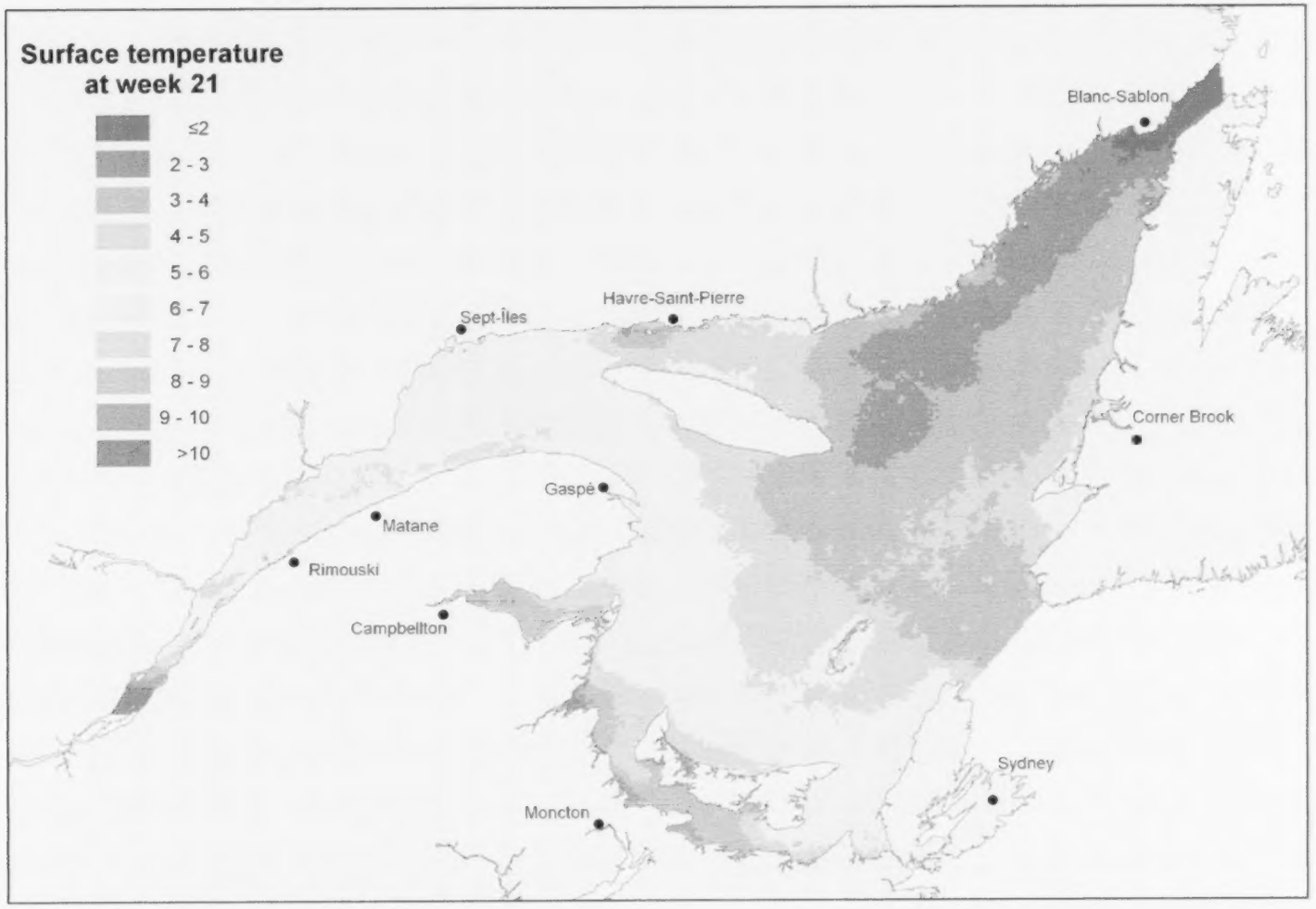

Figure 19. Sea surface temperature (°C) at the end of May (week 21).

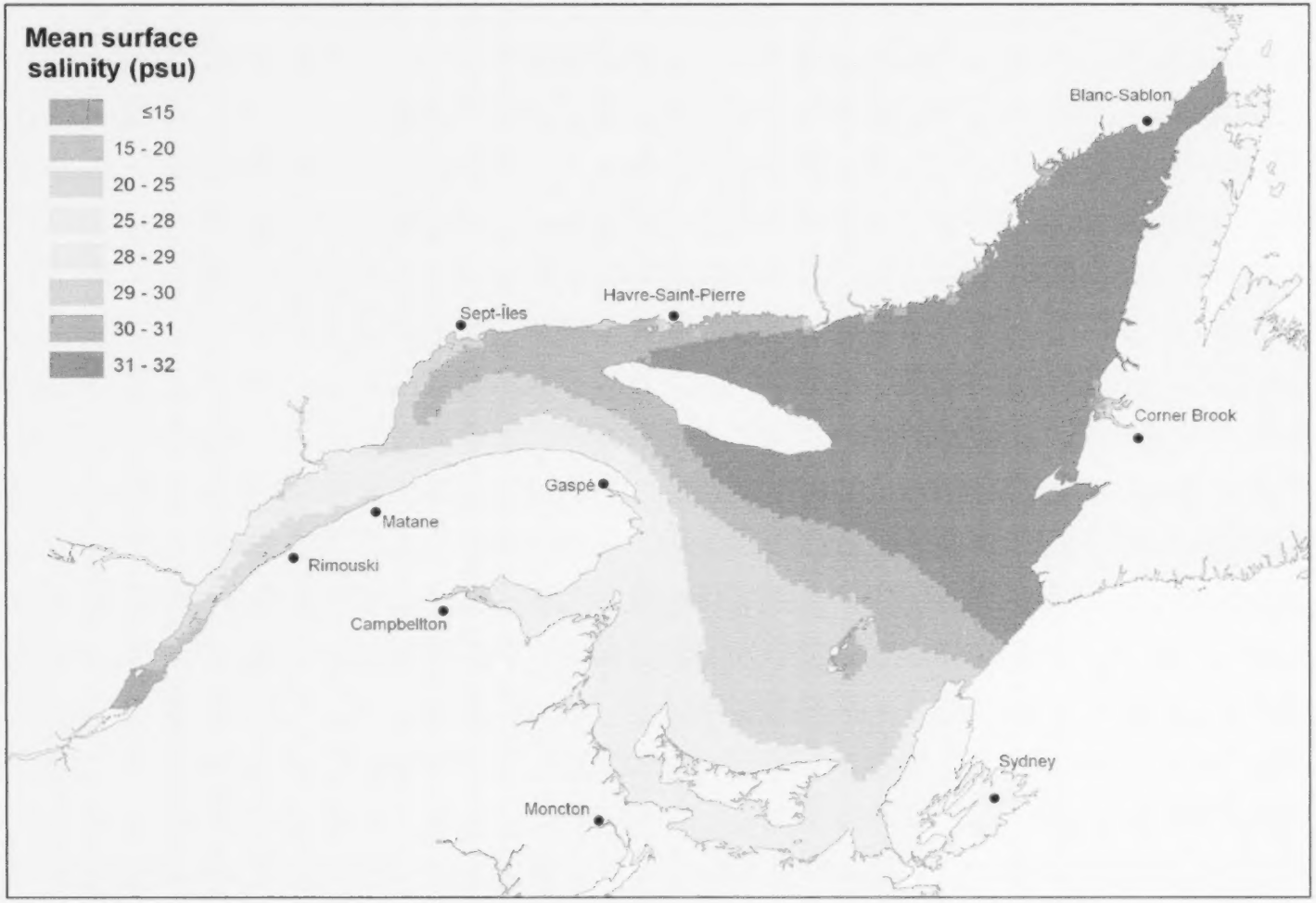

Figure 20. Mean salinity predicted by the 3D model at the surface (0–6.2 m layer).

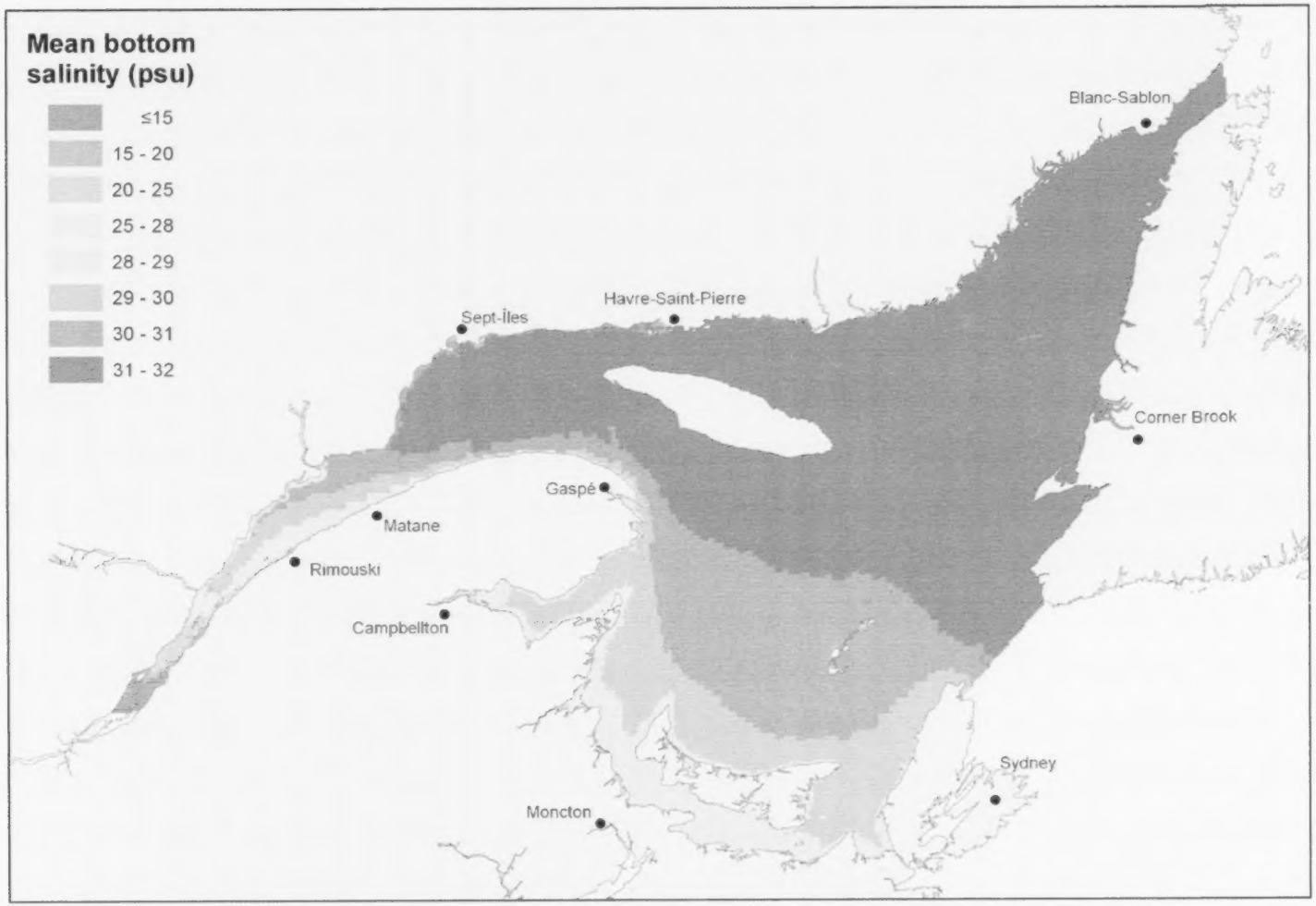

Figure 21. Mean salinity at DEPTHMEAN (on the bottom or at 30 m for BENTHIC_B=0 cells), as predicted from the corresponding layer by the 3D model.

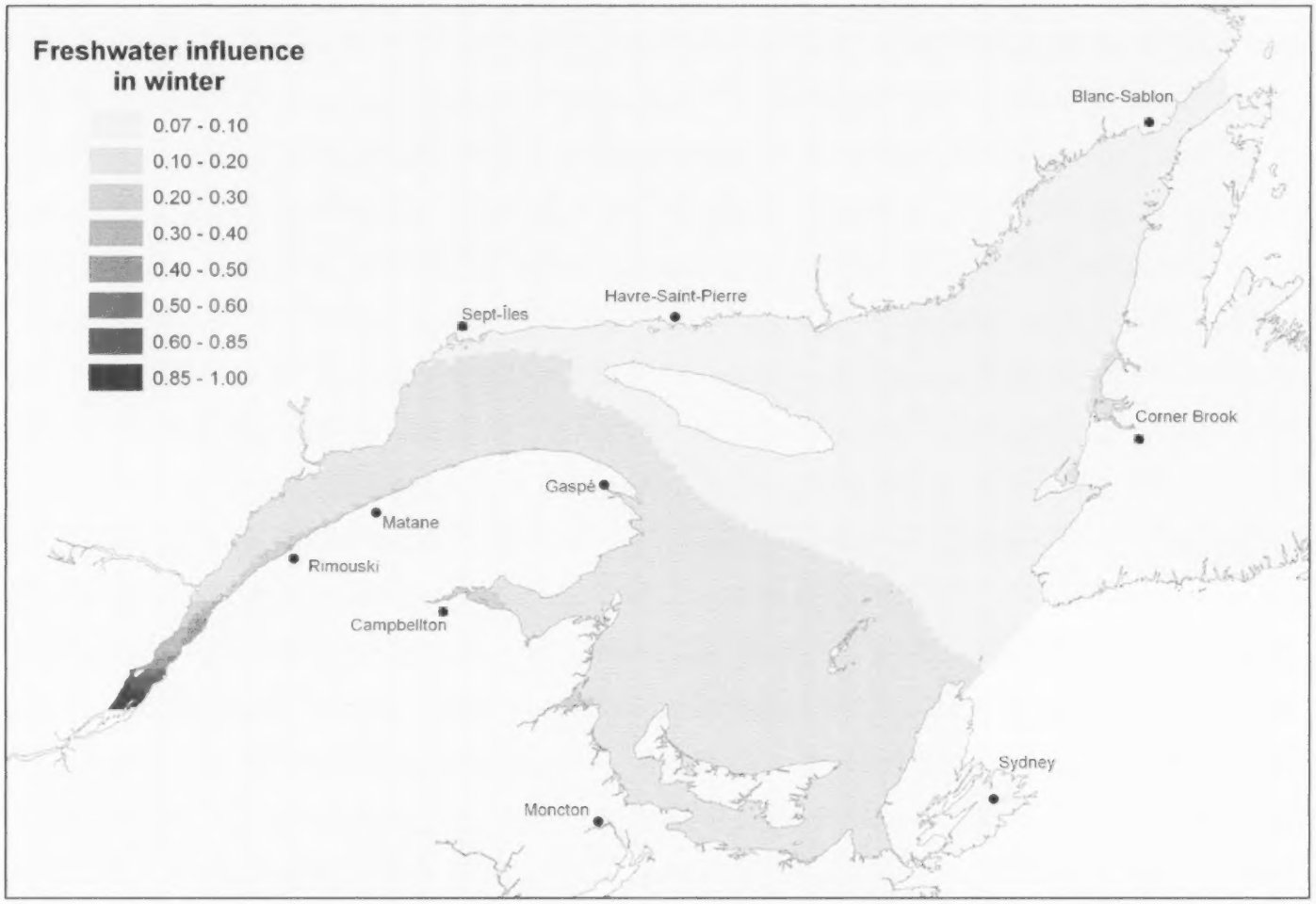

Figure 22. Freshwater runoff influence in winter (period from January to March), as predicted by the 3D model, and calculated as 1-(MSAL/35), where MSAL is the average salinity of the water column from the surface down to 36.7 m, and "35" is the maximum salinity of seawater.

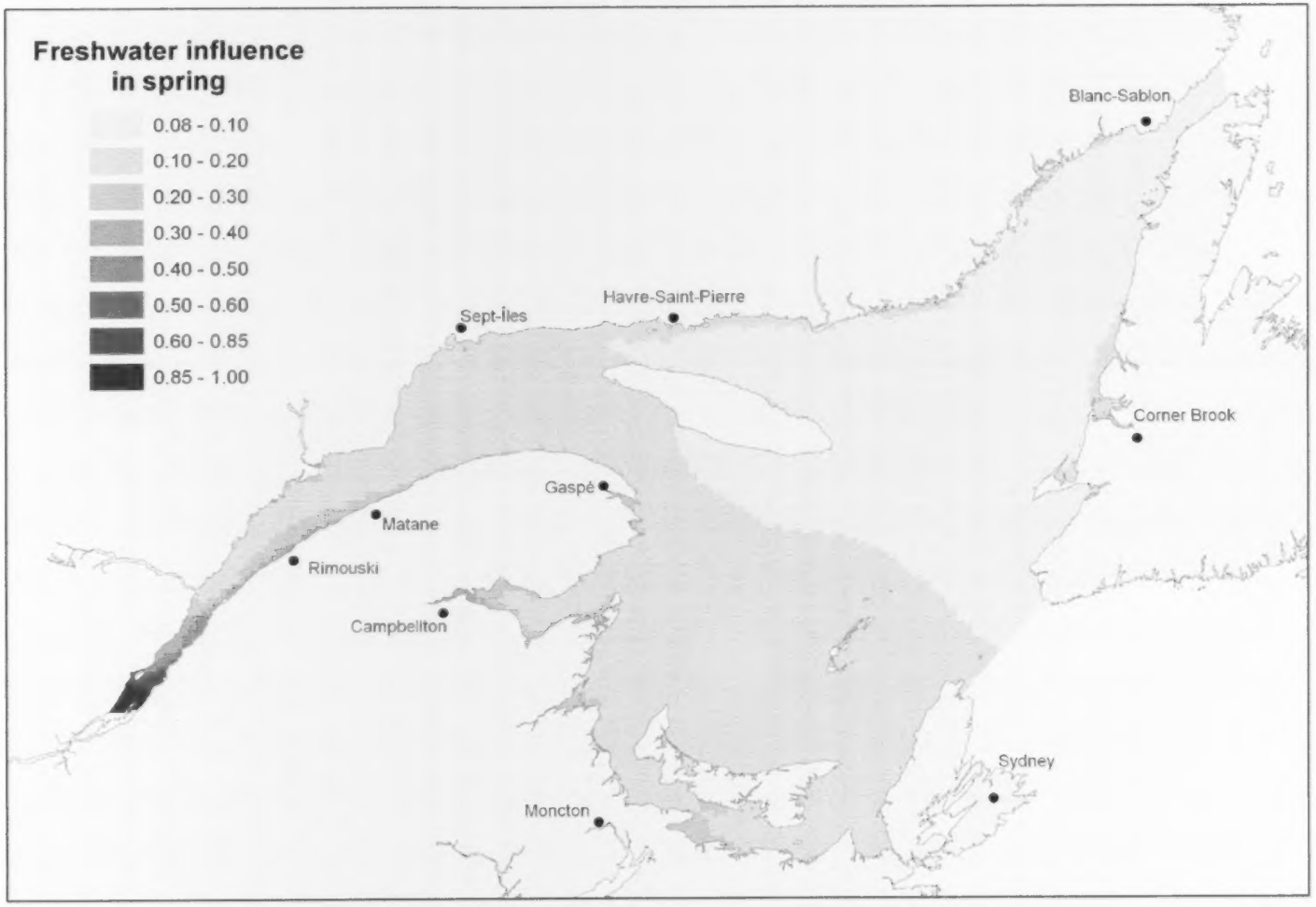

Figure 23. Freshwater runoff influence in spring (period from April to June), as predicted by the 3D model, and calculated as 1-(MSAL/35), where MSAL is the average salinity of the water column from the surface down to 36.7 m, and "35" is the maximum salinity of seawater.

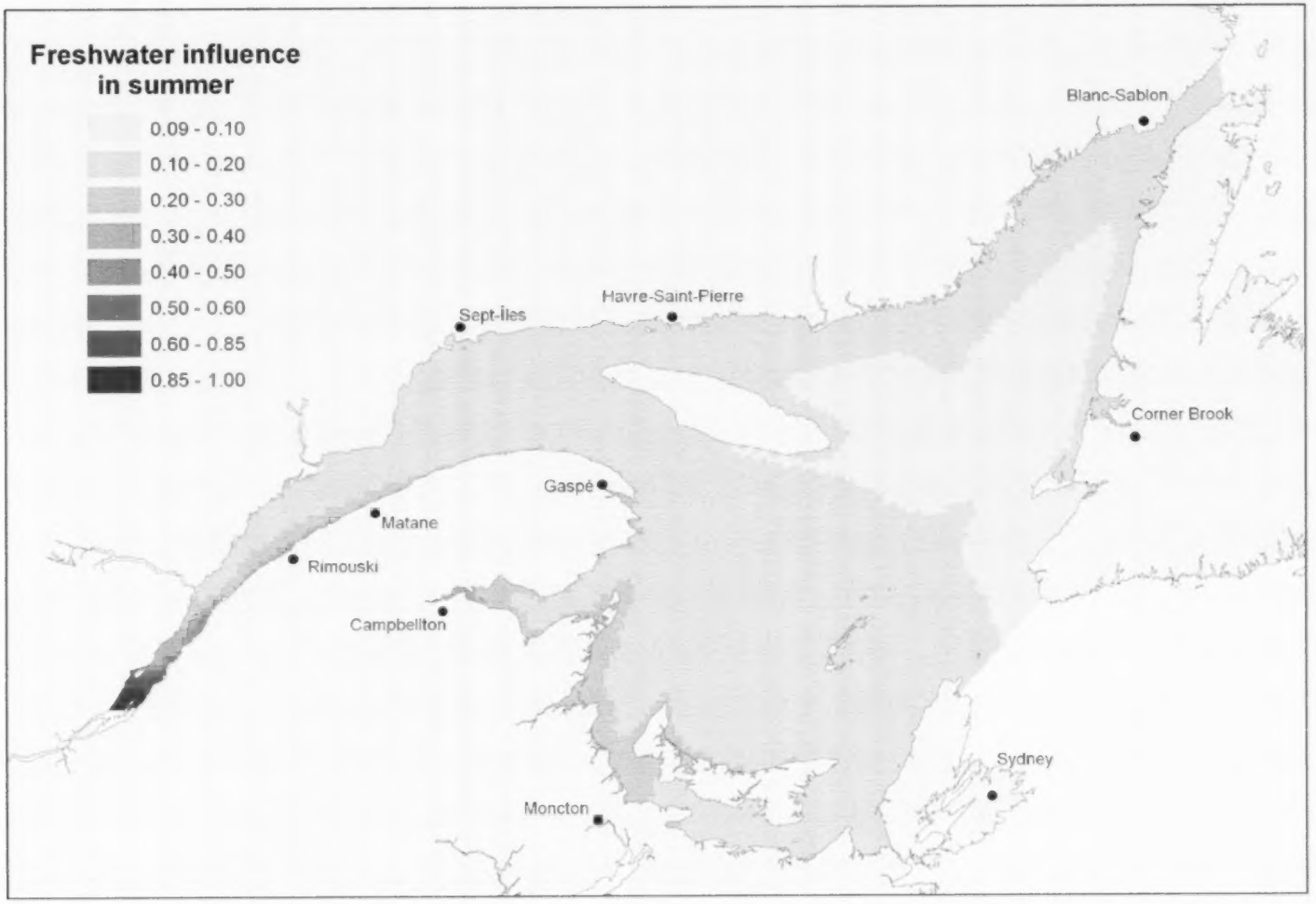

Figure 24. Freshwater runoff influence in summer (period from July to September), as predicted by the 3D model, and calculated as 1-(MSAL/35), where MSAL is the average salinity of the water column from the surface down to 36.7 m, and "35" is the maximum salinity of seawater.

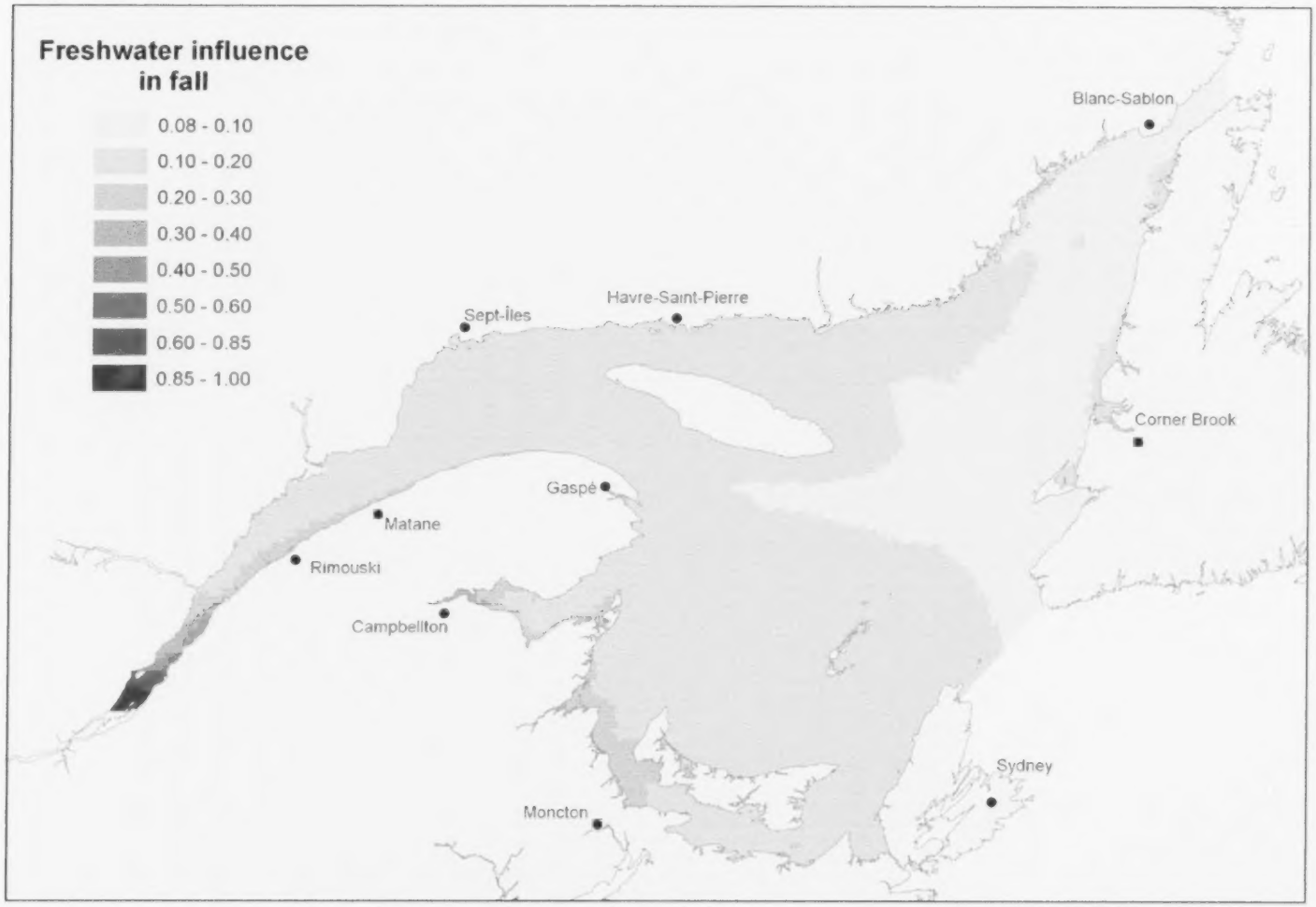

Figure 25. Freshwater runoff influence in fall (period from October to December), as predicted by the 3D model, and calculated as 1-(MSAL/35), where MSAL is the average salinity of the water column from the surface down to 36.7 m, and "35" is the maximum salinity of seawater.

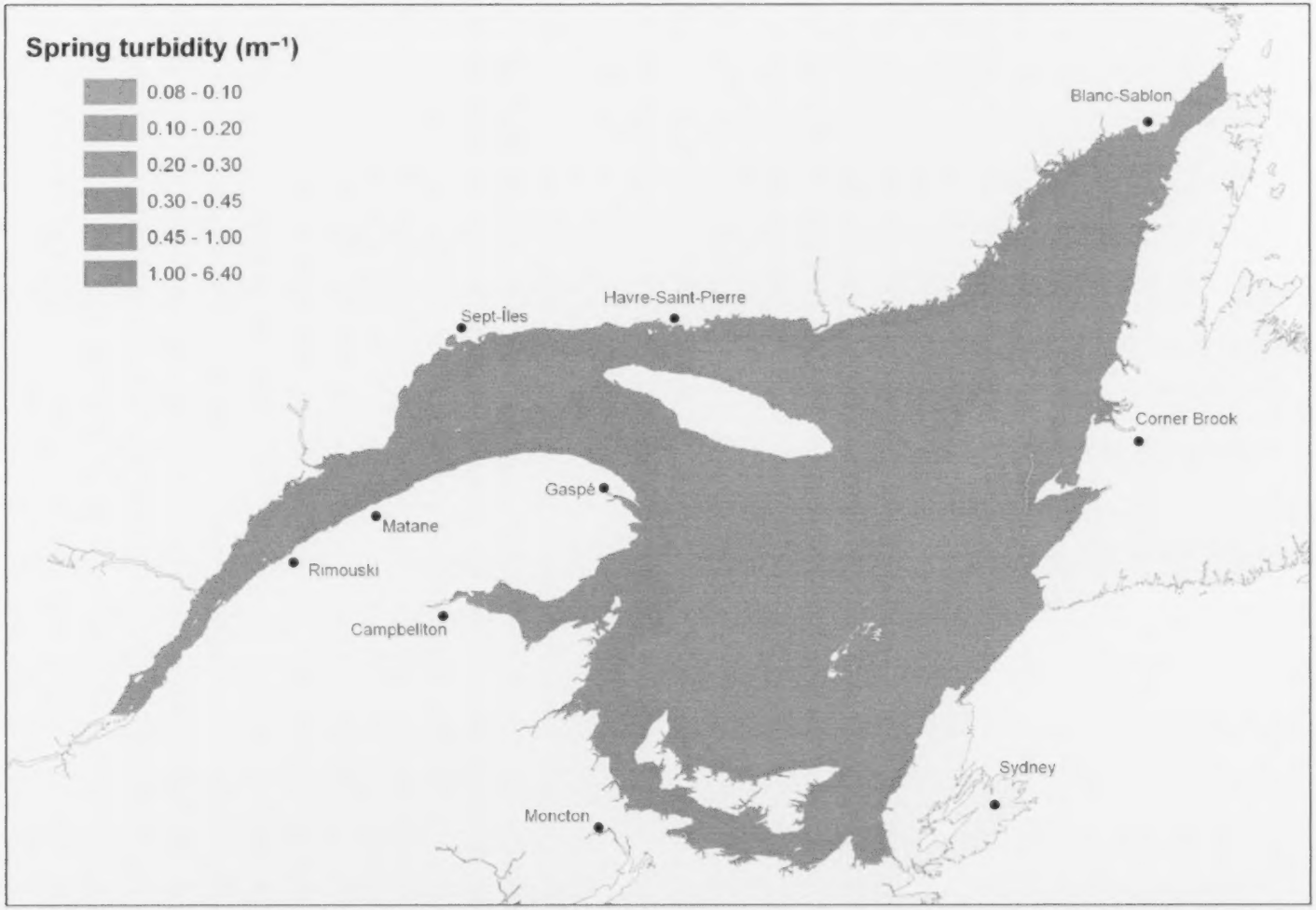

Figure 26. Mean turbidity in spring (period from April to June). Source: NASA, satellite AQUA, MODIS spectroradiometer-based estimate of the diffuse attenuation coefficient of seawater at 490 nm (m^{-1}).

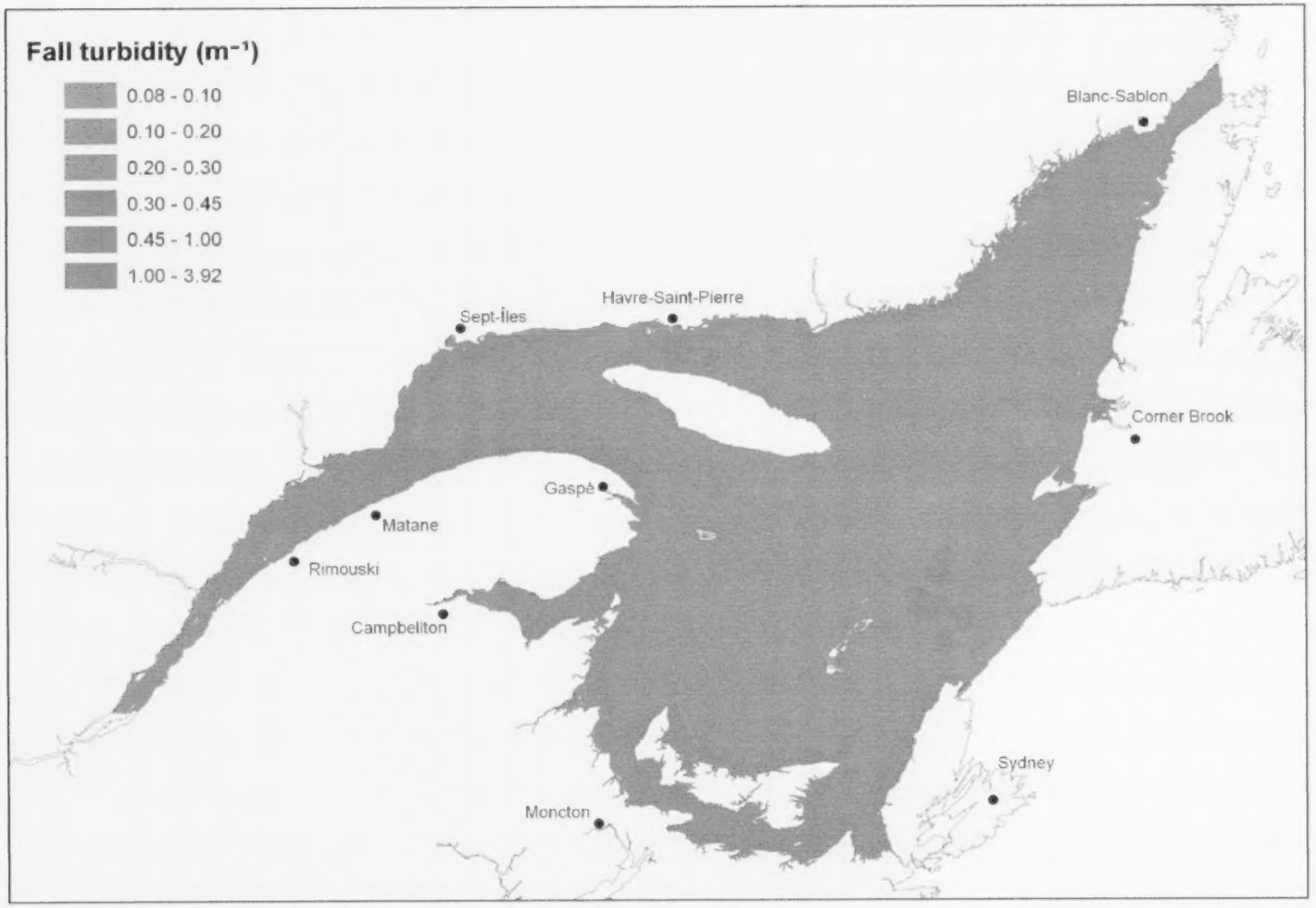

Figure 27. Mean turbidity in fall (period from October to December). Source: NASA, satellite AQUA, MODIS spectroradiometer-based estimate of the diffuse attenuation coefficient of seawater at 490 nm (m^{-1}).

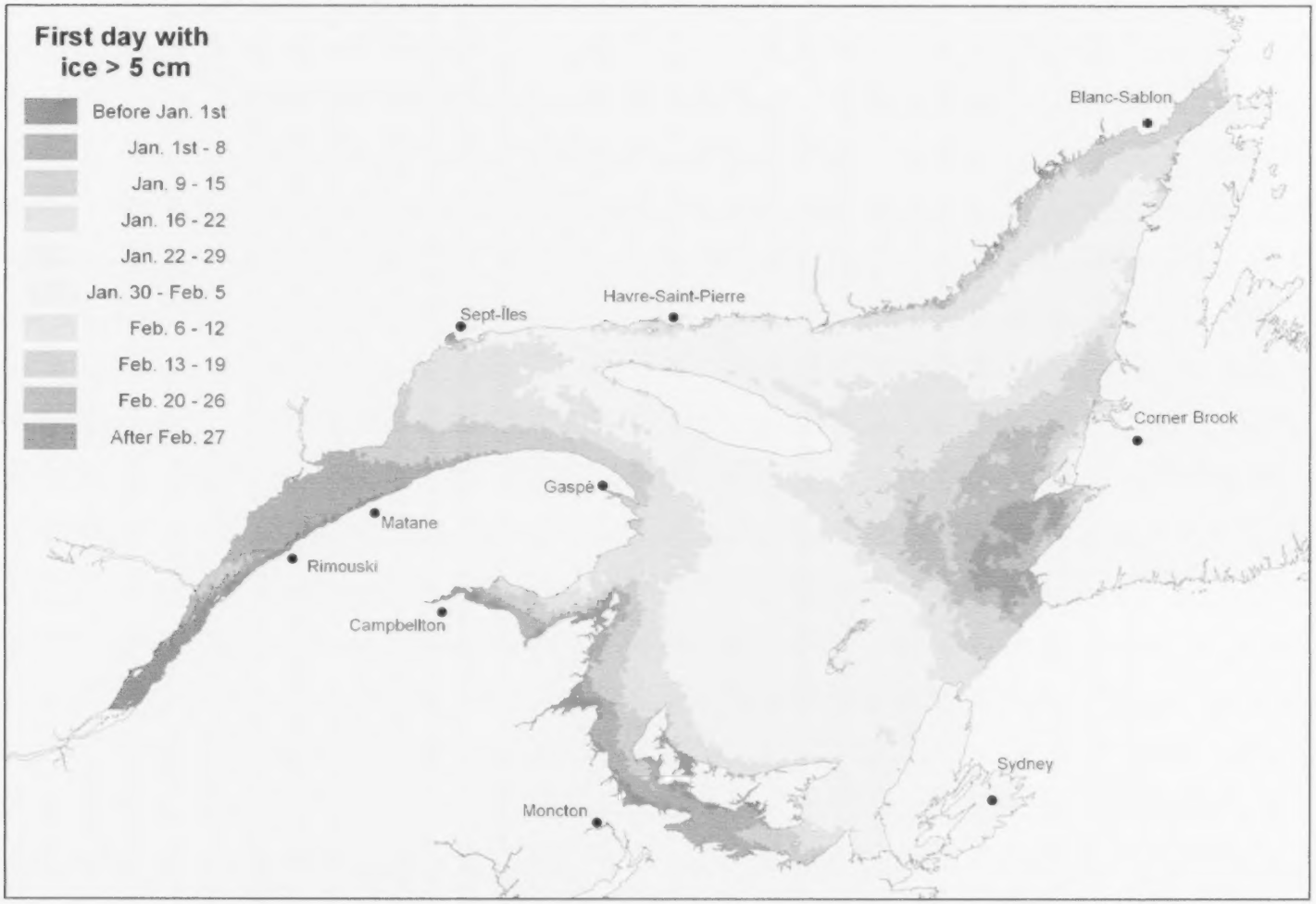

Figure 28. First day of the year when mean ice thickness is greater than 5 cm.

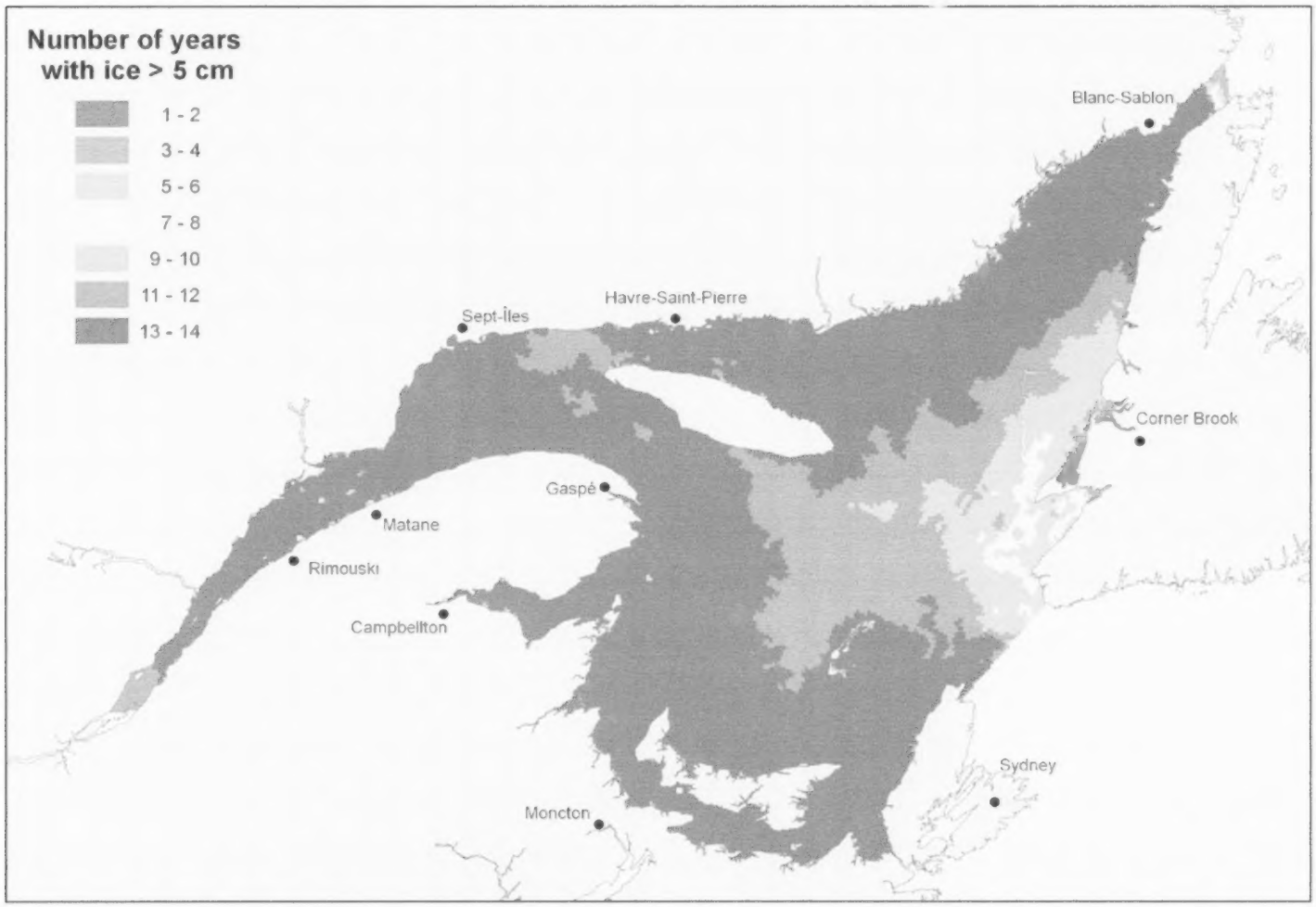

Figure 29. Number of years when ice thickness reached the 5 cm mark (14 years of record).

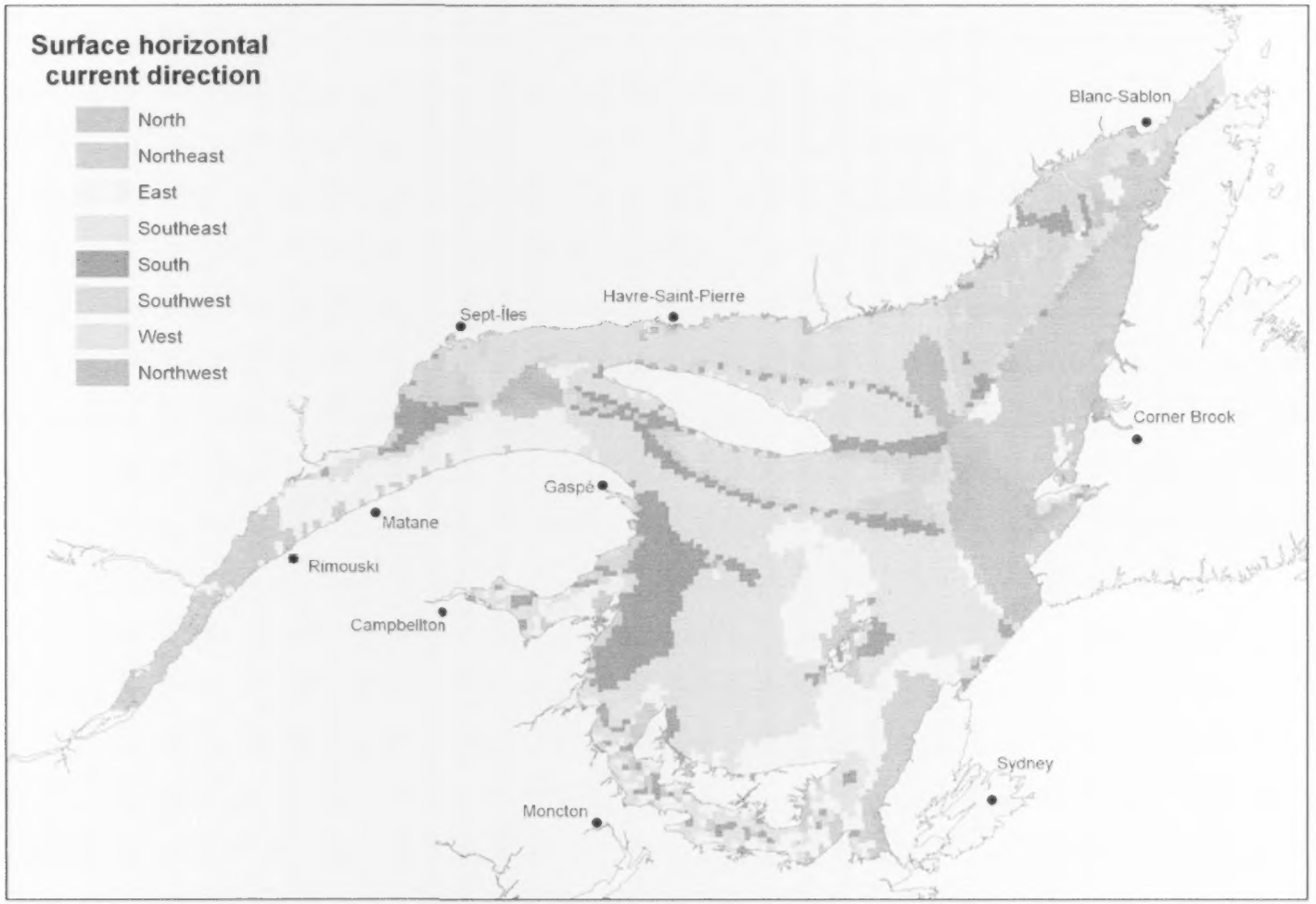

Figure 30. Direction of the horizontal current at the surface (0–6.2 m layer), coded into eight categories of 45 degrees each, code 1 (north) including angles from 337.5 to 360 degrees and from 0 to 22.5 degrees, code 2 angles from 22.5 to 67.5 degrees, etc.

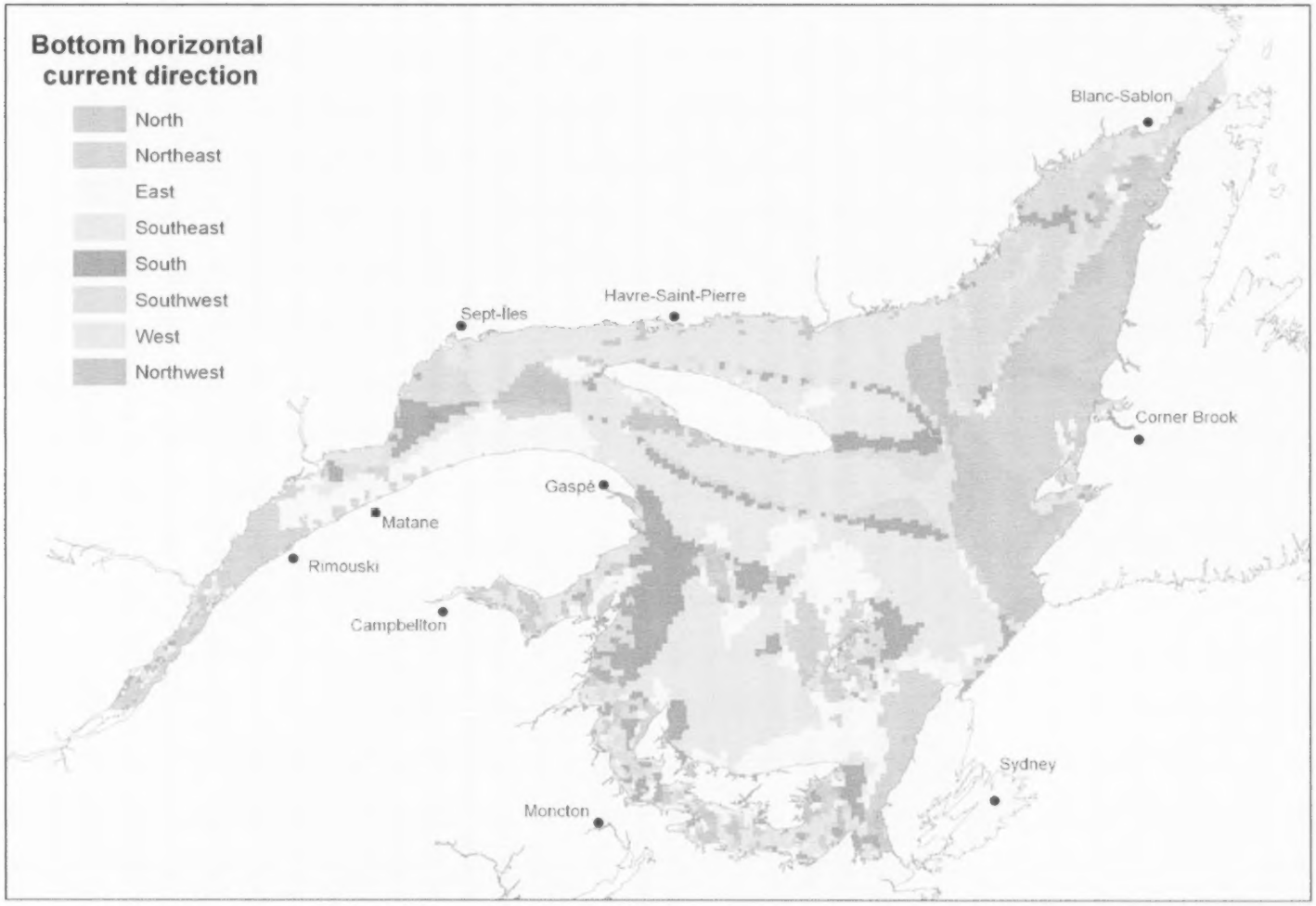

Figure 31. Direction of the horizontal current at DEPTHMEAN (on the bottom or at 30 m for BENTHIC_B=0 cells), coded into eight categories of 45 degrees each, code 1 (north) including angles from 337.5 to 360 degrees and from 0 to 22.5 degrees, code 2 angles from 22.5 to 67.5 degrees, etc.

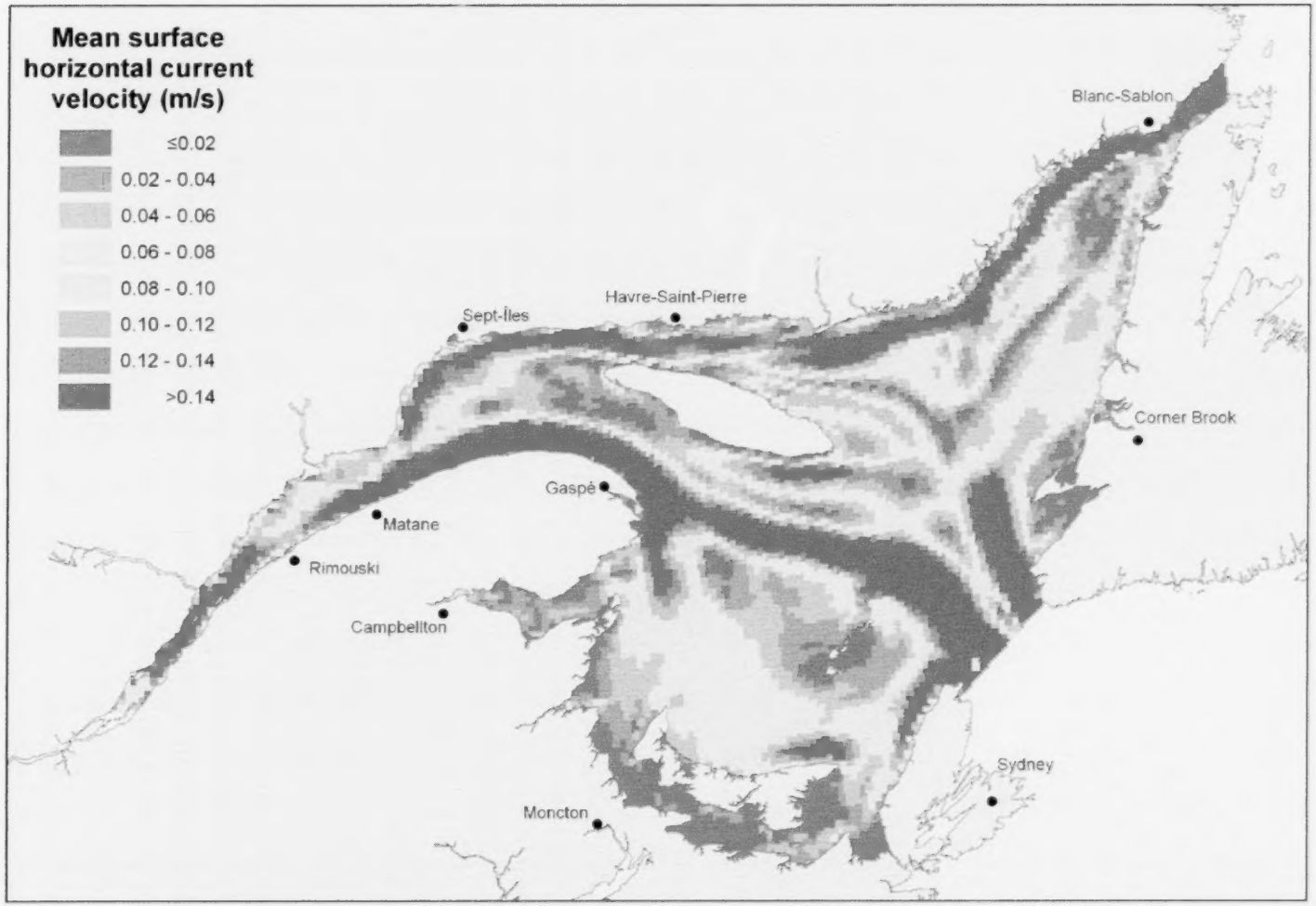

Figure 32. Mean horizontal current velocity (m/s) predicted by the 3D model at the surface (0–6.2 m layer).

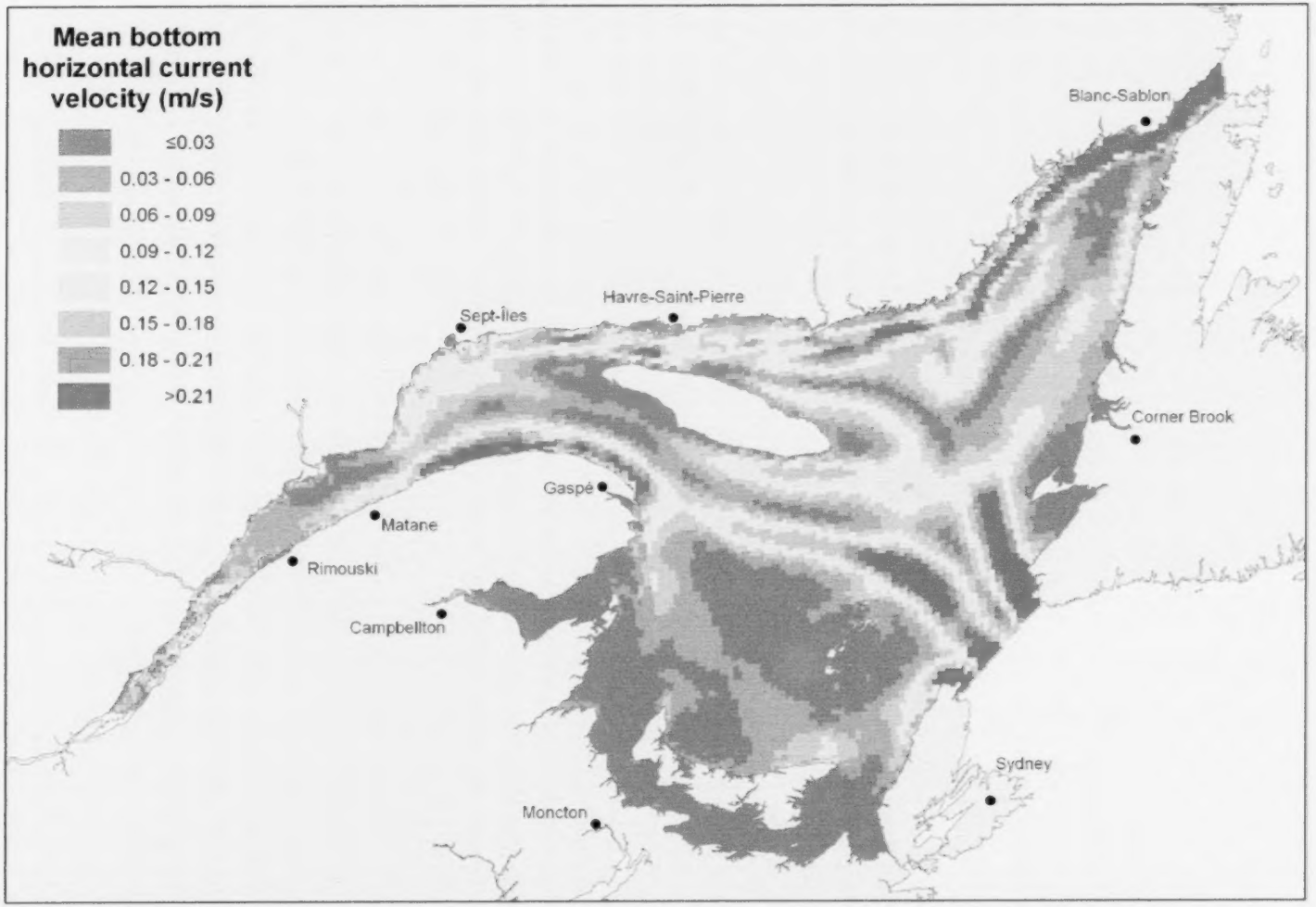

Figure 33. Mean horizontal current velocity (m/s) at the depth value set by DEPTHMEAN (on the bottom or at 30 m for BENTHIC_B=0 cells), as predicted from the corresponding layer by the 3D model.

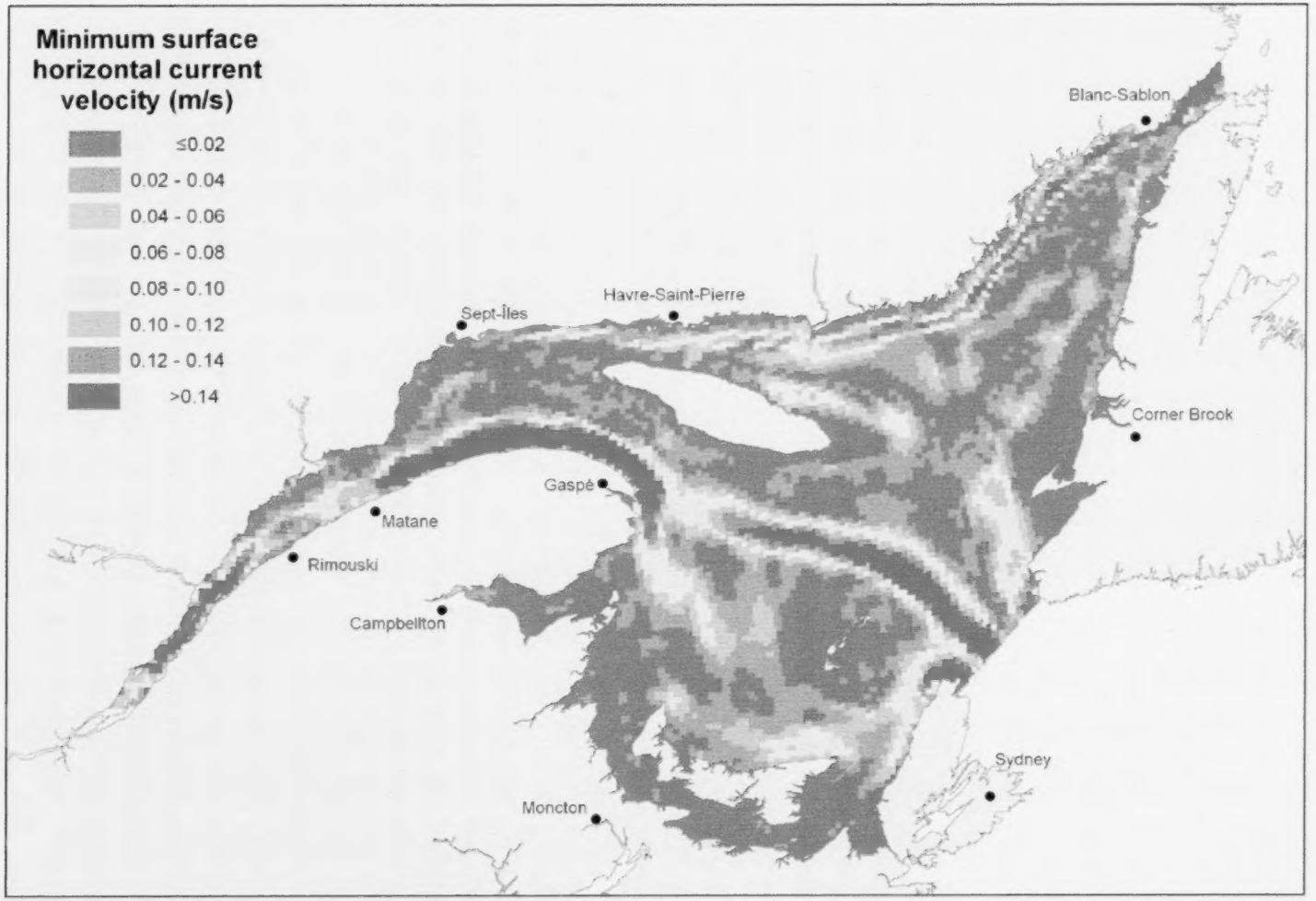

Figure 34. Minimum horizontal current velocity (m/s) predicted by the 3D model at the surface (0–6.2 m layer).

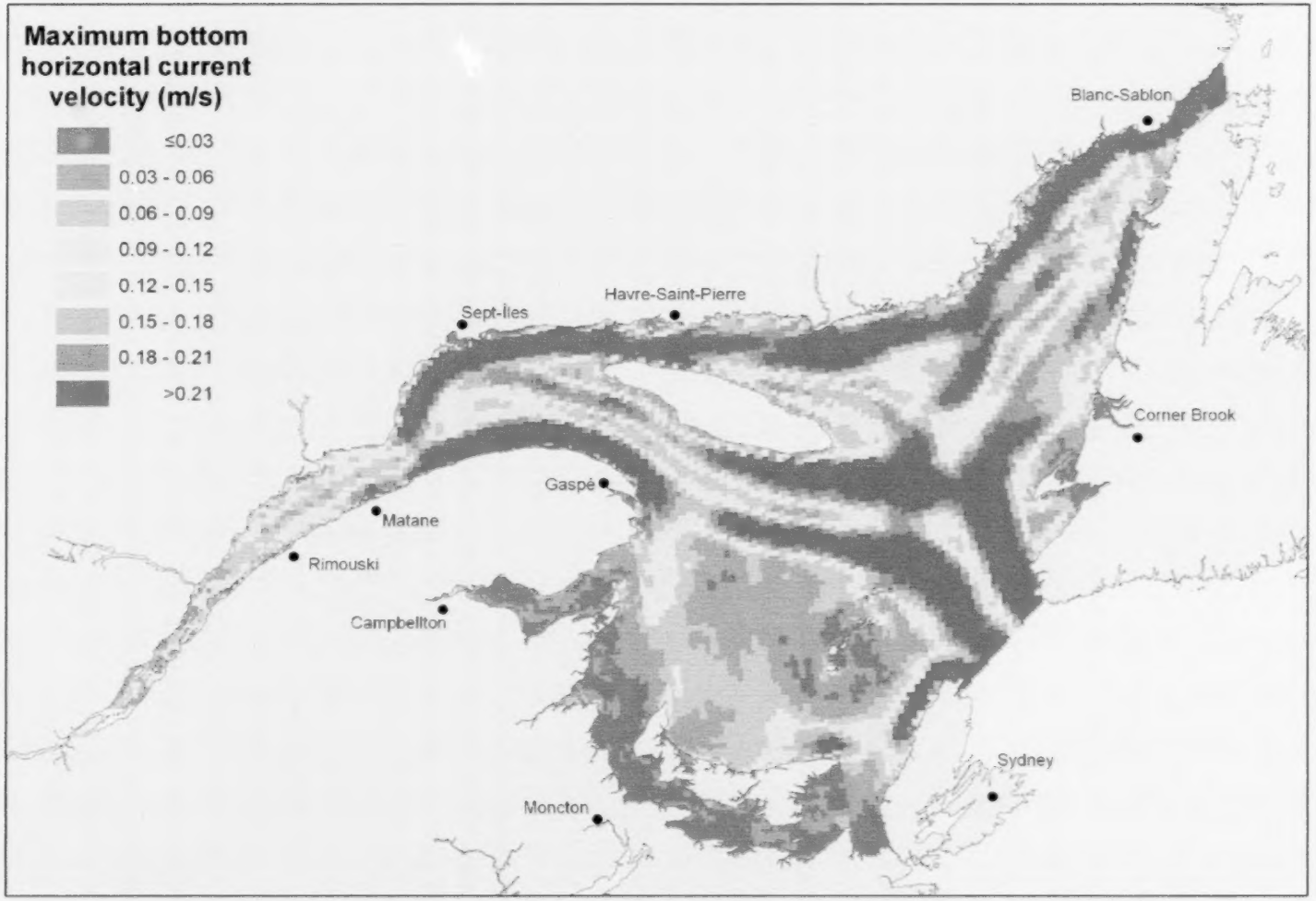

Figure 35. Maximum horizontal current velocity (m/s) at the depth value set by DEPTHMEAN (on the bottom or at 30 m for BENTHIC_B=0 cells), as predicted from the corresponding layer by the 3D model.

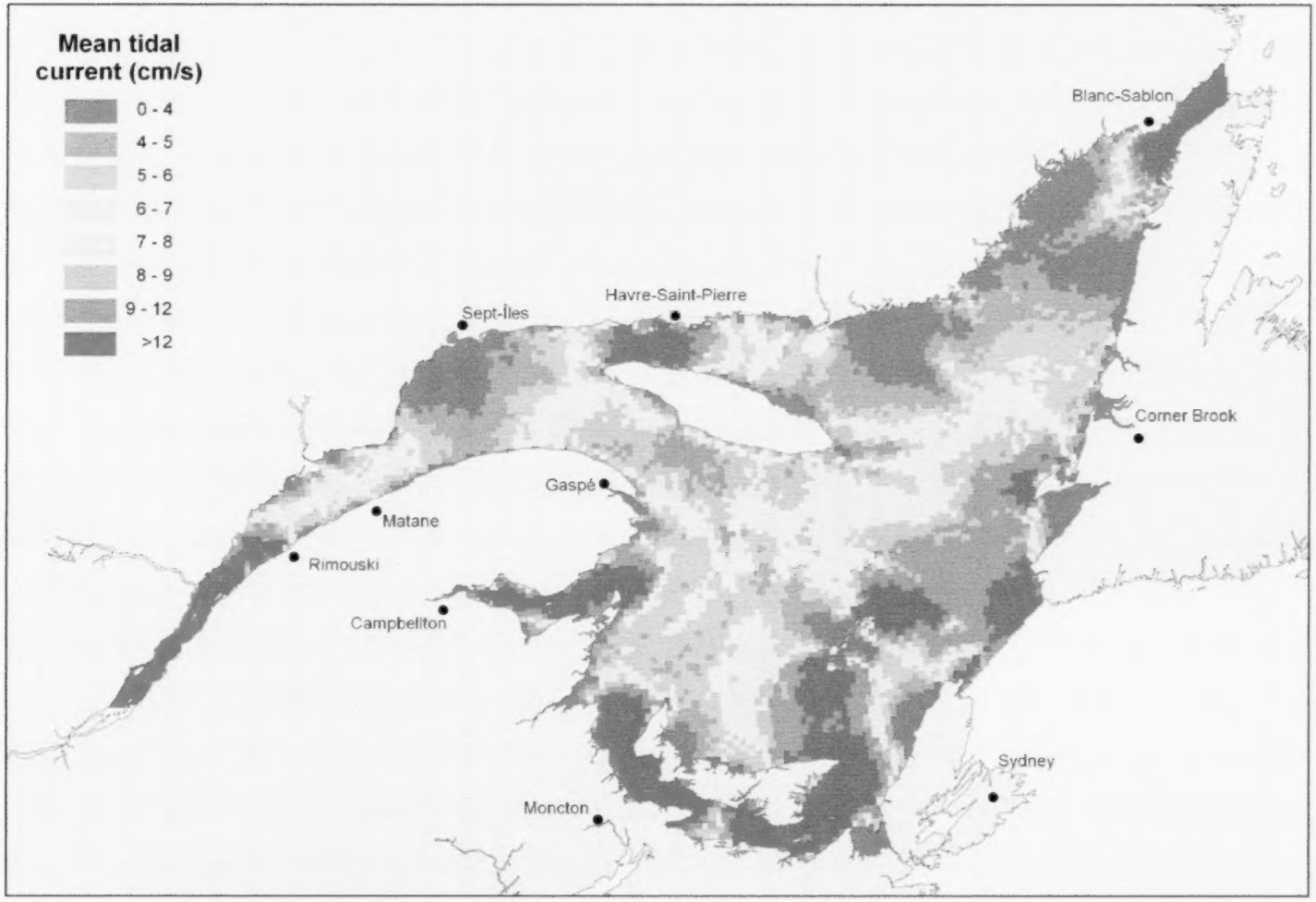

Figure 36. Mean tidal current (cm/sec) associated with the M2 component of the tide.

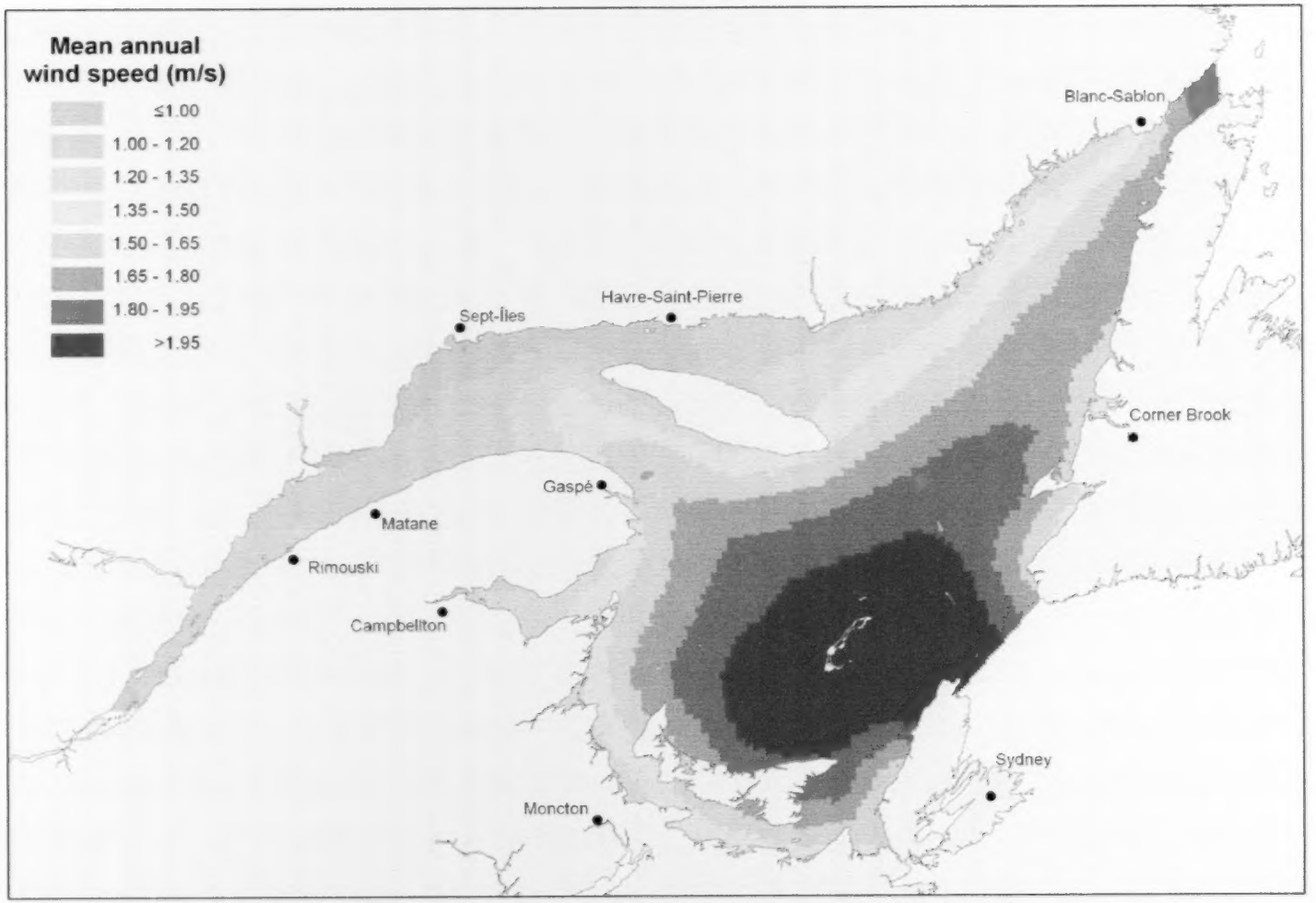

Figure 37. Mean annual wind speed (m/sec)

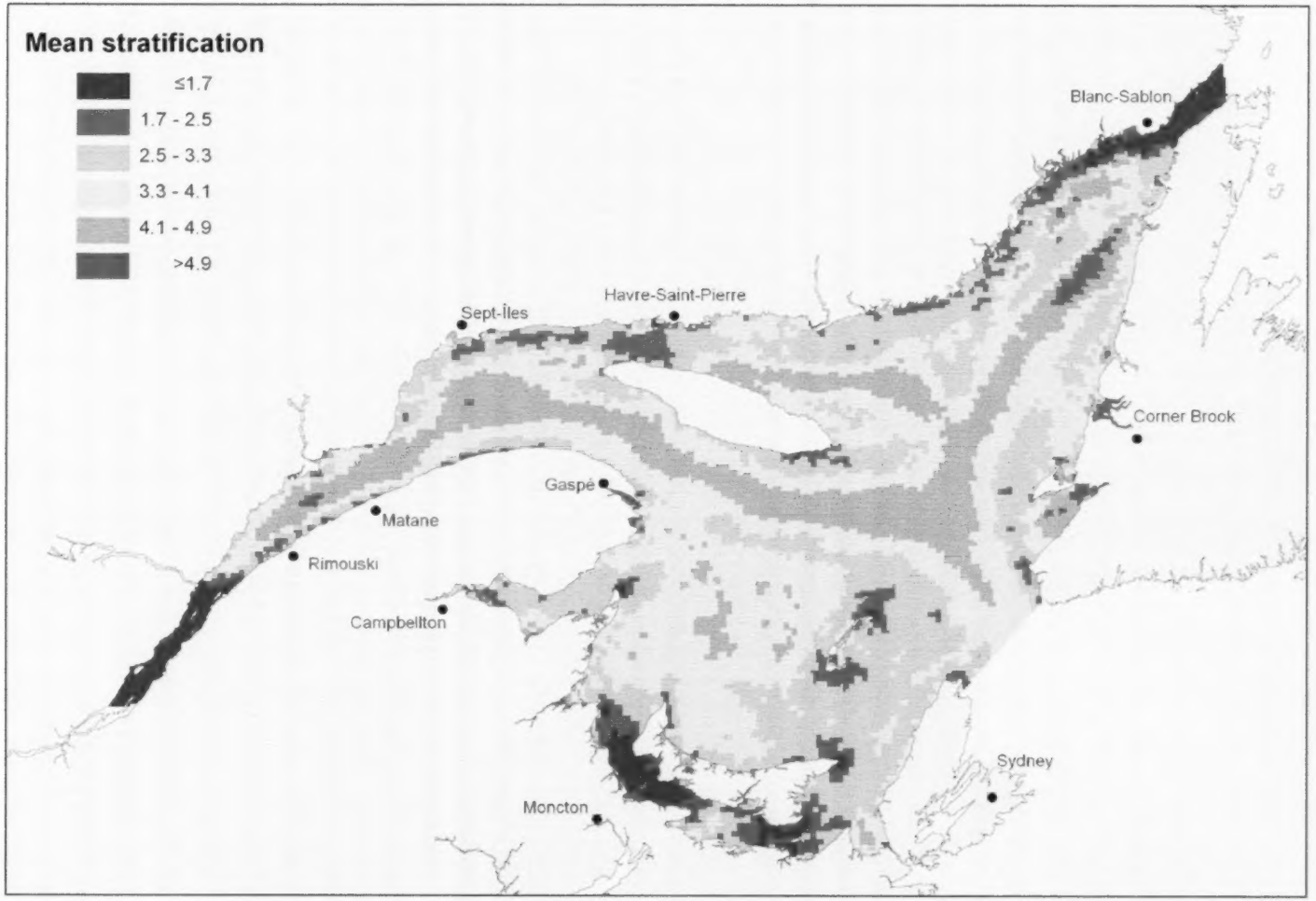

Figure 38. Simpson-Hunter water column stability parameter, mean value for a 50 d period (17 October to 5 December, 2007). This parameter is unitless; values near 0 indicate strong mixing, high values indicate a stratified water column.

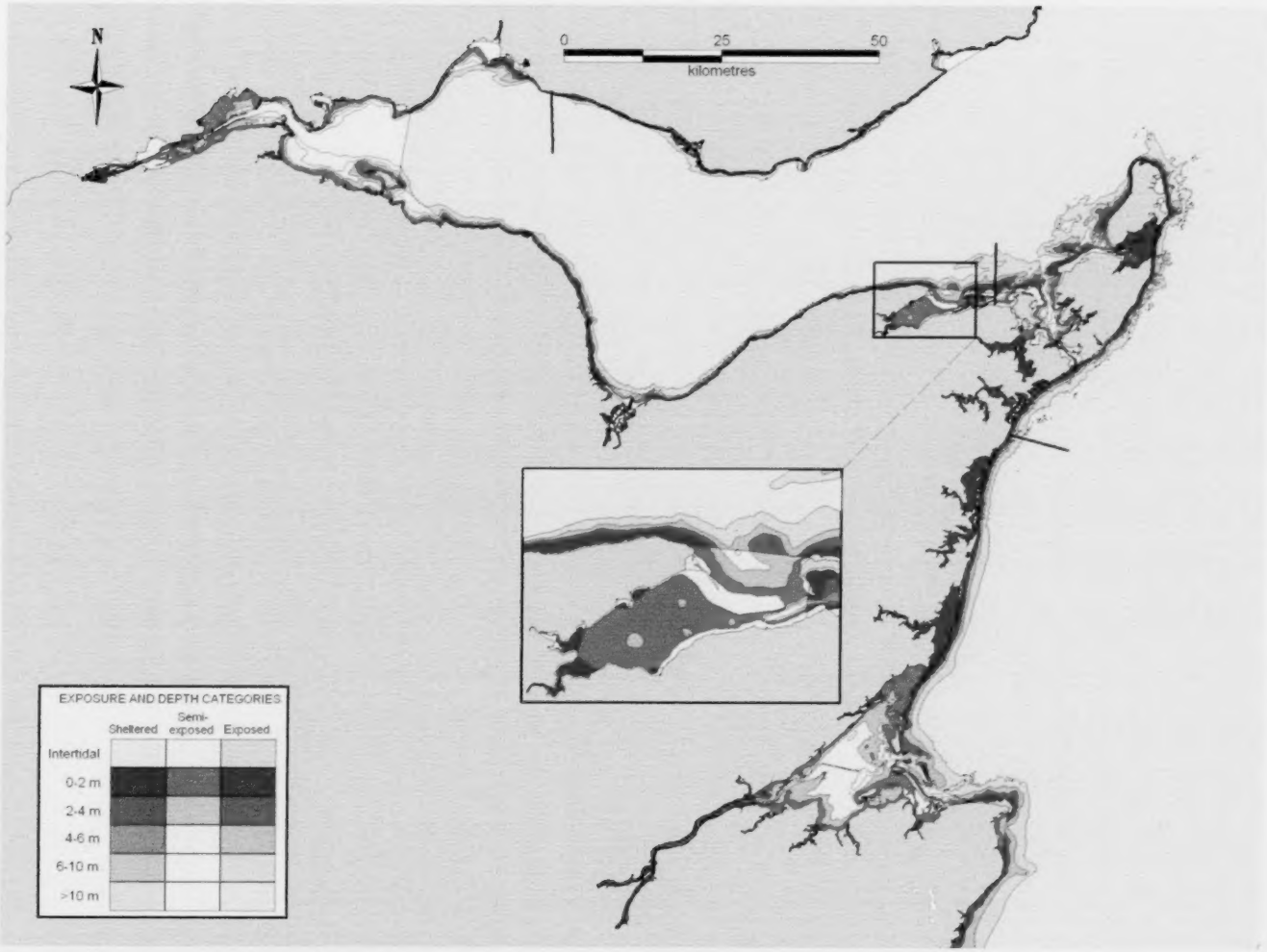

Figure 39. Coastal habitat less than 10 m deep by depth and exposure category in the Baie des Chaleurs, Miscou Island and Miramichi areas. The figure was drawn from Cairns et al. (2012, figure 23).

Figure 40. Cells located within 50 km of all of the following features in the Shoreline Classification and Pre-spill database: sand beach, marsh, and mud flat (light blue areas). Within light blue areas, dark areas indicate cells located within 10 km of known eelgrass beds.

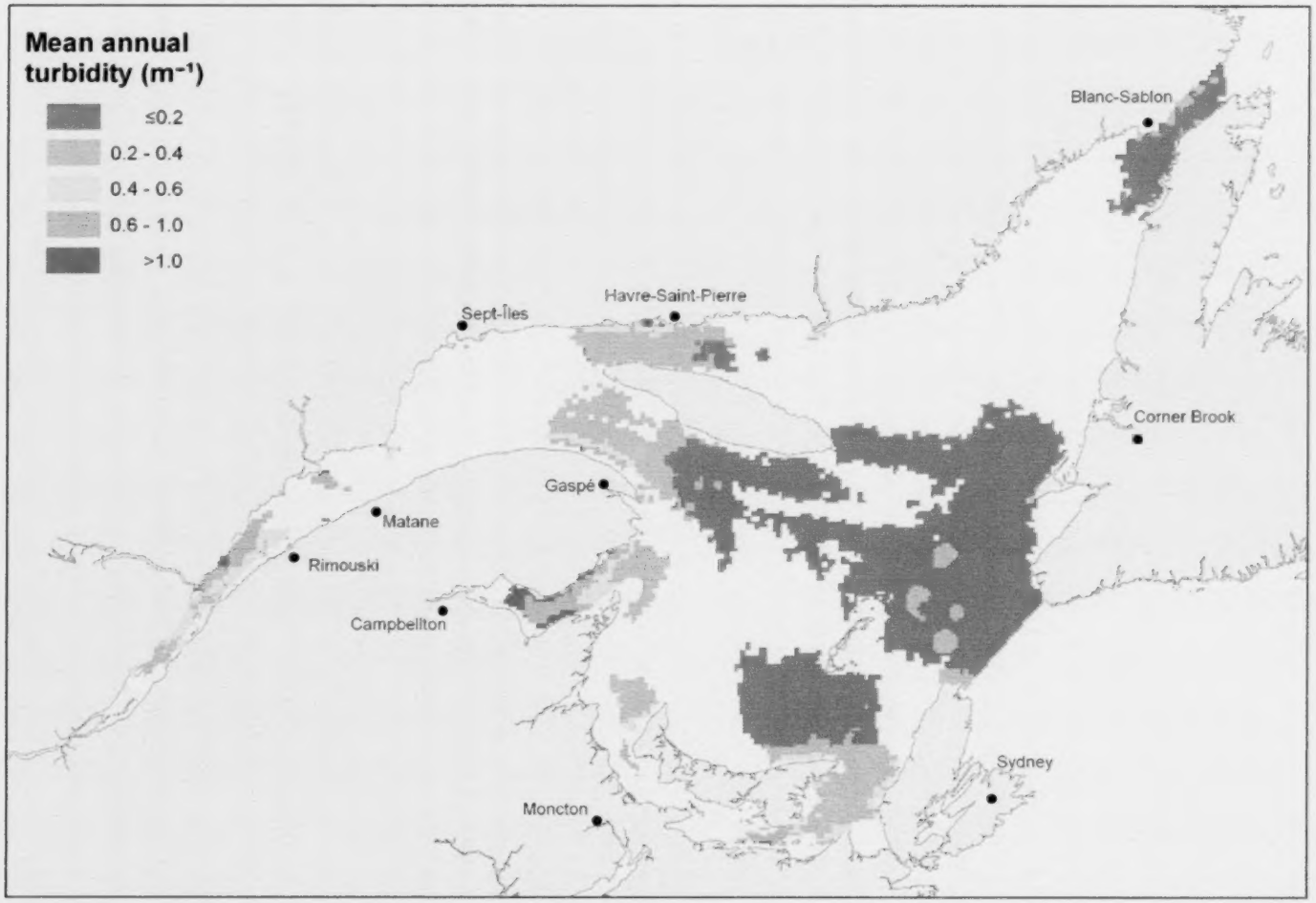

Figure 41. Pelagic cells exhibiting low mean values of the Simpson-Hunter water column stability parameter (< 4.5) and mean tidal current velocities > 7 cm/sec, broken down by mean annual turbidity.

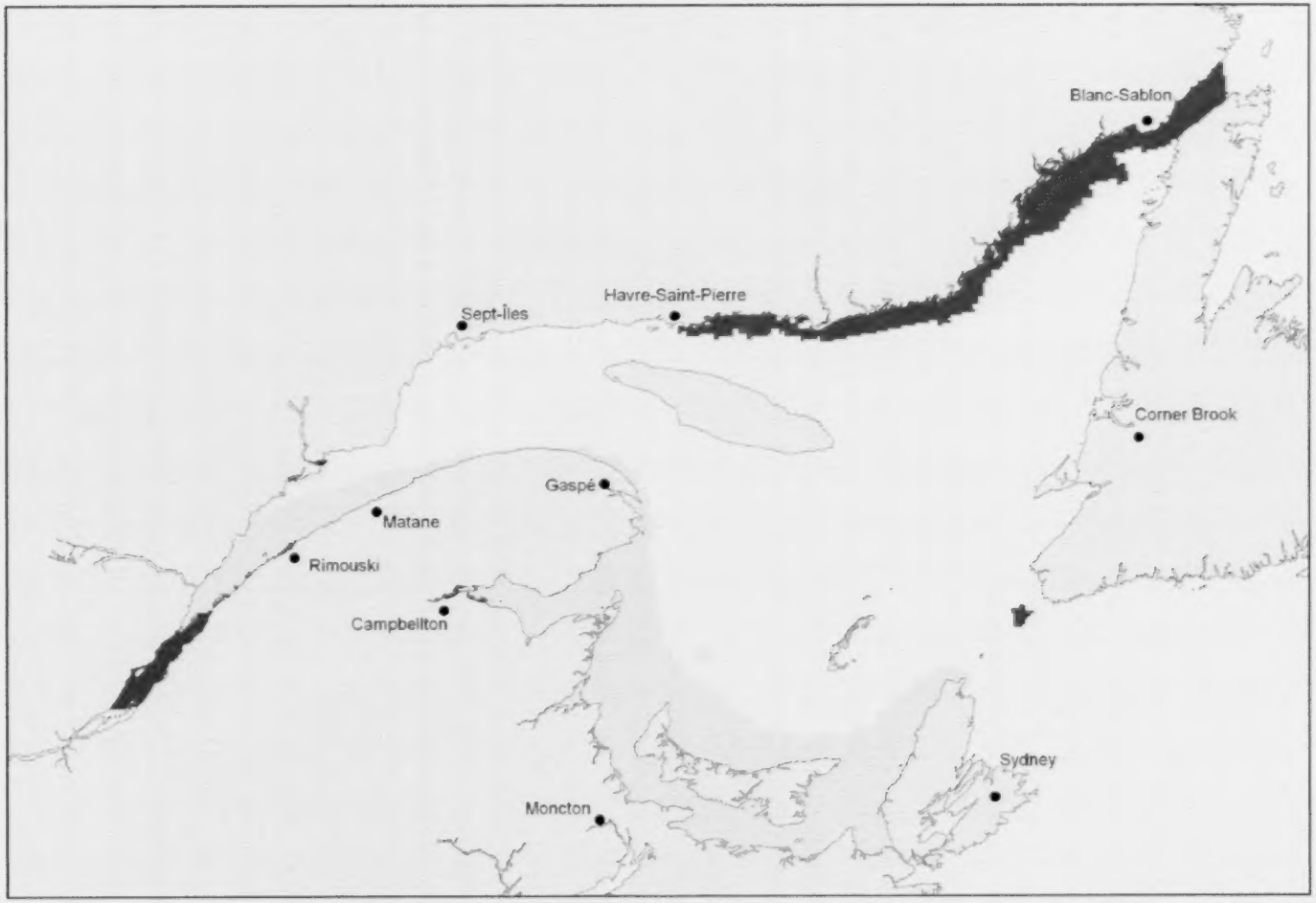

Figure 42. Cells classified as being brackish (brown and beige shades) or more saline (dark blue). Blue: mean bottom salinity > 30, maximum surface salinity > 32, and freshwater influence <0.09; beige: mean bottom salinity < 30, maximum surface salinity < 32, and freshwater influence > 0.08; brown: mean bottom salinity < 24.

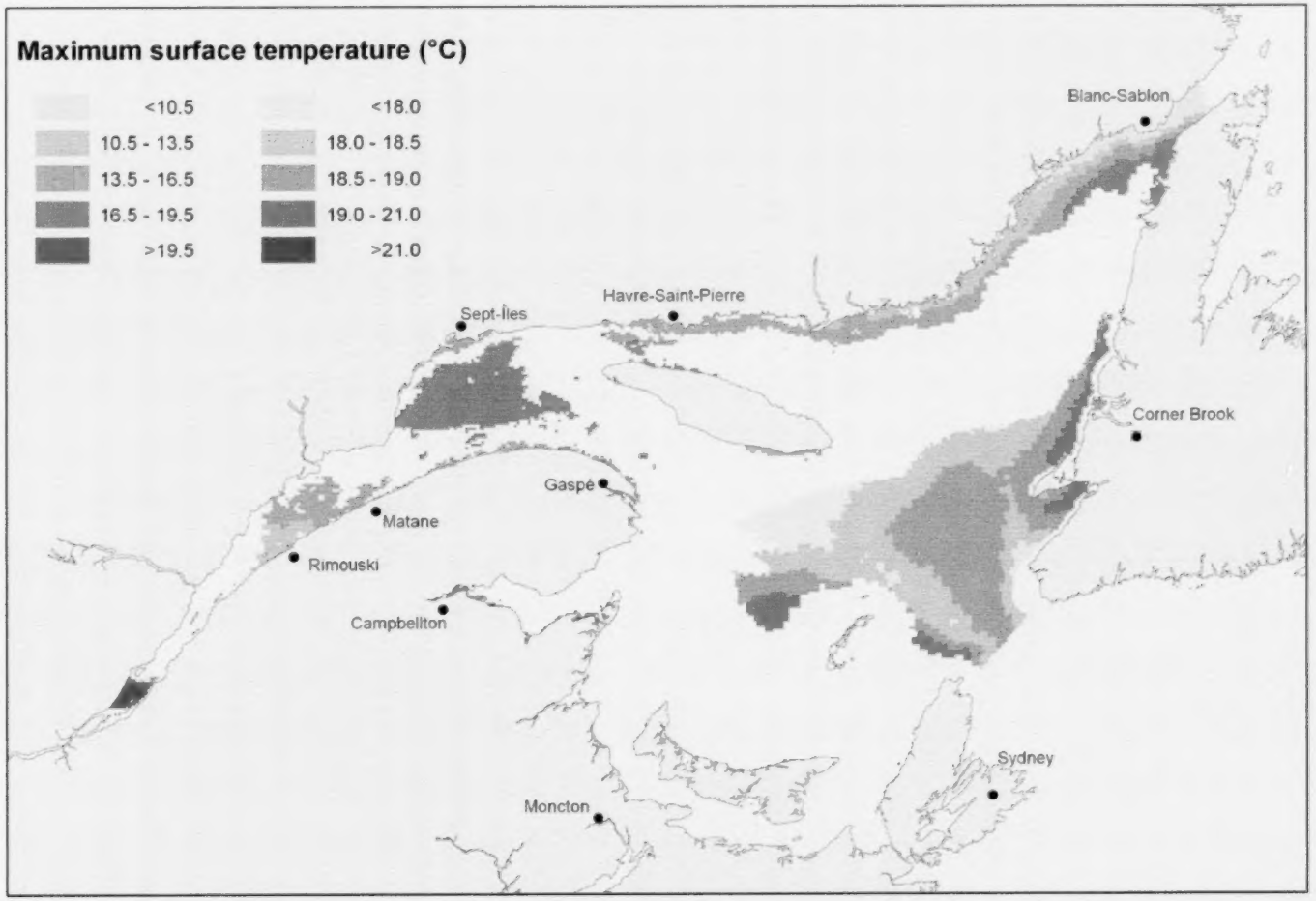

Figure 43. Cells classified as belonging to an arctic environment (blue shades) or a more temperate environment (brown shades). Blue: years with ice > 5 cm = 14, number of weeks with temperature below 2°C > 21, number of degree-days above 2°C from week 31 to week 40 < 850, and minimum surface temperature <-0.5 °C; brown: mirror values for the same parameters. Both categories are broken down by maximum surface temperature.

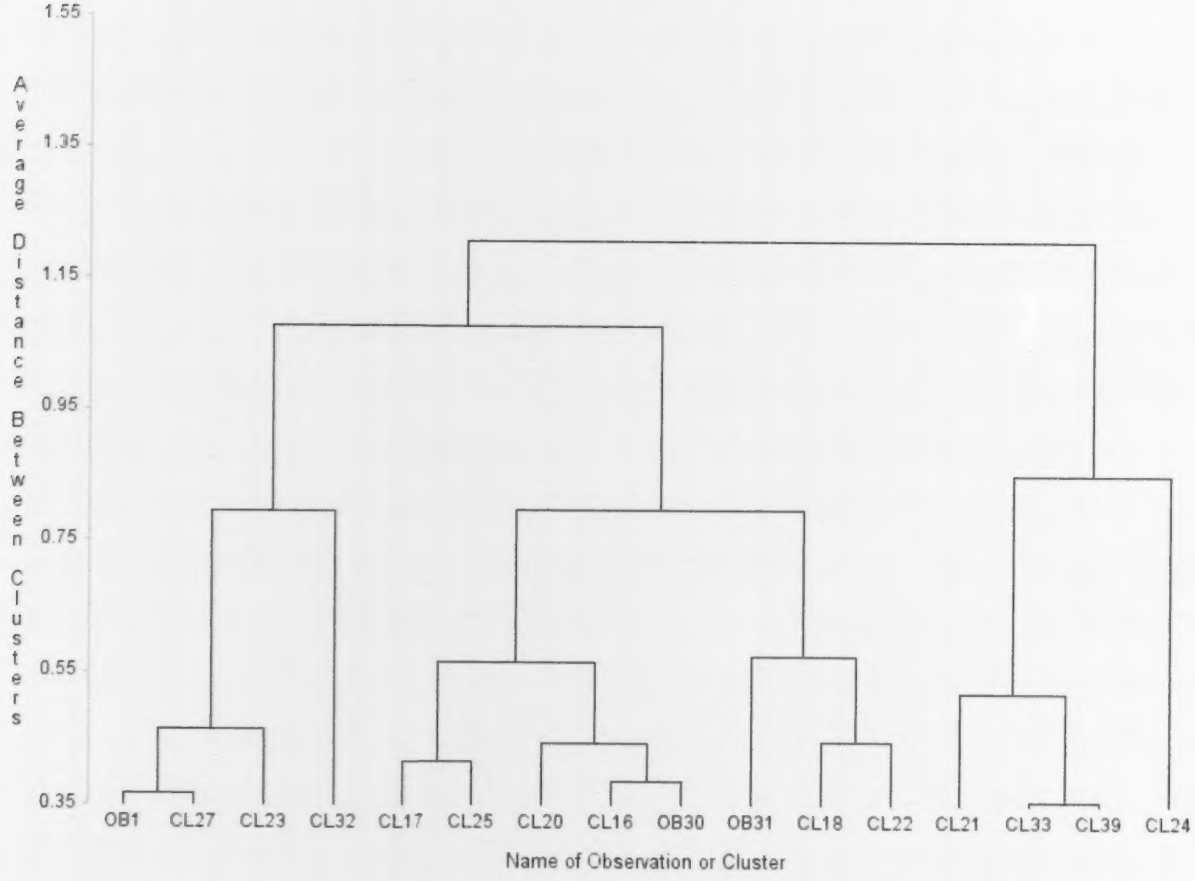

Figure 44. Tree diagram showing 16 clusters formed at an average distance of 0.35. Clusters were determined using a disjoint (i.e., non-hierarchical) cluster analysis based on Euclidean distances (FASTCLUS procedure; SAS software). Outliers (clusters of less than 30 cells) were detected and re-assigned to the remaining clusters. The output from this analysis was analyzed with the CLUSTER procedure (unweighted pair-group averages to determine the hierarchy among clusters and, indirectly, among the 39,337 cells in the study area (see method 2 in Materials and Methods).

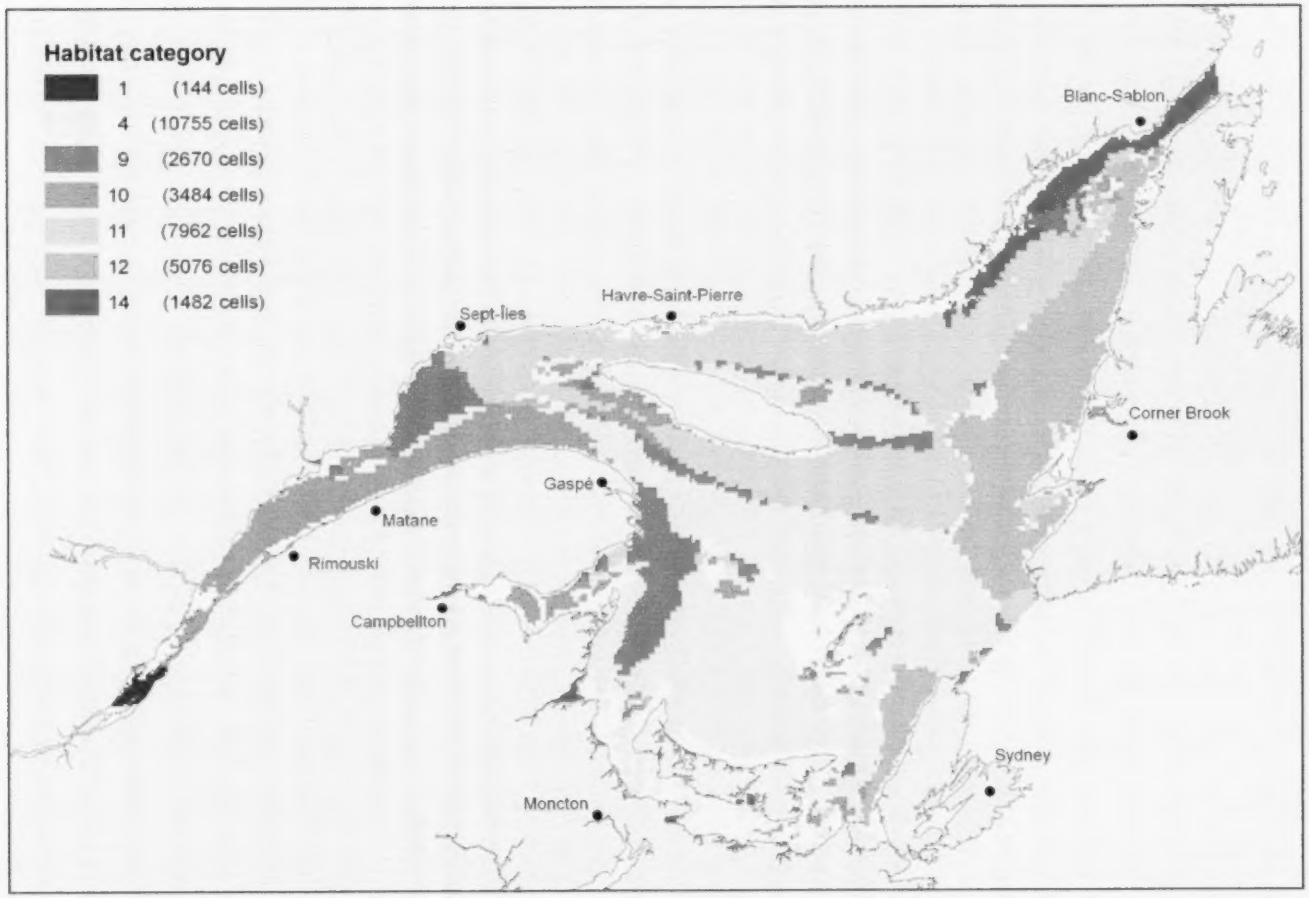

Figure 45. Spatial distribution of seven clusters of cells based on 103 habitat descriptors and representing 80% of all cells in the study area. The analysis suggested 16 different clusters; two small clusters appeared to be made of scattered cells and were grouped with their nearest neighbour, resulting in 14 different clusters considered to represent a classification of the pelagic and coastal habitats in the estuary and Gulf of St. Lawrence (see method 2 in Materials and Methods).

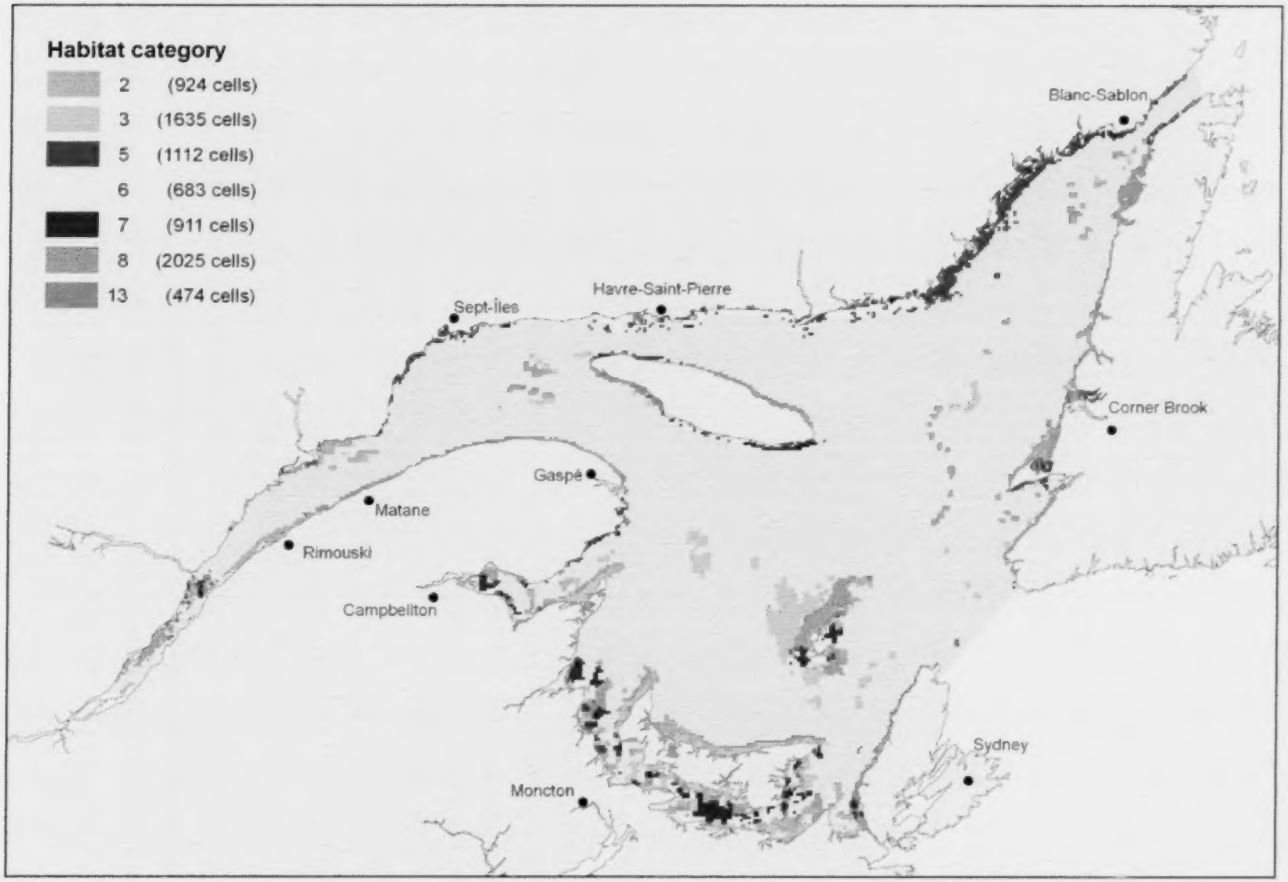

Figure 46. Spatial distribution of seven clusters of cells based on 103 habitat descriptors, mainly located near the coastline and representing 20% of all cells in the study area. The analysis suggested 16 different clusters; two small clusters appeared to be made of scattered cells and were grouped with their nearest neighbour, resulting in 14 different clusters considered to represent a classification of the pelagic and coastal habitats in the estuary and Gulf of St. Lawrence (see method 2 in Materials and Methods).

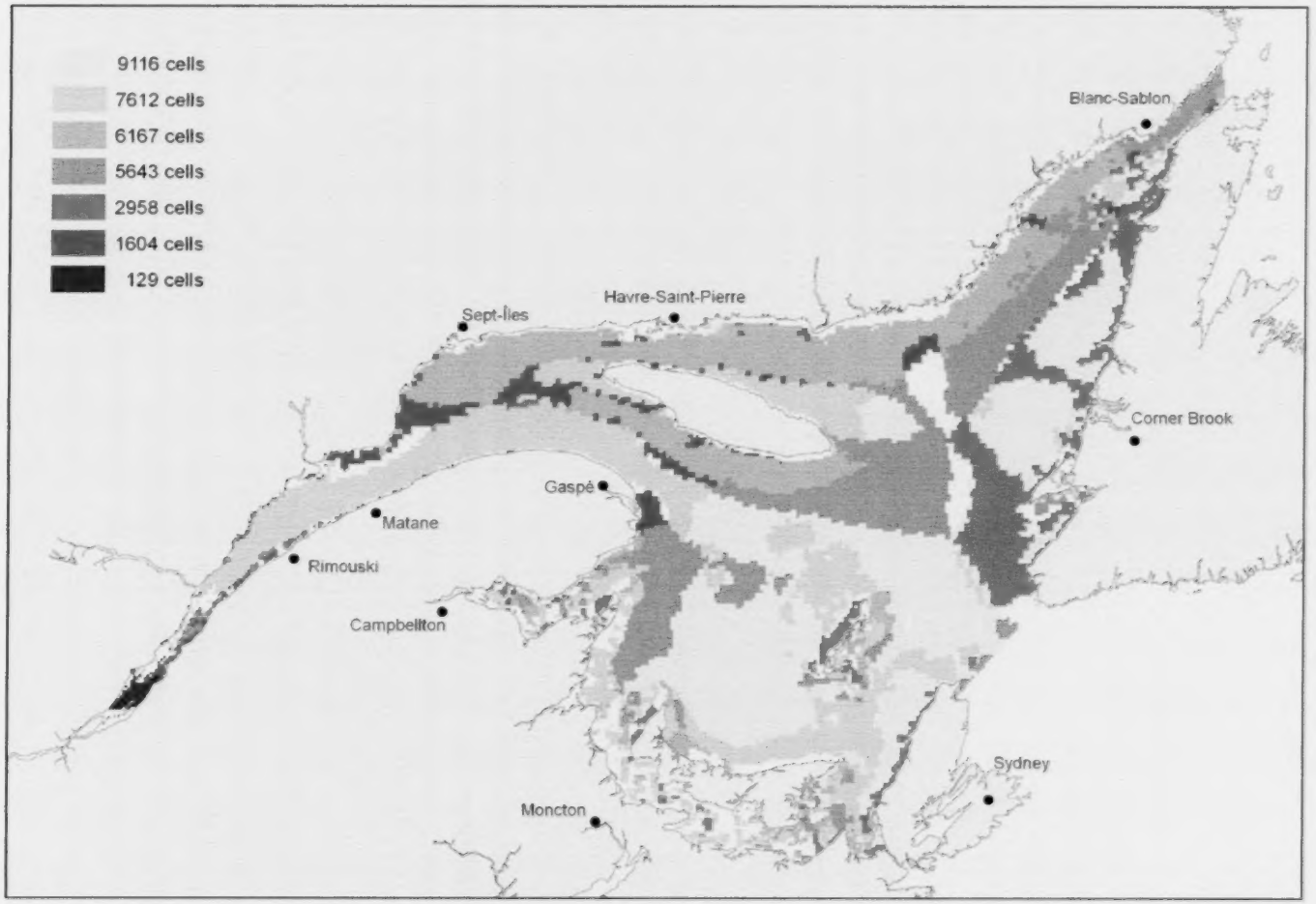

Figure 47. Spatial distribution of seven clusters of cells based on 21 habitat descriptors and representing 84% of all cells in the study area. The 103 original variables were clustered (VARCLUS procedure; SAS software) and a subset of 21 variables selected (see method 4 in Materials and Methods). Different shades indicate different habitat categories.

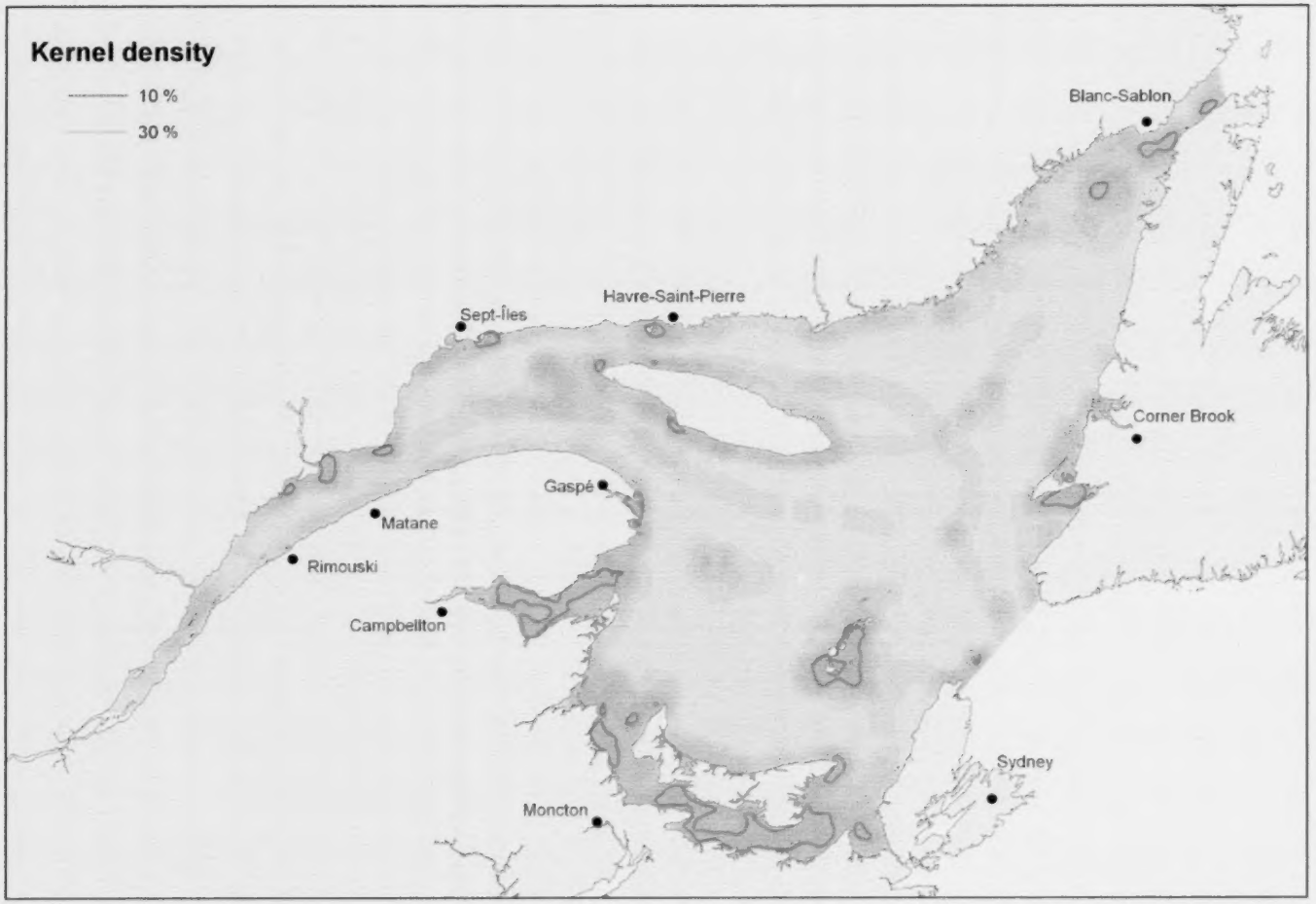

Figure 48. Habitat diversity determined as the number of different habitat categories within a distance of 11.5 km from each cell centroid (shades of blue in the background; deeper colours indicate a higher count, i.e., greater diversity). Kernel density estimation contours are overlaid.

Appendix 1. List of variables used to describe marine cells in the Microsoft Access® database with short descriptions.

Variable	Legend	Description
OBJECTID		Sequential number attributed automatically by the software (ESRI® ArcGIS®)
SHAPE		Vector data type in the geodatabase (Information generated by ESRI® ArcGIS®)
COL_ROW	Cell address (100 km²)	Cell (10 km x 10 km) designation using column number (1 to 115) and row number (1 to 85) from left to right and from top to bottom (Dutil et al. 2011)
CELL_ID	Cell address (6.25 km²)	Smaller cell (2.5 km x 2.5 km) designation by column and row number with a letter suffix ranging from a to p, increasing through the alphabet column-wise and then row-wise. Smaller cells are nested within larger cells
LATITUDE	Latitude	Position of the cell centroid in decimal degrees – WGS84 (World Geodetic System, 1984 revision)
LONGITUDE	Longitude	Position of the cell centroid in decimal degrees – WGS84 (World Geodetic System, 1984 revision)
TIDAL_A[1]	Tidal zone area	Area of the cell between the low tide mark and the high tide mark (km²), excluding tidal pools
NONTIDAL_A	Non-tidal zone area	Total area of the cell minus the area of the tidal zone and minus the area above the high tide mark (km²)
BENTHIC_A	Benthic area	Area of the non-tidal zone less than 30 m deep (km²)
BENTHIC_B[2]	Benthic cell	Cells with BENTHIC_B set to 1 are those having a BENTHIC_A value > 0
PELAGIC_A	Pelagic area	Area of the non-tidal zone more than 30 m deep (km²)
PELAGIC_B	Pelagic cell	Cells with PELAGIC_B set to 1 are those having a PELAGIC_A value > 0
LCOAST	Length of coastline	Length of the coastline as determined by the low tide mark (mainland and islands) (km)
DCOAST	Distance to coastline	Distance between the cell centroid and the coastline (mainland only), as determined by the low tide mark (km)
SCOAST_P[3]	Sinuosity of coastline (mainland)	Sinuosity of the coastline (mainland only) as the ratio of the length of the coastline at low tide and the corresponding straight-line distance
INSULOSI_P	Insulosity-proportion	Ratio of: 1: sum area of islands (islands and tidal zones associated with islands or forming islands at low tide), and 2: sum area of islands and non-tidal zones. Mainland and contiguous tidal zones were excluded.
INSULOSI_F[4]	Insulosity-frequency	Total number of discrete landscape features emerged at low tide: islands with associated tidal zone and

[1] "_A" indicates a planimetric area variable; *Area* herein
[2] "_B" indicates a binary variable
[3] "_P" indicates a proportion or percentage
[4] "_F" indicates a frequency of occurrence

Variable	Legend	Description
		patches of tidal zones forming islands at low tide (see INSULOSI_P)
SHELTERE_P	Proportion sheltered	Proportion of the non-tidal zone area classified as being "sheltered", following a method described in Cairns et al. (2012) and ICES (2009)
SEMIEXPO_P	Proportion semi-exposed	Proportion of the non-tidal zone area classified as being "semi-exposed", following a method described in Cairns et al. (2012) and ICES (2009)
EXPOSED_P	Proportion exposed	Proportion of the non-tidal zone area classified as being "exposed", following a method described in Cairns et al. (2012) and ICES (2009)
RISK1_C[5]	Sensitivity to sea-level rise	Sensitivity of the coast to sea-level rise. Segments of the coast (mainland only) were classified into three categories of sensitivity (low, high, moderate; Shaw et al. 1998). The dominant category within the cell is reported
RISK2	Distance to high sensitivity coast	Distance (km) between the cell centroid and the nearest high-sensitivity coastal segment (most sensitive to sea-level rise, index values > 15.0)
CELLDEPTH	Cell depth	Maximum cell depth (m)
DEPTHMEAN	Mean depth	Mean depth (m) of the portion of the seafloor less than 30 m deep (m)
DEPTHMIN	Minimum depth	Minimum depth of the portion of the seafloor less than 30 m deep (m); 0 m in cells with islands or overlapping the coastline
DEPTHMAX	Maximum depth	Maximum depth of the portion of the seafloor less than 30 m deep (m); 30 m in cells with CELLDEPTH value greater than 30 m
DEPTHSTD	Depth STD	Standard deviation of depth of the portion of the seafloor less than 30 m deep (m)
SLOPEMEAN	Mean slope	Mean slope of the portion of the seafloor less than 30 m deep (degrees). Mean slope was set to 0.0 for strictly pelagic cells (BENTHIC_B=0 and PELAGIC_B=1)
SLOPEMIN	Minimum slope	Minimum slope of the portion of the seafloor less than 30 m deep (degrees). Minimum slope was set to 0.0 for strictly pelagic cells (BENTHIC_B=0 and PELAGIC_B=1)
SLOPEMAX	Maximum slope	Maximum slope of the portion of the seafloor less than 30 m deep (degrees). Maximum slope was set to 0.0 for strictly pelagic cells (BENTHIC_B=0 and PELAGIC_B=1)
SLOPESTD	Slope STD	Standard deviation of slope of the portion of the seafloor less than 30 m deep (degrees). Standard deviation of slope was set to 0.0 for strictly pelagic cells (BENTHIC_B=0 and PELAGIC_B=1)
SSTMAX	SST maximum	Maximum weekly temperature reached (°C)
SSTWKS1_F	SST < 2°C	Number of weeks with temperature below 2°C
SSTWKS2_F	SST 2-6°C	Number of weeks with temperature between 2 and 6°C

[5] "_C" indicates a categorical variable

Variable	Legend	Description
SSTWKS3_F	SST 6-10°C	Number of weeks with temperature between 6 and 10°C
SSTWKS4_F	SST 10-14°C	Number of weeks with temperature between 10 and 14°C
SSTWKS5_F	SST 14-18°C	Number of weeks with temperature between 14 and 18°C
SSTWKS6_F	SST >18°C	Number of weeks with temperature above 18°C
SSTMARK1_F	Weeks to 6°C	Consecutive weeks with temperature below 6°C from 1 January
SSTMARK2_F	Weeks to 10°C	Consecutive weeks with temperature below 10°C from 1 January
SSTMARK3_F	Weeks to 14°C	Consecutive weeks with temperature below 14°C from 1 January
SSTWK21	SST week 21	Surface temperature at week 21 (°C)
SSTWK30	SST week 30	Surface temperature at week 30 (°C)
SSTDD1	DD week 21-30	Number of degree-days above 2°C from week 21 to week 30
SSTDD2	DD week 31-40	Number of degree-days above 2°C from week 31 to week 40
ICEBEG	First day with ice > 5 cm	First day of the year when mean ice thickness is greater than 5 cm
ICEEND	Last day with ice > 5 cm	Last day of the year when mean ice thickness is greater than 5 cm
ICEDUR_F	Days with ice > 5 cm	Duration of the ice season (days with mean ice depth > 5 cm)
ICERECUR_F	Years with ice > 5 cm	Number of years when ice thickness reached the 5 cm mark (maximum 14 years)
ICETHICK	Maximum ice thickness	Average maximal ice thickness (cm)
TURBIDMEAN	Turbidity (mean)	Mean annual turbidity (m^{-1}). Source: NASA, satellite AQUA, MODIS spectroradiometer-based estimate of the diffuse attenuation coefficient of seawater at 490 nm
TURBIDMIN	Turbidity (minimum)	Minimum monthly turbidity (m^{-1}). Source: NASA, satellite AQUA, MODIS spectroradiometer-based estimate of the diffuse attenuation coefficient of seawater at 490 nm
TURBIDMAX	Turbidity (maximum)	Maximum monthly turbidity (m^{-1}). Source: NASA, satellite AQUA, MODIS spectroradiometer-based estimate of the diffuse attenuation coefficient of seawater at 490 nm
TURBIDWR	Turbidity (winter)	Mean turbidity (m^{-1}) in winter (period from January to March). Source: NASA, satellite AQUA, MODIS spectroradiometer-based estimate of the diffuse attenuation coefficient of seawater at 490 nm
TURBIDSG	Turbidity (spring)	Mean turbidity (m^{-1}) in spring (period from April to June). Source: NASA, satellite AQUA, MODIS spectroradiometer-based estimate of the diffuse attenuation coefficient of seawater at 490 nm
TURBIDSR	Turbidity (summer)	Mean turbidity (m^{-1}) in summer (period from July to September). Source: NASA, satellite AQUA, MODIS spectroradiometer-based estimate of the diffuse attenuation coefficient of seawater at 490 nm
TURBIDFL	Turbidity (fall)	Mean turbidity (m^{-1}) in fall (period from October to December). Source: NASA, satellite AQUA, MODIS spectroradiometer-based estimate of the diffuse attenuation coefficient of seawater at 490 nm

Variable	Legend	Description
SSALMEAN	Surface salinity (mean)	Mean salinity predicted by the 3D model at the surface (0–6.2 m layer)
SSALMIN	Surface salinity (minimum)	Minimum salinity predicted by the 3D model at the surface (0–6.2 m layer)
SSALMAX	Surface salinity (maximum)	Maximum salinity predicted by the 3D model at the surface (0–6.2 m layer)
BSALMEAN	Bottom salinity (mean)	Mean salinity at DEPTHMEAN (on the bottom or at 30 m for BENTHIC_B=0 cells), as predicted from the corresponding layer by the 3D model
BSALMIN	Bottom salinity (minimum)	Minimum salinity at DEPTHMEAN (on the bottom or at 30 m for BENTHIC_B=0 cells), as predicted from the corresponding layer by the 3D model
BSALMAX	Bottom salinity (maximum)	Maximum salinity at DEPTHMEAN (on the bottom or at 30 m for BENTHIC_B=0 cells), as predicted from the corresponding layer by the 3D model
FWRINFWR	Freshwater influence (winter)	Freshwater runoff influence in winter (period from January to March), as predicted by the 3D model, and calculated as 1-(MSAL/35), where MSAL is the average salinity of the water column from the surface down to 36.7 m, and "35" is the maximum salinity of seawater; varies from 0 to 1 (0=no influence)
FWRINFSG	Freshwater influence (spring)	Freshwater runoff influence in spring (period from April to June), as predicted by the 3D model, and calculated as 1-(MSAL/35), where MSAL is the average salinity of the water column from the surface down to 36.7 m, and "35" is the maximum salinity of seawater; varies from 0 to 1 (0=no influence)
FWRINFSR	Freshwater influence (summer)	Freshwater runoff influence in summer (period from July to September), as predicted by the 3D model, and calculated as 1-(MSAL/35), where MSAL is the average salinity of the water column from the surface down to 36.7 m, and "35" is the maximum salinity of seawater; varies from 0 to 1 (0=no influence)
FWRINFFL	Freshwater influence (fall)	Freshwater runoff influence in fall (period from October to December), as predicted by the 3D model, and calculated as 1-(MSAL/35), where MSAL is the average salinity of the water column from the surface down to 36.7 m, and "35" is the maximum salinity of seawater; varies from 0 to 1 (0=no influence)
STEMMEAN	Surface temperature (mean)	Mean temperature (°C) predicted by the 3D model at the surface (0–6.2 m layer)
STEMMIN	Surface temperature (minimum)	Minimum temperature (°C) predicted by the 3D model at the surface (0–6.2 m layer)
STEMMAX	Surface temperature (maximum)	Maximum temperature (°C) predicted by the 3D model at the surface (0–6.2 m layer)
BTEMMEAN	Bottom temperature (mean)	Mean temperature (°C) at DEPTHMEAN (on the bottom or at 30 m for BENTHIC_B=0 cells), as predicted from the corresponding layer by the 3D model
BTEMMIN	Bottom temperature (minimum)	Minimum temperature (°C) at DEPTHMEAN (on the bottom or at 30 m for BENTHIC_B=0 cells), as predicted from the corresponding layer by the 3D model
BTEMMAX	Bottom temperature (maximum)	Maximum temperature (°C) at DEPTHMEAN (on the bottom or at 30 m for BENTHIC_B=0 cells), as predicted from the corresponding layer by the 3D model

Variable	Legend	Description
BTEMWIN	Mean winter temperature	Mean temperature (°C) at DEPTHMEAN (on the bottom or at 30 m for BENTHIC_B=0 cells), as predicted from the corresponding layer by the 3D model, during the period from January to March
BTEMSPR	Mean spring temperature	Mean temperature (°C) at DEPTHMEAN (on the bottom or at 30 m for BENTHIC_B=0 cells), as predicted from the corresponding layer by the 3D model, during the period from April to June
BTEMSUM	Mean summer temperature	Mean temperature (°C) at DEPTHMEAN (on the bottom or at 30 m for BENTHIC_B=0 cells), as predicted from the corresponding layer by the 3D model, during the period from July to September
BTEMFAL	Mean fall temperature	Mean temperature (°C) at DEPTHMEAN (on the bottom or at 30 m for BENTHIC_B=0 cells), as predicted from the corresponding layer by the 3D model, during the period from October to December
SVCURMEAN	Surface vertical current (mean)	Mean vertical current velocity (mm/h), based on absolute value, predicted by the 3D model at 0 m. Negative values indicate descending currents
SVCURMIN	Surface vertical current (minimum)	Minimum vertical current velocity (mm/h), based on absolute value, predicted by the 3D model at 0 m. Negative values indicate descending currents
SVCURMAX	Surface vertical current (maximum)	Maximum vertical current velocity (mm/h), based on absolute value, predicted by the 3D model at 0 m. Negative values indicate descending currents
BVCURMEAN	Bottom vertical current (mean)	Mean vertical current velocity on the bottom (mm/h), based on absolute value, as predicted by the 3D model for the top of the layer closest to DEPTHMEAN. Negative values indicate descending currents
BVCURMIN	Bottom vertical current (minimum)	Minimum vertical current velocity on the bottom (mm/h), based on absolute value, as predicted by the 3D model for the top of the layer closest to DEPTHMEAN. Negative values indicate descending currents
BVCURMAX	Bottom vertical current (maximum)	Maximum vertical current velocity on the bottom (mm/h), based on absolute value, as predicted by the 3D model for the top of the layer closest to DEPTHMEAN. Negative values indicate descending currents
SHCURMEAN	Surface horizontal current (mean)	Mean horizontal current velocity (m/s) predicted by the 3D model at the surface (0–6.2 m layer)
SHCURMIN	Surface horizontal current (minimum)	Minimum horizontal current velocity (m/s) predicted by the 3D model at the surface (0–6.2 m layer)
SHCURMAX	Surface horizontal current (maximum)	Maximum horizontal current velocity (m/s) predicted by the 3D model at the surface (0–6.2 m layer)
BHCURMEAN	Bottom horizontal current (mean)	Mean horizontal current velocity (m/s) at DEPTHMEAN (on the bottom or at 30 m for BENTHIC_B=0 cells), as predicted from the corresponding layer by the 3D model
BHCURMIN	Bottom horizontal current (minimum)	Minimum horizontal current velocity (m/s) at DEPTHMEAN (on the bottom or at 30 m for BENTHIC_B=0 cells), as predicted from the corresponding layer by the 3D model
BHCURMAX	Bottom horizontal current (maximum)	Maximum horizontal current velocity (m/s) at DEPTHMEAN (on the bottom or at 30 m for BENTHIC_B=0 cells), as predicted from the corresponding layer by the 3D model
SHCURDIR_C	Surface horizontal current direction	Direction of the horizontal current at 3.1 m, coded into eight categories of 45 degrees each: code 1 (north) including angles from 337.5 to 360 degrees and from 0 to 22.5 degrees, code 2 angles from 22.5 to 67.5 degrees, and so on

Variable	Legend	Description
BHCURDIR_C	Bottom horizontal current direction	Direction of the horizontal current at DEPTHMEAN (on the bottom or at 30 m for BENTHIC_B=0 cells), coded into eight categories of 45 degrees each, as described for SHCURDIR_C
SDIST3D	Distance to 3D node (S)	The distance between the border of the cell and the nearest 3D model prediction value on the 6 km grid (m), surface layer
BDIST3D1	Distance to 3D node (B1)	The distance between the border of the cell and the nearest 3D model prediction value on the 6 km grid (m), grid closest to DEPTHMEAN (on the bottom or at 30 m for BENTHIC_B=0 cells). This does not apply to vertical current velocities
BDIST3D2	Distance to 3D node (B2)	The distance between the border of the cell and the nearest 3D model prediction value on the 6 km grid (m), grid closest to DEPTHMEAN (on the bottom or at 30 m for BENTHIC_B=0 cells). This applies to vertical current velocities only
SIHUMEAN	Stratification (mean)	Simpson-Hunter water column stability parameter, mean value for a 50 d period (17 October to 5 December, 2007). This parameter is unitless: values near 0 indicate strong mixing, high values indicate a stratified water column
SIHUMIN	Stratification (minimum)	Simpson-Hunter water column stability parameter, minimum running average value for 50 h periods. This parameter is unitless: values near 0 indicate strong mixing, high values indicate a stratified water column
SIHUMAX	Stratification (maximum)	Simpson-Hunter water column stability parameter, maximum running average value for 50 h periods. This parameter is unitless: values near 0 indicate strong mixing, high values indicate a stratified water column
TIDEMAX	Maximum tidal range	Maximum sum value of the main five tidal components (cm) during a 50 d period (17 October to 5 December, 2007). Tidal amplitude has been multiplied by 2 to yield tidal range
TIDECUR	Mean tidal current	Mean tidal current (cm/sec) associated with the M2 component of the tide
TIDESDH	Semi-diurnal high tide	Mean tidal range (cm) of the semi-diurnal high tide, estimated as the sum of the M2 (or S2 where the S2 component has the greatest amplitude) and O1 components. Tidal amplitude has been multiplied by 2 to yield tidal range
TIDESDL	Semi-diurnal low tide	Mean tidal range (cm) of the semi-diurnal low tide, estimated as the difference between the M2 (or S2 where the S2 component has the greatest amplitude) and O1 components. Tidal amplitude has been multiplied by 2 to yield tidal range
WINDMEAN	Mean wind speed	Mean annual wind speed (m/sec)
WINDMIN	Minimum wind speed	Minimum monthly wind speed (m/sec)
WINDMAX	Maximum wind speed	Maximum monthly wind speed (m/sec)
WINDDIR_C	Wind direction	Mean annual wind direction, coded into eight categories of 45 degrees each: code 1 (north) including angles from 337.5 to 360 degrees and from 0 to 22.5 degrees, code 2 angles from 22.5 to 67.5 degrees, and so on
SEGMENTID	Segment ID	Corresponds to variable Segment_ID in the Shoreline Classification and Pre-spill (SCP) web tool. Each cell in the study area was assigned the Segment_ID of the nearest segment on the shoreline (Source: Environment Canada)

Variable	Legend	Description
SEGMENTLBL	Segment label	Corresponds to variable Segment_Label in the SCP web tool. Each cell in the study area was assigned the Segment_label of the nearest segment on the shoreline (Source: Environment Canada)
SEGMENTDIS	Distance to segment	Distance from the cell boundary to the nearest segment on the shoreline (km). A value of 0 indicates that the shoreline segment is partially or entirely enclosed within the cell boundary
SHORMOR_C	Shoreline morphology	Corresponds to the lower intertidal form variable LI_FORM in the SCP database
SHORMAT_C	Shoreline material	Corresponds to the upper intertidal shoreline category variable UI_Scat in the SCP database
SANDBEACH	Distance to sand beach	Distance between the cell and the nearest sand beach (SANDBEACH) on the shoreline (km)
MUDFLAT	Distance to mud flat	Distance between the cell and the nearest mud flat (MUDFLAT) on the shoreline (km)
MARSH	Distance to marsh	Distance between the cell and the nearest salt marsh (MARSH) on the coast (shoreline and backshore) (km)
MANMADE	Distance to modified shoreline	Distance between the cell and the nearest anthropogenic structure and material (MANMADE) on the shoreline (km)
TACCESS_A	Access to tidal areas	Sum of TIDAL_A of the cell and its adjacent neighbours (km^2, maximum 8 neighbours)
SEDIMENT_C	Type of sediment	Type of soft sediment reported for the nearest zone in Loring and Nota's (1973) map, Loring and Nota's code (1973). Benthic cells (BENTHIC_B=1) only
OUTCROP_C	Type of outcrop	Type of rocky outcrop reported for the nearest zone in Loring and Nota's (1973) map, Loring and Nota's code (1973). Benthic cells (BENTHIC_B=1) only
LORNOTDIST	Distance to sediment zone	Distance (km) between the cell centroid and the nearest zone in Loring and Nota's (1973) map. Benthic cells (BENTHIC_B=1) only
SEDIMENTF	Description du sédiment	Description française du sédiment meuble en surface (Loring et Nota, 1973). Benthic cells (BENTHIC_B=1) only
SEDIMENTE	Sediment description	English description for the soft surface sediment (Loring and Nota, 1973). Benthic cells (BENTHIC_B=1) only
OUTCROPF	Description des affleurements rocheux	Description française des affleurements rocheux (Loring et Nota, 1973). Benthic cells (BENTHIC_B=1) only
OUTCROPE	Description of outcrops	English description for the rocky outcrops (Loring and Nota, 1973). Benthic cells (BENTHIC_B=1) only
ZOSTERA_B	Proximity to eelgrass bed	ZOSTERA_B set to 1 when an eelgrass bed is known to occur within 10 km of the cell centroid; ZOSTERA_B set to 0 otherwise. Data from various sources described in Materials and Methods
FWINPUT	Nearest stream/river	CELL_ID of the nearest cell located at the junction between a stream or river mouth (drainage area > 70 km^2) and the low tide mark. When a cell overlaps the low tide mark at the point of entry of a stream or river, CELL_ID and FWINPUT have the same code
FWDIST	Distance to nearest stream/river	Calculated distance between the cell centroid (km) and the nearest cell identified as a point of entry of a stream or river. When CELL_ID and FWINPUT have the same code, FWDIST=0

Variable	Legend	Description
FWDRAIN	Drainage area of nearest stream/river	Drainage area of the nearest stream/river (km^2) within the study area
FWFLOW	Mean annual flow of nearest stream/river	Mean annual flow of the nearest stream/river (m^3/sec) within the study area
HAB_BEN	Benthic megahabitat	Classification of cells (100 km2) into 13 benthic megahabitats based on Dutil, J.-D., S. Proulx, P.-M. Chouinard, D. Borcard (2011)
HAB_C_E	Coastal and pelagic habitat	Classification of cells (6.25 km2) into 14 coastal and epipelagic habitats (this dataset)
REGION	Geographic region	Geographic region within the study area: estuary, northern and southern Gulf of St. Lawrence

Appendix 2. Description of variables in the Microsoft Access® database with regard to their characteristics and scale of measurement.

Variable	Variable category	Type of variable	Type of variable	Scale of measurement *	Minimum	Maximum
OBJECTID	ArcGIS® generated	Qualitative	Label	N/A	N/A	N/A
SHAPE	ArcGIS® generated	Qualitative	Format	N/A	N/A	N/A
COL_ROW	Geographic	Qualitative	Label	Local	N/A	N/A
CELL_ID	Geographic	Qualitative	Label	Local	N/A	N/A
LATITUDE	Geographic	Quantitative	Continuous	Local	45.5769	51.9093
LONGITUDE	Geographic	Quantitative	Continuous	Local	-70.7603	-55.9734
TIDAL_A[1]	Topographic	Quantitative	Continuous	Local	0.00	6.25
NONTIDAL_A	Topographic	Quantitative	Continuous	Local	0.00	6.25
BENTHIC_A	Topographic	Quantitative	Continuous	Local	0.00	6.25
BENTHIC_B[2]	Topographic	Qualitative	Binary	Local	0	1
PELAGIC_A	Topographic	Quantitative	Continuous	Local	0.00	6.25
PELAGIC_B	Topographic	Qualitative	Binary	Local	0	1
LCOAST	Topographic	Quantitative	Continuous	Local	0.00	34.06
DCOAST	Geographic	Quantitative	Continuous	Local	0.00	107.52
SCOAST_P[3]	Topographic	Quantitative	Continuous	Local	1.00	6.79
INSULOSI_P	Geographic	Quantitative	Continuous	Local	0.00	1.00
INSULOSI_F	Geographic	Quantitative	Discrete	Local	0	87
SHELTERE_P	Topographic	Quantitative	Continuous	Regional	0.00	1.00
SEMIEXPO_P	Topographic	Quantitative	Continuous	Regional	0.00	1.00
EXPOSED_P	Topographic	Quantitative	Continuous	Regional	0.00	1.00
RISK1_C[4]	Multiple categories	Quantitative	Categorical	Regional	Low (0–4.9)	High (15.0 and more)

[1] "_A" indicates a planimetric area variable; *Area* herein
[2] "_B" indicates a binary variable
[3] "_P" indicates a proportion or percentage
[4] "_F" indicates a frequency of occurrence

Variable	Variable category	Type of variable	Type of variable	Scale of measurement *	Minimum	Maximum
RISK2	Multiple categories	Quantitative	Continuous	Regional	0.00	107.52
CELLDEPTH	Topographic	Quantitative	Continuous	Local	0.0	532.3
DEPTHMEAN	Topographic	Quantitative	Continuous	Local	0.0	30.0
DEPTHMIN	Topographic	Quantitative	Continuous	Local	0.0	30.0
DEPTHMAX	Topographic	Quantitative	Continuous	Local	0.0	30.0
DEPTHSTD	Topographic	Quantitative	Continuous	Local	0.0	11.2
SLOPEMEAN	Topographic	Quantitative	Continuous	Local	0.0	27.6
SLOPEMIN	Topographic	Quantitative	Continuous	Local	0.0	18.5
SLOPEMAX	Topographic	Quantitative	Continuous	Local	0.0	70.1
SLOPESTD	Topographic	Quantitative	Continuous	Local	0.0	16.7
SSTMAX	Physico-chemical	Quantitative	Continuous	Local	8.01	24.83
SSTWKS1_F[5]	Physico-chemical	Quantitative	Discrete	Local	11	37
SSTWKS2_F	Physico-chemical	Quantitative	Discrete	Local	1	19
SSTWKS3_F	Physico-chemical	Quantitative	Discrete	Local	2	19
SSTWKS4_F	Physico-chemical	Quantitative	Discrete	Local	0	15
SSTWKS5_F	Physico-chemical	Quantitative	Discrete	Local	0	15
SSTWKS6_F	Physico-chemical	Quantitative	Discrete	Local	0	11
SSTMARK1_F	Physico-chemical	Quantitative	Discrete	Local	8	30
SSTMARK2_F	Physico-chemical	Quantitative	Discrete	Local	17	52
SSTMARK3_F	Physico-chemical	Quantitative	Discrete	Local	17	52
SSTWK21	Physico-chemical	Quantitative	Continuous	Local	-1.68	13.65
SSTWK30	Physico-chemical	Quantitative	Continuous	Local	-1.44	21.54
SSTDD1	Physico-chemical	Quantitative	Continuous	Local	30.73	1053.92
SSTDD2	Physico-chemical	Quantitative	Continuous	Local	263.20	1174.81
ICEBEG	Physico-chemical	Quantitative	Discrete	Local	-11	68

[5] "_C" indicates a categorical variable

Variable	Variable category	Type of variable	Type of variable	Scale of measurement *	Minimum	Maximum
ICEEND	Physico-chemical	Quantitative	Discrete	Local	40	134
ICEDUR_F	Physico-chemical	Quantitative	Discrete	Local	16	136
ICERECUR_F	Physico-chemical	Quantitative	Discrete	Local	1	14
ICETHICK	Physico-chemical	Quantitative	Continuous	Local	4.9	107.8
TURBIDMEAN	Physico-chemical	Quantitative	Continuous	Local	0.09	6.40
TURBIDMIN	Physico-chemical	Quantitative	Continuous	Local	0.05	6.40
TURBIDMAX	Physico-chemical	Quantitative	Continuous	Local	0.10	6.40
TURBIDWR	Physico-chemical	Quantitative	Continuous	Local	0.07	5.01
TURBIDSG	Physico-chemical	Quantitative	Continuous	Local	0.09	6.40
TURBIDSR	Physico-chemical	Quantitative	Continuous	Local	0.08	4.91
TURBIDFL	Physico-chemical	Quantitative	Continuous	Local	0.08	3.92
SSALMEAN	Physico-chemical	Quantitative	Continuous	Local	1.09	32.05
SSALMIN	Physico-chemical	Quantitative	Continuous	Local	1.01	31.58
SSALMAX	Physico-chemical	Quantitative	Continuous	Local	1.29	32.81
BSALMEAN	Physico-chemical	Quantitative	Continuous	Local	1.09	32.07
BSALMIN	Physico-chemical	Quantitative	Continuous	Local	1.01	31.73
BSALMAX	Physico-chemical	Quantitative	Continuous	Local	1.29	32.83
FWRINFWR	Physico-chemical	Quantitative	Continuous	Local	0.07	0.97
FWRINFSG	Physico-chemical	Quantitative	Continuous	Local	0.08	0.97
FWRINFSR	Physico-chemical	Quantitative	Continuous	Local	0.09	0.97
FWRINFFL	Physico-chemical	Quantitative	Continuous	Local	0.09	0.97
STEMMEAN	Physico-chemical	Quantitative	Continuous	Local	1.59	10.13
STEMMIN	Physico-chemical	Quantitative	Continuous	Local	-1.71	1.79
STEMMAX	Physico-chemical	Quantitative	Continuous	Local	5.07	23.76
BTEMMEAN	Physico-chemical	Quantitative	Continuous	Local	1.24	10.13
BTEMMIN	Physico-chemical	Quantitative	Continuous	Local	-1.71	2.26
BTEMMAX	Physico-chemical	Quantitative	Continuous	Local	4.23	23.76

Variable	Variable category	Type of variable	Type of variable	Scale of measurement *	Minimum	Maximum
BTEMWIN	Physico-chemical	Quantitative	Continuous	Local	-1.59	3.28
BTEMSPR	Physico-chemical	Quantitative	Continuous	Local	0.06	10.20
BTEMSUM	Physico-chemical	Quantitative	Continuous	Local	2.67	22.45
BTEMFAL	Physico-chemical	Quantitative	Continuous	Local	1.75	11.06
SVCURMEAN	Hydrographic	Quantitative	Continuous	Local	41.3	-1238.7
SVCURMIN	Hydrographic	Quantitative	Continuous	Local	37.3	-513.7
SVCURMAX	Hydrographic	Quantitative	Continuous	Local	2.2	-1996.8
BVCURMEAN	Hydrographic	Quantitative	Continuous	Local	2654.0	-3590.7
BVCURMIN	Hydrographic	Quantitative	Continuous	Local	1521.3	-1599.7
BVCURMAX	Hydrographic	Quantitative	Continuous	Local	4061.1	-5160.7
SHCURMEAN	Hydrographic	Quantitative	Continuous	Local	0.00	1.10
SHCURMIN	Hydrographic	Quantitative	Continuous	Local	0.00	0.44
SHCURMAX	Hydrographic	Quantitative	Continuous	Local	0.00	1.74
BHCURMEAN	Hydrographic	Quantitative	Continuous	Local	0.00	0.92
BHCURMIN	Hydrographic	Quantitative	Continuous	Local	0.00	0.39
BHCURMAX	Hydrographic	Quantitative	Continuous	Local	0.00	1.45
SHCURDIR_C	Hydrographic	Qualitative	Categorical	Local	1	8
BHCURDIR_C	Hydrographic	Qualitative	Categorical	Local	1	8
SDIST3D	Validation criterion	Quantitative	Continuous	Local	0.00	45.35
BDIST3D1	Validation criterion	Quantitative	Continuous	Local	0.00	45.35
BDIST3D2	Validation criterion	Quantitative	Continuous	Local	0.00	50.31
SIHUMEAN	Physico-chemical	Quantitative	Continuous	Local	-0.60	11.10
SIHUMIN	Physico-chemical	Quantitative	Continuous	Local	-0.95	10.79
SIHUMAX	Physico-chemical	Quantitative	Continuous	Local	0.03	11.91
TIDEMAX	Hydrographic	Quantitative	Continuous	Local	35.3	697.2
TIDECUR	Hydrographic	Quantitative	Continuous	Local	0.2	164.4
TIDESDH	Hydrographic	Quantitative	Continuous	Local	20.6	485.9

Variable	Variable category	Type of variable	Type of variable	Scale of measurement *	Minimum	Maximum
TIDESDL	Hydrographic	Quantitative	Continuous	Local	0.0	387.1
WINDMEAN	Atmospheric	Quantitative	Continuous	Local	0.73	2.19
WINDMIN	Atmospheric	Quantitative	Continuous	Local	0.00	0.80
WINDMAX	Atmospheric	Quantitative	Continuous	Local	1.39	4.86
WINDDIR_C	Atmospheric	Qualitative	Categorical	Local	3	4
SEGMENTID	Geographic	Qualitative	Label	Regional	N/A	N/A
SEGMENTLBL	Geographic	Qualitative	Label	Regional	N/A	N/A
SEGMENTDIS	Validation criterion	Quantitative	Continuous	Regional	0.0	103.6
SHORMOR_C	Topographic	Qualitative	Categorical	Regional	N/A	N/A
SHORMAT_C	Geologic	Qualitative	Categorical	Regional	N/A	N/A
SANDBEACH	Topographic	Quantitative	Continuous	Regional	0.0	235.6
MUDFLAT	Topographic	Quantitative	Continuous	Regional	0.0	300.7
MARSH	Topographic	Quantitative	Continuous	Regional	0.0	286.0
MANMADE	Topographic	Quantitative	Continuous	Regional	0.0	138.1
TACCESS_A	Topographic	Quantitative	Continuous	Local	0.00	37.36
SEDIMENT_C	Geologic	Qualitative	Categorical	Regional	N/A	N/A
OUTCROP_C	Geologic	Qualitative	Categorical	Regional	N/A	N/A
LORNOTDIST	Validation criterion	Quantitative	Continuous	Regional	0.00	77.96
SEDIMENTF	Geologic	Qualitative	Label	Regional	N/A	N/A
SEDIMENTE	Geologic	Qualitative	Label	Regional	N/A	N/A
OUTCROPF	Geologic	Qualitative	Label	Regional	N/A	N/A
OUTCROPE	Geologic	Qualitative	Label	Regional	N/A	N/A
ZOSTERA_B	Biological	Qualitative	Binary	Regional	0	1
FWINPUT	Hydrographic	Qualitative	Label	Regional	N/A	N/A
FWDIST	Hydrographic	Quantitative	Continuous	Regional	0.00	157.54
FWDRAIN	Hydrographic	Quantitative	Continuous	Regional	70.0	86954.5
FWFLOW	Hydrographic	Quantitative	Continuous	Regional	1.5	1597.5

Variable	Variable category	Type of variable	Type of variable	Scale of measurement *	Minimum	Maximum
HAB_BEN	Habitat	Qualitative	Categorical	Local	N/A	N/A
HAB_C_E	Habitat	Qualitative	Categorical	Local	N/A	N/A
REGION	Geographic	Qualitative	Label	Regional	N/A	N/A

* When the data for a given variable were obtained from observations made within the limits of a cell, they are referred to as local measurements; properties attributed to a cell on the basis of its localization in a broader area, in which all cells share a common value for that variable, are referred to as regional measurements.

Appendix 3. Variables issued from remote sensing observations (italics) and 3D modelling (plain text).

	Temperature	Salinity	Hor. current	Ver. current	Stratification	Turbidity	Ice	Tide	Wind
Surface layer	STEMMEAN	SSALMEAN	SHCURMEAN	SVCURMEAN					WINDMEAN
(annual)	STEMMIN	SSALMIN	SHCURMIN	SVCURMIN					WINDMIN
	STEMMAX	SSALMAX	SHCURMAX	SVCURMAX					WINDMAX
	SSTMAX		SHCURDIR_C						WINDDIR_C
	SSTWKS1_F								
	SSTWKS2_F								
	SSTWKS3_F								
	SSTWKS4_F								
	SSTWKS5_F								
	SSTWKS6_F								
	SSTMARK1_F								
	SSTMARK2_F								
	SSTMARK3_F								
	SSTWK21								
	SSTWK30								
	SSTDD1								
	SSTDD2								
Bottom layer	BTEMMEAN	BSALMEAN	BHCURMEAN	BVCURMEAN					
(annual)	BTEMMIN	BSALMIN	BHCURMIN	BVCURMIN					
	BTEMMAX	BSALMAX	BHCURMAX	BVCURMAX					
			BHCURDIR_C						
Bottom layer	BTEMWIN								
(seasonal)	BTEMSPR								

	Temperature	Salinity	Hor. current	Ver. current	Stratification	Turbidity	Ice	Tide	Wind
	BTEMSUM								
	BTEMFAL								
Not layer-specific	*TURBIDMEAN*						*ICEBEG*		
(annual)	*TURBIDMIN*						*ICEEND*		
	TURBIDMAX						*ICEDUR_F*		
							ICERECUR_F		
							ICETHICK		
Not layer-specific		FWRINFWR				*TURBIDWR*			
(seasonal)		FWRINFSG				*TURBIDSG*			
		FWRINFSR				*TURBIDSR*			
		FWRINFFL				*TURBIDFL*			
Not layer-specific					SIHUMEAN			TIDEMAX	
(50-day period in fall)					SIHUMIN			TIDECUR	
					SIHUMAX			TIDESDH	
								TIDESDL	

Appendix 4. Variables and number of cells with null or missing data. Cells with null data were coded "-8888", those with missing data were coded "-9999". Variables not listed had no null or missing data.

Variable	Cells with null or missing data	Cells with null data
SCOAST_P	35341	Null data when cell does not overlap mainland coastline
RISK1_C	35290	Null data when cell does not overlap mainland coastline, missing data for most islands
TURBIDMEAN	233	Missing data in narrow bays and estuaries
TURBIDMIN	233	Missing data in narrow bays and estuaries
TURBIDMAX	233	Missing data in narrow bays and estuaries
TURBIDWR	320	Missing data in narrow bays and estuaries
TURBIDSG	292	Missing data in narrow bays and estuaries
TURBIDSR	306	Missing data in narrow bays and estuaries
TURBIDFL	251	Missing data in narrow bays and estuaries
SHORMOR_C	8813	Missing data in the Environment Canada database
SHORMAT_C	13076	Missing data in the Environment Canada database
SEDIMENT_C	29948	Null data for non-benthic cells
OUTCROP_C	29948	Null data for non-benthic cells
LORNOTDIST	29948	Null data for non-benthic cells
SEDIMENTF	29948	Null data for non-benthic cells
SEDIMENTE	29948	Null data for non-benthic cells
OUTCROPF	29948	Null data for non-benthic cells
OUTCROPE	29948	Null data for non-benthic cells
HAB_BEN	2189	Null data for cells out of the range for the benthic megahabitats study

Coastal and epipelagic habitats of the estuary and Gulf of St. Lawrence.

Can. Tech. Rep. Fish. Aquat. Sci.
3009: ix + 87 pages.

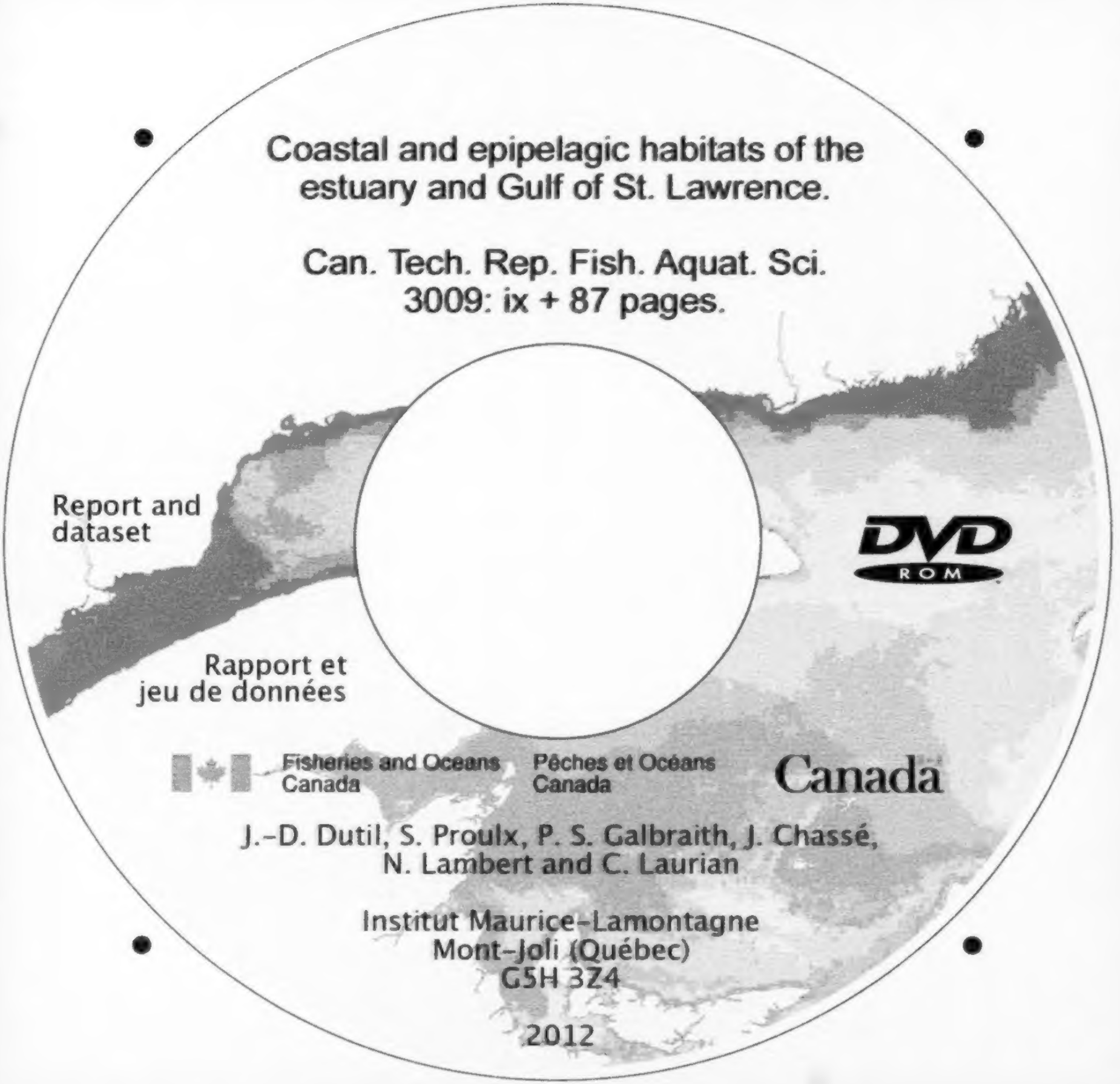

Fisheries and Oceans Canada | Pêches et Océans Canada

Canada

J.-D. Dutil, S. Proulx, P. S. Galbraith, J. Chassé, N. Lambert and C. Laurian

Institut Maurice-Lamontagne
Mont-Joli (Québec)
G5H 3Z4

2012